Schlafen12, a novel HIV restriction factor involved in latency

Katarína Smutná

TESI DOCTORAL UPF / 2018

DIRECTORS DE LA TESI

Dr. Andreas Meyerhans i Dra. Juana Díez

DEPARTAMENT DE CIÈNCIES EXPERIMENTALS I DE LA SALUT

Celej vedeckej komunite

ACKNOWLEDGEMENTS

In science one never works alone. It is always a teamwork. I have been lucky to have amazing people around me, and because of that, I want to thank everyone who has helped me achieve my PhD.

First of all, I would like to thank both of my supervisors; Andreas and Juana. Not only for giving me the opportunity to do my PhD and providing the material for my experiments but also for being mentors who were able to encourage me to work hard on myself and lead me in the right direction.

Javier! Thank you for being supportive during my first period of PhD. Teaching me how to deal with bosses, meetings, deadlines, data presenting and lots of other necessary stuff in order to continue and survive in the world of science. On top of everything, one big thanks for forcing me to be responsible for myself from the beginning. I have appreciated that later a lot.

Mie! The most lovely, hard-working, and caring colleague. I couldn't ask for anyone better. There have been many changes going on during my PhD, but you coming to our lab and joining me was definitely the best one. Thank you so much for giving me useful advice and correcting my work to the fine detail. I have learned so much from working with you.

Huge thanks to you Jordi! Not only for the work you have done in this project but also for the time you have spent with me, explaining the things to the detail and showing me the proper way of thinking while dealing with problems.

Jenni, Jenni, Jenni!! I love the way you work! Thank you for having patience with me and helping out with problematic stuff. It has been a pleasure to work with you.

To all my labmates and people I have met whilst working in the lab. Graciela, Mireia, Valentina, Eva, Gemma, Marc, Leire, Rene and Maria-Eugenia, you guys made every day a little bit easier. Thank you for helping, sharing and supporting.

To my students Noujan, Selina and Florencia who has also contributed to the project. Thank you for being a part of my work.

To the guys from Genomic Core Facility who advised me whenever I needed it.

I also appreciate the help of Dr Nick Berrow who took his time to talk to me and explain me cloning strategies step by step. It was very supportive and helpful moment for the beginner like me.

Veľké ďakujem patrí aj mojej rodine. Mami, oci, ďakujem za všetko. Aj keď na diaľku, ale boli ste mojou obrovskou oporou. Bez Vás by som to už dávno vzdala. A moji dvaja “malí” smradi!! Ďakujem za to, že ste. Najlepší. Nevymenila by som Vás za nič na svete.

To Helder, who was standing by my side no matter what. Seeing you working so hard, was helping me to carry on and not to give up. Thank you for your patience and understanding.

Thanks to all my friends and people who have always believed in me!

Kat.

SUMMARY

The process of HIV latency establishment and maintenance is not clearly understood. Homeostatic proliferation (HSP) is a major mechanism by which long-lived naive and memory CD4 T cells are maintained *in vivo*. HSP also contributes to the persistence of HIV latent reservoir. Furthermore, HIV-infected naive CD4 T cells cultured under HSP condition are refractory to reactivation, in contrast to TCR-activated memory CD4 T cells. This might be due to the suggested post-transcriptional block in naive HSP-cultured cells. Here we compared a transcriptomic signature of naive and memory CD4 T cells. Among differentially expressed genes that may influence HIV latency, we identified Schlafen 12 (SLFN12) as an interesting candidate for a potential HIV restriction factor. Our results showed that SLFN12 establishes post-transcriptional block in HIV infected cells and thus inhibits both, HIV production as well as its reactivation from latently infected cells. These findings may help to better understand the mechanisms underlying HIV latency and its reversal in HSP-maintained naive CD4 T cells. All together it might contribute to the design of novel HIV eradication strategies.

RESUMEN

El proceso por el cual el virus de la Inmunodeficiencia Humana (VIH) establece y mantiene un estado de latencia no se conoce en su totalidad. La proliferación homeostática (HSP, de sus siglas en ingés “Homeostatic proliferation”) es uno de los mecanismos por el cual las células T CD4 “naive” y de memoria se mantienen in vivo. Además, HSP también contribuye al mantenimiento del reservorio de virus en forma latente. Además, las células T CD4 “naive” infectadas y cultivadas en condiciones de HSP no son capaces de reactivarse a diferencia de las células T CD4 de memoria activadas vía TCR. Estudios previos sugieren que esta observación se debe a un bloqueo post-transcripcional en células T “naive” cultivadas en condiciones de HSP. En esta tesis comparamos la perfil del transcriptoma de células T CD4 “naive” y de memoria. Entre los genes diferencialmente expresados que podrían participar en el proceso de latencia del VIH, identificamos Schlafen 12 (SLFN12) como un candidato interesante que podría ser un factor de restricción del virus. Los resultados de este trabajo muestran que SLFN12 establece un bloqueo post-transcripcional en células infectadas por VIH, y de esta forma inhibe tanto la producción del virus como su reactivación en células infectadas de forma latente. Estas observaciones pueden ser de gran ayuda para entender mejor los mecanismos subyacentes a la latencia del VIH así como su reactivación en células CD4 T “naive” mantenidas bajo condiciones de HSP. En su conjunto, estos resultados podrían contribuir al diseño de nuevas estrategias para erradicar el VIH.

PROLOGUE

The Human Immunodeficiency Virus (HIV) is the causative agent of acquired immunodeficiency syndrome (AIDS). Although current antiretroviral therapy effectively suppresses HIV replication, rapid viral rebound is observed in patients after treatment interruption. This is due to the existence of a reservoir of treatment-resistant virus-infected cells, most importantly latently-infected T cell subsets such as resting naive and memory CD4 T cells. This reservoir is the main obstacle for curing an HIV infection.

The so-called “kick and kill” strategy involves the use of latency reversal agents (LRAs) to switch dormant-infected cells to virus-producing cells that can be targeted by antivirals and depleted by cytotoxic T lymphocytes (CTLs). While this strategy seems to work using *in vitro* models, the efficiency of “kick and kill” *in vivo* is far less efficient. This highlight the need for a deeper understanding of the mechanism driving HIV latency.

Naive and memory CD4 T cells are *in vivo* maintained mainly by homeostatic proliferation (HSP). HSP was also suggested to contribute to the persistence of latent HIV-1 reservoir. However, studies of the dormant switch in naive CD4 T cells are lacking as many *in vitro* latency models rely on CD4 T cells that were first differentiated via T-cell receptor (TCR) into memory/effector cells. To fill this gap we have previously, in collaboration with Professor Yasuko Tsunetsugu-Yokota, developed an *in vitro* system to study HIV infection in HSP-maintained primary cells. Using this approach, we showed that HIV-infected naive T cells are refractory to reactivation upon TCR or LRA stimuli.

In this thesis, we have performed a transcriptomic analysis of HSP-cultured naive CD4 T cells in order to identify cellular factors that might contribute to HIV provirus persistence in these physiological relevant conditions. The presented results contribute to better understand mechanisms governing HIV latency and its reversal in naive CD4 T cells, moreover, they might also contribute to therapeutic intervention.

TABLE OF CONTENTS

INTRODUCTION

1 Human Immunodeficiency Viruses

1.1 General facts about HIV

The Human Immunodeficiency Viruses HIV-1 and HIV-2 are the causative agents of the Acquired Immune Deficiency Syndrome (AIDS). They were discovered at the Pasteur Institute in Paris in 1983 and 1986, respectively (Barré-Sinoussi et al. 1983; Clavel et al. 1986). Initial discrepancies in the naming of the AIDS-causing viruses as Lymphadenopathy-Associated Virus (LAV) or HTVL III were settled in 1986 and HIV became the official name (Case 1986).

HIV belongs to the family of *Retroviridae*, genus *Lentivirus*. In Latin, “lentus” means slow. Lentiviruses got this name because of their long incubation period. Based on genetic characteristics, HIV is classified into two types (HIV-1, HIV-2). Both types have been evolved from simian immunodeficiency viruses (SIV). HIV-1, from Central African chimpanzees (SIVcpz) and gorillas (SIVgor), and HIV-2, from West African sooty mangabeys (SIVsm) (Gao et al. 1999; Paul M. Sharp and Hahn 2011; Huet et al. 1990; Van Heuverswyn et al. 2006). HIV is a very variable pathogen. HIV-1 is divided into four groups: group M (main), group O (outlier), group N (new) and group P (closely related to gorilla SIV). Group M has been subdivided into several genetically associated clades (A1, A2, B, C, D, F1, F2, G, H, J, and K). For HIV-2 different subtypes also exist (A, B, C, F, and G). Furthermore, HIV can be also classified as macrophage tropic (M-tropic), T-cell tropic (T-tropic) or dual tropic based on its ability to infect macrophages, T cells or both (Al-Jabri 2003; Korber et al. 2000).

HIV-1 and HIV-2 share the same mechanism of replication. Both can be transmitted by sexual contact, by blood products or by vertical transmission (mother-to-child). Infection by both viruses eventually leads to AIDS in nearly all cases. However, HIV-2 infection progresses more slowly compared to HIV-1. Viral load is lower during HIV-2 infection than in HIV-1, which explains the lower transmission rate of HIV-2. Based on geography, HIV-1 spreads worldwide while HIV-2 infection is mostly limited to West Africa and countries linked to it socioeconomically, for example,

Portugal (Nyamweya et al. 2013). Today, HIV is present on each continent, however, the majority of HIV-infected people is living in low- or middle- income countries of sub-Saharan Africa **(Figure I1)**. The latest data from 2017 report 36,9 million HIV-infected people worldwide. From these, 35,1 million are adults, the rest are children under the age of 15. Deaths of AIDS-related illnesses reached 940 000/year and 1,8 million individuals were newly infected. The most affected groups within the population are men who have sex with men (MSM), clients of sex workers and intravenous drugs users (IVDU) (**Figure I2**). Although the number of new infections per year dropped by 47% compared to the peak of infections in 1996, the annual number does not vary so much in the last years. Nevertheless, the current decline in newly infected individuals does not meet the global targets of HIV infection elimination (www.unaids.org).

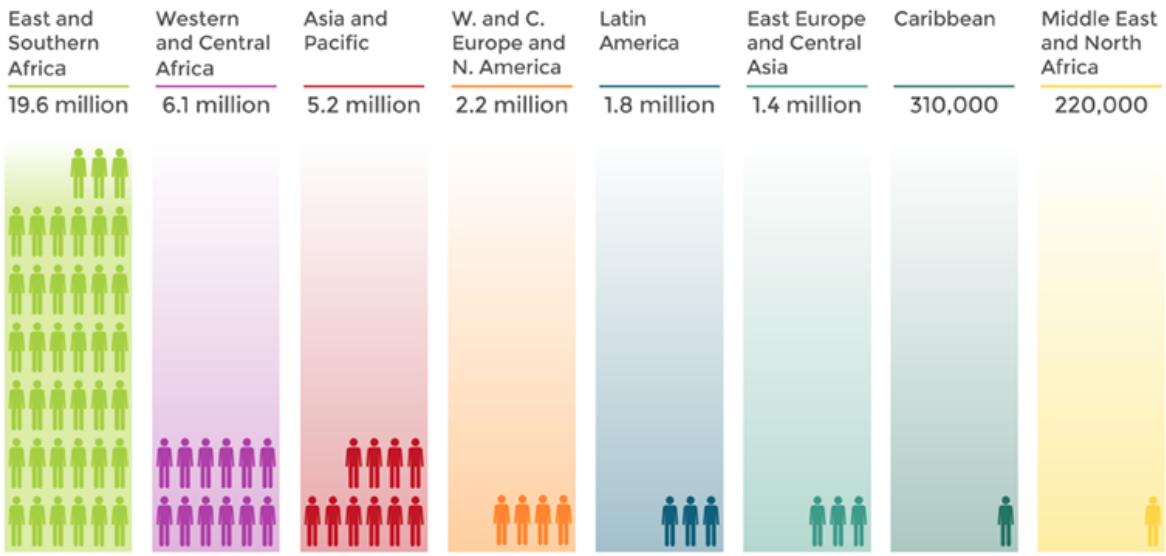

Figure I1. Distribution of people living with HIV in 2017. The global statistic shows that the least people infected with HIV are living in the Middle East, North Africa and the Caribbean. Europe and America contribute with higher numbers, but the vast majority of HIV-infected people lives in the rest of Africa and in Asia. Figure is taken from (www.avert.org).

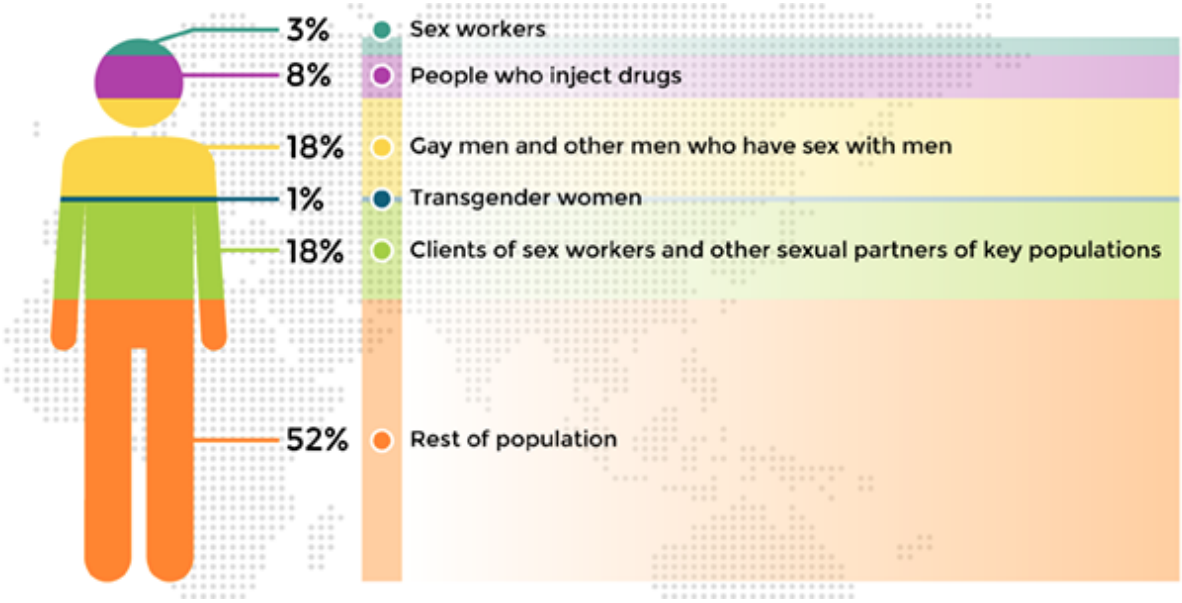

Figure I2. Distribution of new HIV infections among different groups of the population in 2017. 1,8 million people were newly infected with HIV in 2017. Transgender women (1%) and sex workers (3%) represent the least affected groups. Drug-addicted people who share needles to inject the drugs participate in these infections by 8%. Unprotected sexual contact is the most common way of HIV transmission. 18% of new HIV infections occurred in the homosexual community as well as within the clients of sex workers. The remaining 52% were people infected by unprotected sexual intercourse, contaminated blood or mother-to-child transmission. Figure is taken from (www.avert.org).

1.2 HIV genome and virion structure

The viral particle of HIV is around 100 nm in diameter. It contains two copies of single-stranded RNA (ssRNA) protected by a conical capsid which is coated by a lipidic membrane derived from the cell surface. The 5´end of the HIV genomic RNA contains a cap sequence and the 3´end is polyadenylated. Upon entering a cell, the genomic viral RNA is reverse transcribed into DNA (Montagnier 1999; Castelli and Levy 2002). Viral DNA has long terminal repetitions (LTR) flanking both sides **(Figure I3 A)**. The 5´-LTR region encodes the HIV promotor. The first open reading frame (ORF) is *gag* (group-specific antigen) which encodes structural proteins that build the core of the HIV virion. These are matrix protein (MA, p17), capsid protein (CA, p24), and nucleocapsid protein (NC, p7). The *Gag* gene is followed by the *pol* (polymerase) ORF encoding viral integrase (IN, p32), reverse transcriptase (RT, p51) together with RNase H (p15) and protease (PR, p12). These enzymes are located within the capsid, close to the viral RNA. Next to *pol* is the last typical retroviral ORF *env* (envelope) from which the surface glycoprotein (SU, gp120) and the transmembrane glycoprotein (TM, gp41) are transcribed **(Figure I3 B)**. Apart

from structural proteins, HIV-1 encodes proteins that have regulatory functions: Rev (RNA splicing regulator) and Tat (transactivator protein). And also small accessory proteins: Vif (viral infectivity factor) is necessary for infectious viral production, Nef (negative regulating factor) affecting HIV replication, Vpu (virus protein unique) required for release of new viral particles and Vpr (virus protein r) which also has an impact on virus infectivity. HIV-2 encodes Vpx (virus protein x) instead of Vpu (Frankel and Young 1998; Levy 1989). Like all viruses, HIV requires the cell machinery to replicate and produce progeny.

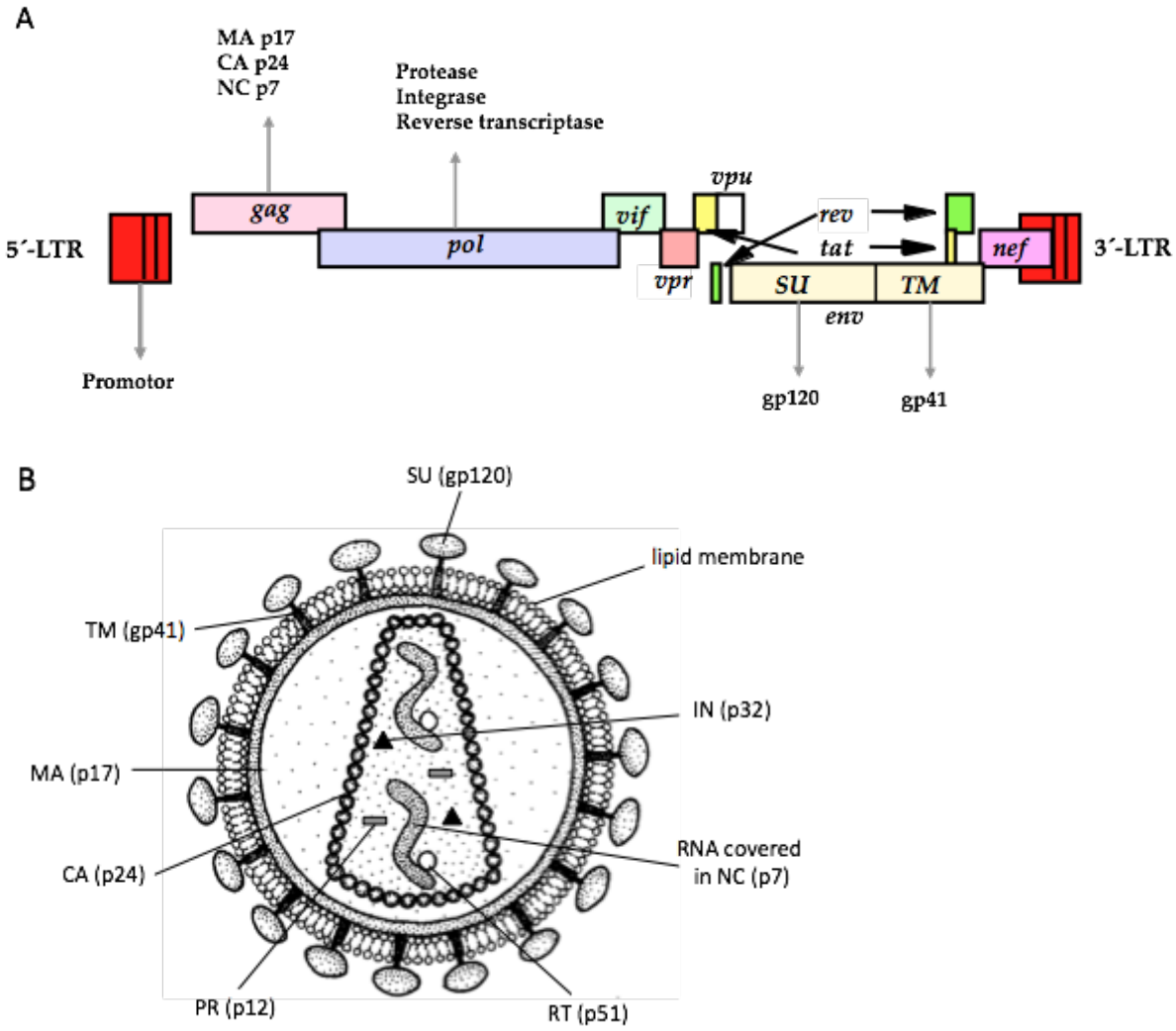

Figure I3. HIV-1 genome organization and virion structure. A - The HIV genome is around 10kb long. Long terminal repetitions (LTRs) are flanking both sides of the genome. The HIV promoter is encoded in the 5´-LTR region. Open reading frame (ORF) *gag* encodes structural proteins (matrix protein p17, capsid protein p24, nucleocapsid protein p7). All viral enzymatic activities are transcribed from segment *pol*. Gene *env* is coding surface and transmembrane glycoproteins (gp120, gp41). Proteins of *tat* and *rev* are composed of two different regions. The figure was provided by Andreas Meyerhans. **B** - Schematic view of an HIV viral particle. The surface of HIV is composed by the surface glycoprotein 120 (SU, gp120) and the transmembrane glycoprotein 41 (TM, gp41). The lipid

bilayer together with the matrix protein (MA, p17) forms a border between inner and outer side of the virion. The conical capsid (CA, p24) contains two identical copies of HIV-RNA which are covered by the nucleocapsid protein (NC, p7). Viral integrase (IN, p32), reverse transcriptase (RT, p66) and protease (PR, p12) are located together with the HIV-RNA as the process of reverse transcription is happening in the capsid. Modified from (http://biodidac.bio.uottawa.ca).

1.3 HIV life cycle and cellular restriction factors

During HIV infection at the level of a cell, host defense mechanisms compete with viral counterparts, and dampen down virus expansion. The HIV life cycle is divided into several stages **(Figure I4)**. The first step is an interaction between the host cell and the virus followed by virus entry into the cell. HIV glycoprotein gp120 interacts with a CD4 receptor expressed on the surface of the host cell (Dalgleish et al. 1984). CD4 T lymphocytes and macrophages have been identified as major targets for HIV (Gendelman et al. 1990; Shioda, Levy, and Cheng-Mayer 1991). Although the CD4 receptor is an essential factor in the interaction between a host cell and HIV, additional cellular co-receptors are also required. Small proteins, CCR5 and CXCR4, have been identified to interact with gp120 and thus permit HIV to finally enter a target cell (Moore, Trkola, and Dragic 1997). CCR5 is mainly expressed on memory CD4 T cells and macrophages while naive CD4 T cells express CXCR4 (Kitchen and Zack 1999; Zhang et al. 1998). Once HIV is attached to the target cell, gp120 changes its conformation and enables the fusion of the viral and cell membranes via gp41 (Weissenhorn et al. 1997; Sherer, Jin, and Mothes 2010; Wilen, Tilton, and Doms 2012). The virion content is then delivered into the cell. At this step, the cellular restriction factor TRIM5α (tripartite motif 5 alpha protein) detects viral capsid structures and triggers immune defense mechanisms to destroy it (Stremlau et al. 2006).

In the cytoplasm, the viral capsid is uncoated and the viral reverse transcriptase (RT) converts two copies of HIV single-stranded (ss)RNA to one linear double-stranded (ds) DNA. The reverse transcription depends on the presence of deoxynucleotide triphosphates (dNTPs) (Meyerhans et al. 1994). The cellular factor SAMHD1 (sterile alpha motif and histidine/aspartic domain-containing protein) can repress this step by downregulation of dNTPs (Schaller, Goujon, and Malim 2012; Goldstone et al. 2011). RT uses a cellular Lys3 tRNA as a primer to start the process of reverse

transcription. The tRNA is complementary to a sequence called primer binding site (PBS) within the 5´- region of the HIV genome. DNA synthesis begins and first generates an RNA-DNA duplex from which the viral RNase H removes the RNA part of the duplex. The viral (-) cDNA strand is then completed after strand transfer to the complementary R region at the 3´end of the viral RNA genome and further polymerisation. The (+) DNA synthesis is initiated from the RNA polypurine tract that is more stable against RNAse H breakdown (Hu and Hughes 2012a). Once ds HIV DNA synthesis is completed, it is translocated to the nucleus and used as a substrate for chromosomal integration. Import of ds HIV DNA to the nucleus can be suppressed by cellular myxovirus resistance protein B (MxB) (Goujon et al. 2013; Z. Liu et al. 2013). Without this restriction, viral integrase incorporates the viral dsDNA into the host chromosome. This so-called HIV provirus can then be activated and transcribed that finally will lead to new viral particles, or can remain silent in a latent form (Hu and Hughes 2012b; Bocharov et al. 2012). In case of productive infection, the HIV provirus is transcribed into mRNAs, and all viral proteins are translated in the cytoplasm. The cell tries to restrict this step by expression of Schlafen11 (SLFN11) which selectively inhibits translation of HIV proteins (M. Li et al. 2012). Once all viral components are produced, the assembly step starts. During this step, new virions are built. Assembling virions package two copies of viral RNA, structural proteins, viral enzymes and cellular tRNA (as a primer for DNA synthesis). As a cellular defense mechanism, apolipoprotein B mRNA-editing enzyme catalytic polypeptide-like 3G (APOBEC3G or A3G) can be also packed into the new virions. When a new target cell is infected with virions containing A3G, single-stranded DNA is deaminated at cytidine residues leading to hypermutated genes (Bishop et al. 2008; Harris and Liddament 2004; J. P. Vartanian et al. 1991).

New HIV virions bud from the cell through the cytoplasmic membrane as immature, non-infectious particles. Release of new viral particles can be restricted by bone marrow stromal antigen 2 (BST2/tetherin). The last step of the HIV life cycle is maturation of the immature particles. The viral protease cleaves Gag proteins which evokes the rearrangement of viral structural proteins. This changes the particle morphology and generates the typical conical capsid structure of lentiviruses, and leads to a clustering of the Env proteins on the virion surface (Mattei, Schur, and

Briggs 2016; Chojnacki et al. 2012). The mature HIV particles are infectious and can now start a new round of infection.

To counteract virus restriction by cellular factors, HIV uses its own proteins Vif and Vpu. They can target host restriction factors for degradation (Van Damme et al. 2008; Sheehy, Gaddis, and Malim 2003; Neil, Zang, and Bieniasz 2008; Neil et al. 2007).

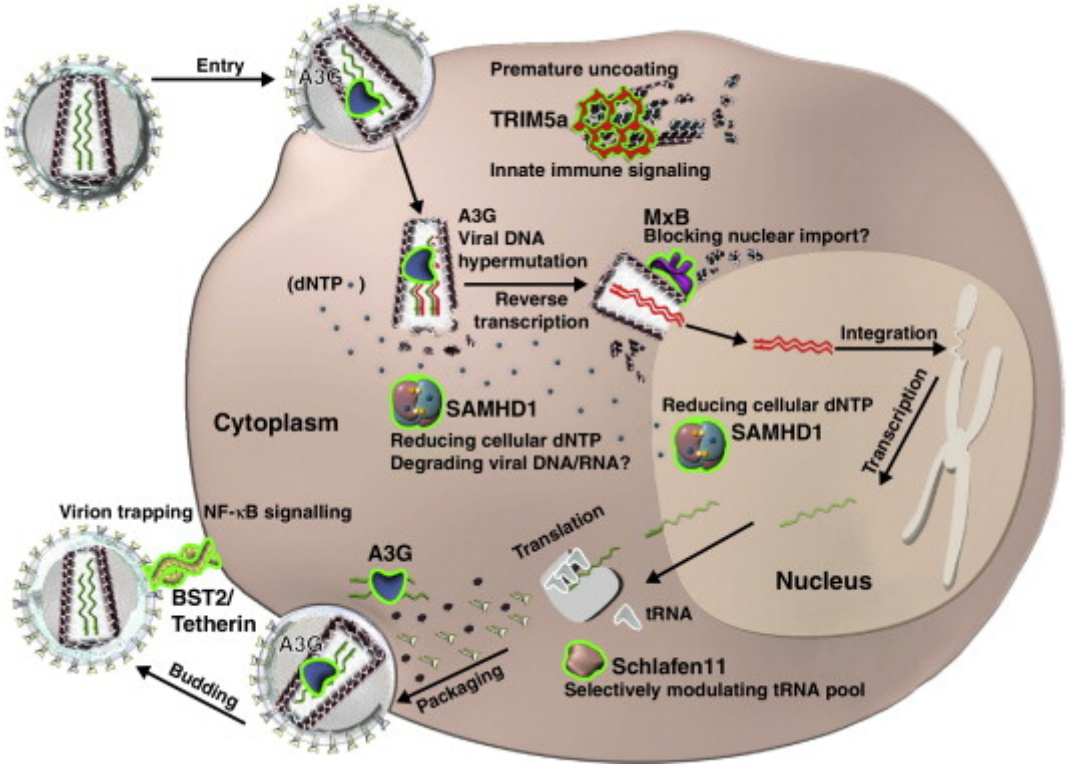

Figure I4. The restriction of the HIV life cycle by cellular restriction factors. Once HIV is attached to the CD4 receptor of a target cell, viral and cell membranes fuse and HIV enters the cytoplasm. At this step, TRIM5a recognizes viral capsid and evokes cell immune mechanisms. The HIV genome is transcribed by RT. The cell tries to suppress this process by A3G hypermutation on newly transcribed viral DNA or by a decrease of dNTP caused by expression of SAMHD1. Nuclear import and integration of HIV into the cell chromosome is inhibited by MxB protein. Schlafen11 affects the translation of HIV proteins. The late stages are repressed by A3G which is inserted into the new virions and BST2/Tetherin blocks the budding of the new virions. The figure is taken from (Jia, Zhao, and Xiong 2015).

1.4 HIV infection at the level of a host organism

During an HIV infection *in vivo*, the virus expands rapidly. Viral growth then activates host immune mechanisms including innate and adaptive responses (Katsikis, Mueller, and Villinger 2011; Stacey et al. 2009; Goonetilleke et al. 2009; Levesque et al. 2009; Kramer et al. 2010). Based on the CD4 T cell count and viral loads, different stages of an infection have been identified **(Figure I5)**. During the first couple of weeks of an HIV infection, viral load in the blood (viremia) reaches its peak which is associated with a decrease in CD4 T cells. These events characterize a primary HIV infection. Then, CD4 T cells slightly recover and viremia levels drop. A dynamic quasi-equilibrium between CD4 T cell counts and viral load is established which results in a long, asymptomatic infection phase that usually lasts for years. However, during this time, the CD4 cell counts in blood continue to decline. When CD4 T cells drop below 200 cells per microliter blood, a state defined as AIDS (Lloyd 1996), opportunistic infections become apparent and the health of the infected individual deteriorates due to opportunistic infections like those caused by *Pneumocystis jiroveci (former P. carinii), Mycobacterium tuberculosis, Candida albicans, Toxoplasma gondii*, diverse Herpesviruses or malignant diseases such as Kaposi´s sarcoma and non-Hodgkin´s lymphoma and others (Chereshnev et al. 2013).

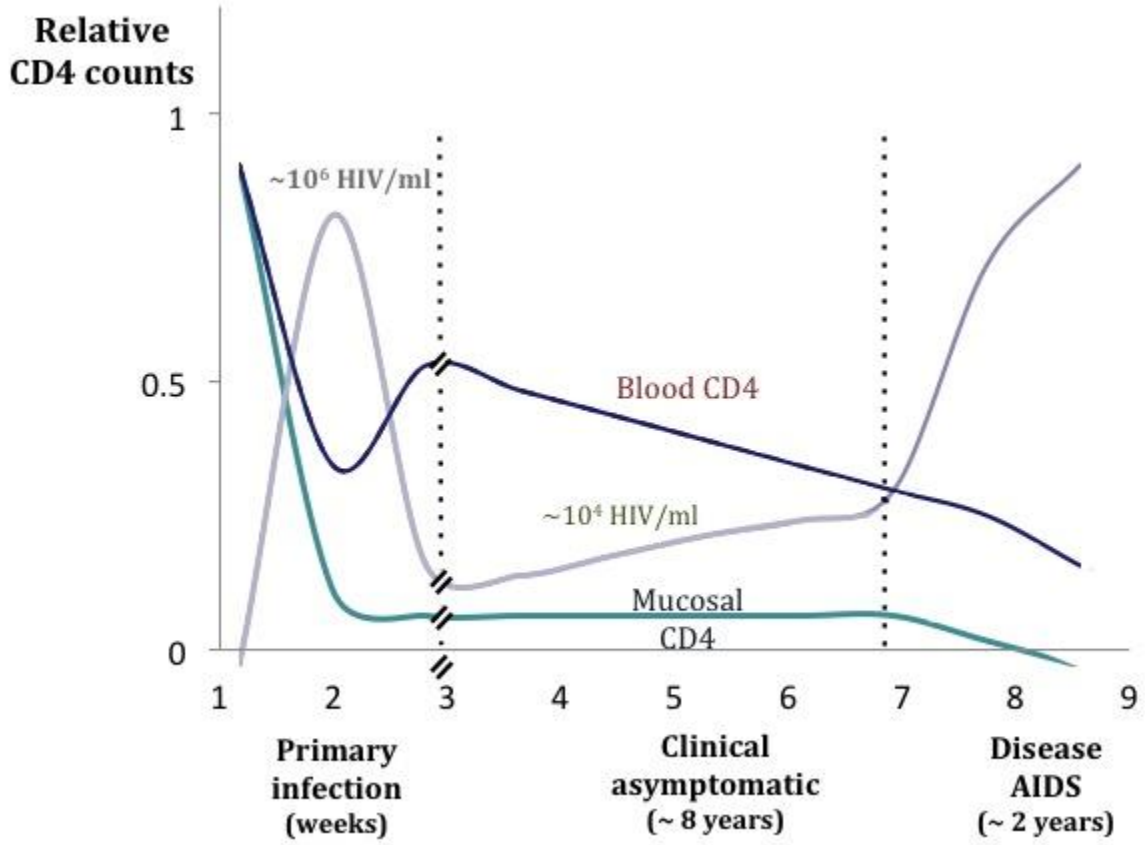

Figure I5. Characteristics of an HIV infection *in vivo*. HIV infection is divided into three clinical stages based on virus load (grey curve) in the blood and CD4 T cell counts (blue curve for blood CD4 T cells and green line for mucosal CD4 T cell). The typical features of a **primary infection** is a peak in viremia and rapid decrease in CD4 T cells. This stage lasts for a couple of weeks until CD4 T cells in blood slightly recover and viremia dropped down. Mucosal CD4 T cells remain at a low level. This is the **asymptomatic phase.** The last stage is the **AIDS disease phase**, which is defined as CD4 T cell counts below 200/mm^3 of blood. This phase is associated with opportunistic infections and various malignancies, and finally leads to the death of the infected individual. Figure is modified from (Bocharov et al. 2012).

2 HIV latency

The main obstacle in curing an established HIV infection is the reservoir of treatment-resistant, latently infected cells. HIV productive infection can be nowadays controlled by combination antiretroviral therapy (cART). cART is used as a combination of three or more drugs that suppress virus loads to below levels of detection (below 50 copies of HIV RNA/ ml of plasma). Under these conditions, HIV replication is well controlled and disease progression is inhibited (Hirsch et al. 1999; Perelson et al. 1997; Gulick et al. 1997). However, some of the infected cells are not

affected by cART. HIV persists in these cells in a latent form which is characterized by very low or no viral gene expression (Whitney et al. 2014; Davey et al. 1999). Upon cART interruption, HIV rapidly rebounds from this treatment-resistant latent reservoir and HIV disease progresses (Tae-Wook Chun et al. 1999).

2.1 HIV latency, forms and establishment

HIV latency development bears on the physiology of CD4 T cells (Bleul et al. 1997; Sengupta and Siliciano 2018). Following maturation in the thymus, naive CD4 T cells remain in a quiescent state until they encounter an antigen (Ag) and get activated through their T cell receptor (TCR) (Jenkins et al. 2001). After the drop of Ag i.e. when an infectious agent is controlled, most of the CD4 T cells undergo programmed cell death. However, a small fraction survives as memory cells and revert into a resting state. Modified gene expression patterns of these cells allow their long-term survival and their ability to be susceptible to Ag re-encounter (R. F. Siliciano and Greene 2011).

Two types of HIV latency has been defined, pre-integration and post-integration latency **(Figure I6)**. HIV infection of activated CD4 T cells results in integration of the viral genome into the host chromosome which is followed by replication and successful production of new viral particles. However, productive infection fails in resting CD4 T cells. Viral DNA may fail to integrate into the cell genome as a result of insufficient levels of deoxynucleotide triphosphates, essential for the import of the viral genome into the nucleus (Bukrinsky et al. 1991; Korin and Zack 1999; T. C. Pierson et al. 2002). Another study suggested that restriction of integration is due to incomplete reverse transcription (Zack et al. 1990, 1992). The non-integrated HIV genome is unstable with a fast decay (Y. Zhou et al. 2005). However, if infected resting CD4 T cells become activated, HIV pre-integration complex-containing cells can complete the HIV life cycle and subsequently produce virus progeny. Thus, HIV may establish a state of pre-integration latency in resting CD4 T cells that can convert into a productive infection upon T cell stimulation (T. C. Pierson et al. 2002). Due to the short half-life of the non-integrated viral genome, pre-integration latency is not considered as the main barrier for HIV eradication (Marsden and Zack 2010).

The second form of latency is established when HIV infects activated CD4 T cells and integrates into the host chromosome. Part of these infected cells may then revert into a resting state as part of their natural behavior during memory cell formation. This so-called post-integration latency may also occur when HIV infects resting CD4 T cells (Shan and Siliciano 2013; Marsden and Zack 2010). However, due to the low expression of the CCR5 coreceptor, the infection of these cells is usually less effective (Bleul et al. 1997; Maier et al. 2000). Another hypothesis suggests that if HIV infects CD4 T cells during their reversion into resting cells, the virus will be able to complete chromosome integration, but proviral gene expression may be restricted (Marsden and Zack 2010; Sengupta and Siliciano 2018; Murray et al. 2016).

Post-integration latency, and thus a stable virus reservoir, is established at an early stage of an HIV infection (Chomont et al. 2009; T. Pierson et al. 2000; T. W. Chun et al. 1998). As resting CD4 T cells naturally survive for long time periods, the major impediment to eradicate HIV is the stability of the HIV reservoir with a half-life ranging from 6 to 44 months. Based on this half-live, complete elimination of the HIV reservoir by decay under efficient cART would require more than 70 years (J. D. Siliciano et al. 2003; Finzi et al. 1997; Zhang et al. 1999; Ramratnam et al. 2000).

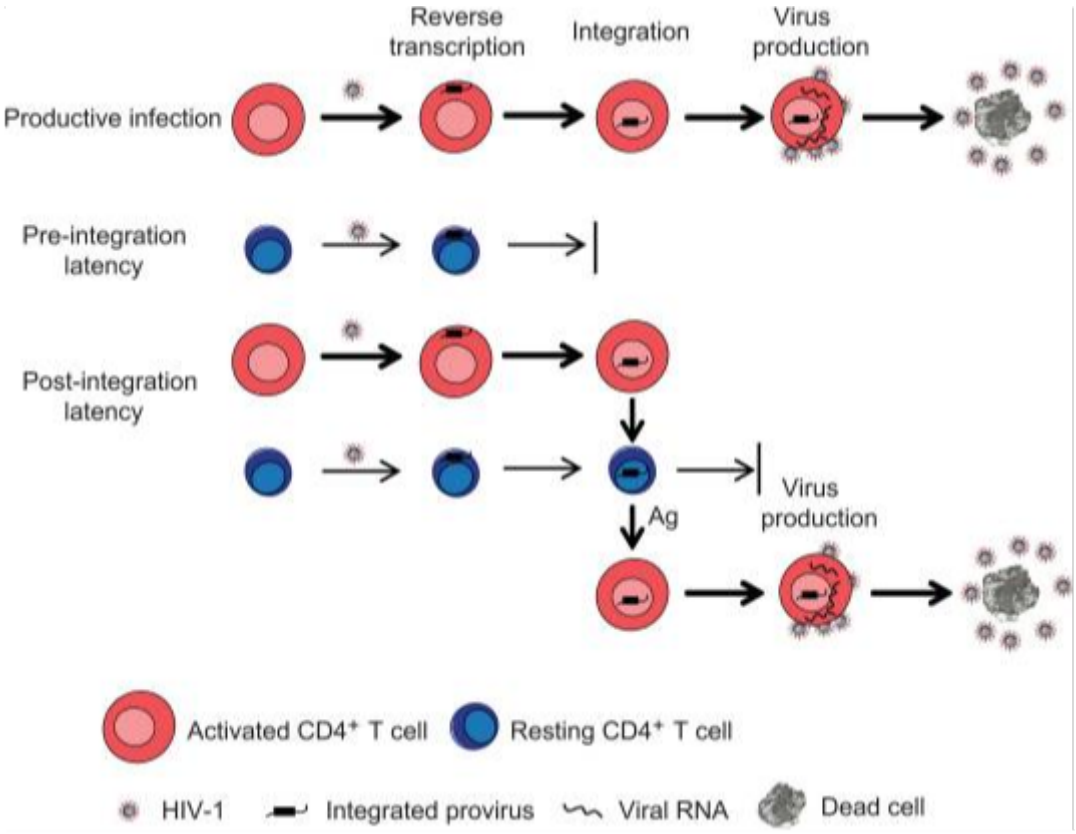

Figure I6. Scheme of HIV productive and latent infection. During HIV infection of activated CD4 T cells, HIV achieves all necessary steps which lead to virus production and possibly death of infected cells (productive infection). Apart from productive infection, two forms of latency exist: Pre-integration latency is established when HIV infects resting CD4 T cells, but HIV fails to integrate into the host genome. It is labile form of latency and eases with time. Post-integration latency is caused when HIV infects activated CD4 T cells, and completes provirus formation while these cells revert to a resting state in which gene transcription is shut down. HIV can also infect resting CD4 T cells and complete provirus integration albeit at low efficiency. Once latently infected resting CD4 T cells encounter an antigen (Ag), they may get activated and produce HIV progeny. Figure is taken from (Shan and Siliciano 2013).

2.2 Strategies to eradicate HIV reservoirs

As current cART alone cannot cure an HIV infection, additional approaches to fight the HIV/AIDS pandemic have been designed. One of the proposed strategies is called “Kick and kill”. Latent HIV provirus is reactivated or “kicked” by latency-reversing agents (LRAs) which induce viral transcription and protein production. The host immune system will then be able to recognize viral antigens and eliminate, “kill”, reactivated cells via CTLs (Spivak and Planelles 2018; Shan et al. 2012; Castro-Gonzalez, Colomer-Lluch, and Serra-Moreno 2018). Different groups of LRAs have been classified according to their mechanism of action. (i) Protein kinase C (PKC)

agonists like bryostatin, prostatin or phorbol myristate acetate (PMA). They initiate NF-κB signaling by PKC pathway activation that enhances viral transcription (Rullas et al. 2004; Bullen et al. 2014). (ii) Histone deacetylase inhibitors (HDACi) like SAHA/vorinostat, romidepsin or panobinostat. Histone deacetylation of provirus-containing chromatin regions usually lead to inhibition of HIV transcription (Van Lint et al. 1996). Inhibition of histone deacetylation then reactivates HIV RNA synthesis as shown *in vitro* as well as *in vivo* (N. M. Archin et al. 2012; Nancie M. Archin et al. 2009; Ke et al. 2015). (iii) Disulfiram. This drug is usually used for alcoholic addiction therapy. In addition, it has been proven to reactivate latently infected primary cells through protein kinase B (Akt) pathway activation (Doyon et al. 2013). (iv) Bromo and Extra-terminal domain inhibitors (BETi) has been also classified as LRAs, but their mechanisms of action remain unclear (Castro-Gonzalez, Colomer-Lluch, and Serra-Moreno 2018). (v) In 2018, a new compound with latency reversal activity has been identified. Maraviroc, a novel LRA which binds to the CCR5 coreceptor and induces HIV transcription through NF-κB activation (Madrid-Elena et al. 2018). Even though this strategy seems to be working *in vitro*, there have been some difficulties in clinical trials. Different scientific groups are still trying to design the right combination of LRAs to achieve HIV reservoir reductions (Ho et al. 2013; Dolgin 2013; Laird et al. 2015).

An alternative approach, called “Block and lock”, has been described recently. The aim of this strategy is to “block” the HIV promoter by using latency-promoting agents (LPAs) and then secure the shut-off or “lock” of HIV transcription. Various compounds are being tested for use in this procedure - Levosimendan (Hayashi et al. 2017), telomerase-derived peptide G1V001 (Kim et al. 2016), or Curaxin 100 and Didehydro-Cortisatin repressing the step of transcriptional elongation (Jean et al. 2017; Mousseau et al. 2015). It is still unclear how LPAs can effectively target the latently infected cells, hence more detailed studies are required in this area (Castro-Gonzalez, Colomer-Lluch, and Serra-Moreno 2018).

2.3 HIV latency maintenance and regulation

Within an adult organism, the T cell pool is maintained by antigen-driven proliferation or homeostatic proliferation (HSP) mediated by cytokines (Boyman et al. 2007). Interleukin 7 (IL-7) and interleukin 15 (IL-15) are mediating memory CD4 T cell homeostasis (Surh and Sprent 2008; Seddon, Tomlinson, and Zamoyska 2003). As memory CD4 T cells form the biggest part of the HIV reservoir, HSP has been suggested to be a major component of its maintenance (J. D. Siliciano et al. 2003; Chomont et al. 2009). Indeed, our own work and that of others suggest that HSP does not per se lead to re-activation of latent HIV or SIV (Tsunetsugu-Yokota et al. 2016a; Kumar et al. 2018). Thus, T cell homeostasis by HSP seems compatible with maintenance of the latent HIV reservoir (Surh and Sprent 2008; Seddon, Tomlinson, and Zamoyska 2003).

On the mechanistic level of a single HIV-infected cell, latency means lack of viral protein production. This may be due to inhibition of transcription or post-transcriptional blocks. The process of transcription can be silenced by (i) lack of transcription factors NF-κB or NFAT (nuclear factor of activated T cells) (Kinoshita et al. 1997; Nabel and Baltimore 1987), (ii) DNA methylation (Harbers et al. 1981; Lavie et al. 2005; Marsden and Zack 2010) or (iii) histone modification (Marsden and Zack 2010; Verdin, Paras, and Van Lint 1993). Other studies hint to post-transcriptional blocks in HIV latency. HIV cannot be efficiently reactivated from latently infected memory CD4 T cells (Mohammadi et al. 2014). Upon the treatment with SAHA and disulfiram, only the viral RNA level has been enhanced but protein expression remained low. A post-transcriptional block has also been described in naive latently infected CD4 T cells (Tsunetsugu-Yokota et al. 2016b). While viral protein expression remains low, HIV provirus transcripts have been found. Another study identified RNA surveillance protein UPF1 which stabilizes HIV RNA at post-transcriptional level (Ajamian et al. 2008). Depletion of UPF1 protein in latently infected J-lat cell line resulted in reduced viral RNA levels and thus attenuated HIV reactivation (Rao et al. 2018). According to all these facts, HIV latency is a process that might be controlled and regulated by various mechanisms (Marsden and Zack 2010; Kobayashi-Ishihara et al. 2018).

3 The Schlafen family

3.1 Characteristic of Schlafen genes (*Slfns*)

The Schlafen gene family has been discovered in 1998 as regulators of T cell maturation in mice. The name Schlafen, which in German means “to sleep”, was based on the observation that enhanced expression of *Schlafen1* (prototype in mice) resulted in G_0/G_1 cell cycle arrest (Schwarz, Katayama, and Hedrick 1998).

Slfns are broadly expressed genes, mostly conserved in human and mice. Ten mouse *Slfns* have been described (*m-Slfn1, m-Slfn1L, m-Slfn2, m-Slfn3, m-Slfn4, m-Slfn5, m-Slfn8, m-Slfn9, m-Slfn10* and *m-Slfn14*) clustered on chromosome 11 (Mavrommatis, Fish, and Platanias 2013a; Geserick et al. 2004a). There are six human *Slfns* (*h-Slfn5, h-Slfn-11, h-Slfn12, h-Slfn12L, h-Slfn13* and *h-Slfn14*) clustered on chromosome 17 (van Zuylen et al. 2011; Recher et al. 2014). Both, human and mouse *Slfns*, are divided into three groups according to the structure and size of the proteins they encode **(Figure I7)**. The shortest Schlafen proteins (SLFNs) with a molecular weight from 37 to 42 kDa belong to Group I (Bustos et al. 2009; Neumann et al. 2008). All SLFNs harbour an AAA domain that plays a role in ATP/GTP binding and a unique motif called “Schlafen box” whose function is not yet clearly understood. SLFNs with 58 to 68 kDa are in Group II while the longest SLFNs (~100 kDa) are part of Group III (Mavrommatis, Fish, and Platanias 2013b; Geserick et al. 2004b). Group II and Group III share the common SWADL domain. The function of this specific amino-acid motif (Ser-Trp-Ala-Asp-Leu) is unknown. Only the SLFNs from Group III contain a C’ terminal extension with a helicase domain corresponding to RNA/DNA helicases of superfamily I which are known to be involved in DNA and RNA metabolism (Mavrommatis, Fish, and Platanias 2013b; Geserick et al. 2004b; Patel et al. 2009). Mouse SLFNs are differentially localized in the cell. Group I and II SLFNs are cytoplasmic proteins while long SLFNs were found in the nucleus. This finding is also supported by the appearance of a nuclear localization sequence (NLS) in the C’ terminal extension of SLFNs from Group III. Similar studies about human SLFNs have not been reported yet (Neumann et al.

2008). Although the Schlafen protein family has been now studied for 20 years, information about this family is still incomplete.

3.2 Functions of Schlafen proteins

SLFNs are involved in multiple mechanisms in several cell types. **(i)** They play a role in cell proliferation and T cell differentiation. SLFN1 indirectly regulates the fate of NIH 3T3 cells by blocking the induction of cyclin D1 which is an essential factor for cell proliferation (Brady et al. 2005). SLFN2, 5, 8, 9 and 10 affect the cellular pathways that control T cell development and activation (Mavrommatis, Fish, and Platanias 2013c; Geserick et al. 2004a; Berger et al. 2010). **(ii)** SLFNs are associated with cancer. SLFN5 regulates the expression of matrix metalloproteinase genes and thus inhibits the aggressive growth and invasiveness of renal carcinoma cells (Sassano et al. 2015). SLFN11 was suggested as a novel biomarker for colorectal carcinoma treatment (Tian et al. 2014). It was also found to increase resistance to platinum-based chemotherapy in patients with lung cancer (Nogales et al. 2016). SLFN12 is affecting differentiation of prostate cancer cells (Kovalenko and Basson 2014) and its interaction with the phosphodiesterase 3A increases sensitivity to the DNMDP treatment in cancer cell lines (de Waal et al. 2016). **(iii)** SLFNs possess RNA cleavage activity. SLFN13 was termed RNase S13 because of its ability to cleave transfer (t)RNA and ribosomal (r)RNA. A structural study revealed that the N-terminus of SLFN13 cuts RNA at a specific cleavage site (Yang et al. 2018). Endoribonuclease SLFN14 was described as one of the main ribosome-associated proteins in rabbit reticulocytes. It preferentially cleaves rRNA over different kinds of RNA (Pisareva et al. 2015).

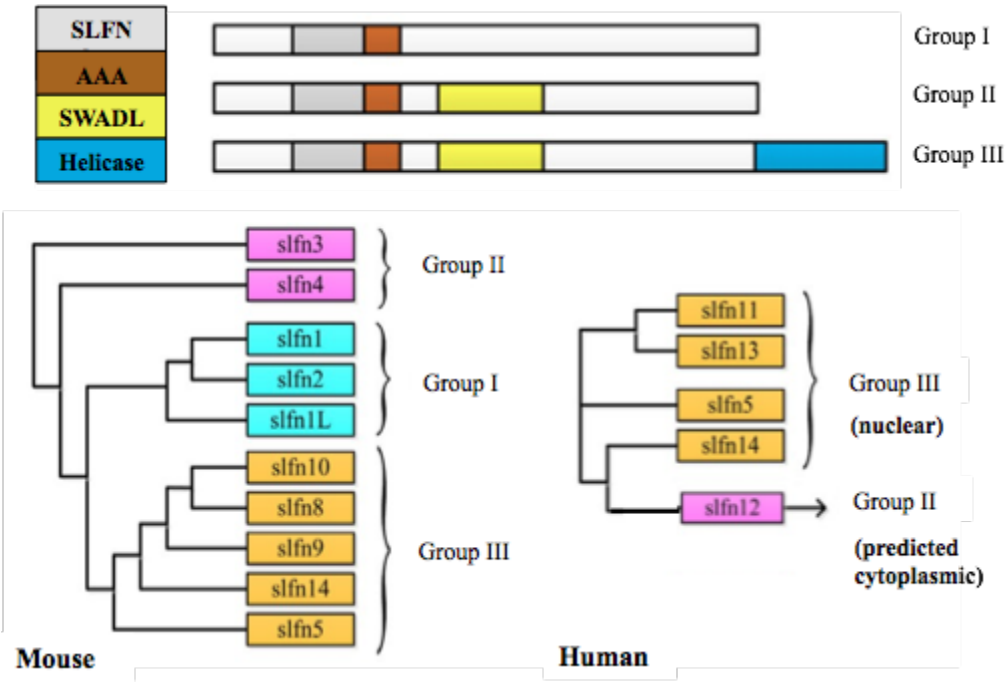

Figure I7. The Schlafen protein family of human and mouse: Schlafen genes are divided into three groups. Group I (in light blue colour) contain only mouse members (*Slfn1, Slfn2 and Slfn1L*). In Group II (purple) are two mouse members (*Slfn3 and Slfn4*) and human *Slfn12*. Group III (orange) has 4 mouse (*Slfn10, Slfn8, Slfn9, Slfn14 and Slfn5*) and 4 human Schlafen genes (*Slfn11, Slfn13, Slfn5 and Slfn14*). Human *Slfn12L* (green) does not belong to any group. All SLFNs contain an AAA domain (brown) and a SLFN box (grey) attached to it. The SWADL sequence (yellow) is shared between the members of Group II and III. Group III has an additional C-terminal extension with a helicase domain (dark blue). The figure is modified from (F. Liu et al. 2018).

3.3 Schlafen proteins suppress production of different viruses

Viral infection triggers type I interferon (IFN-I) production and signaling. Infected cells produce IFN-I when viral components are recognized. IFN-I then stimulates expression of many interferon-stimulated genes (ISGs). Products of these genes show antiviral activity (Schoggins and Rice 2011; Schoggins 2014; Calonge et al. 2017; Kane et al. 2016; Short 2009). As SLFN gene expression is also induced by IFN-I, SLFNs are categorized as ISGs (Mavrommatis, Fish, and Platanias 2013c; F. Liu et al. 2018). An antiviral activity of some of the SLFN proteins against RNA and DNA viruses has been demonstrated during the last years.

In 2012, human SLFN11 has been described as a novel host restriction factor which suppresses HIV-1 protein synthesis in a codon-usage-dependent manner (M. Li et

al. 2012). Later, it was found that human SLFN11 is also able to inhibit other retroviruses such as murine leukemia virus (MLV) and feline immunodeficiency virus (FIV) (Stabell et al. 2016). Therefore the antiretroviral effect of SLFN11 was classified as host-specific but virus-independent. This conclusion was supported by another study where broad screening of ISGs revealed macaque and human SLFN12 antiretroviral activity (Kane et al. 2016). Equine SLFN11 restricts late but not early proteins of equine infectious anemia virus (EIAV). This selective inhibition is based on codon optimality which confirmed the same mechanism as in the case of human SLFN11 (Lin et al. 2016). In 2017, inhibition of influenza wild-type PR8 virus (wtPR8) and varicella-zoster virus (VZV) by SLFN14 has been reported (Seong et al. 2017). The authors suggested a mechanism involving the enhancement of RIG-I-mediated IFN-beta signaling. Furthermore, in the same work, SLFN13 was also proven to suppress wtPR8. Most recently, the inhibitory effect of SLFN13 on HIV-1 and ZIKA virus production was shown (Yang et al. 2018). The authors proposed that SLFN13 might use nucleolytic activity to suppress HIV-1 replication. Together these data suggest that the SLFN protein family participates in the defence against a variety of viruses with diverse mechanisms.

OBJECTIVES

The process of homeostatic proliferation (HSP) contributes to the persistence of the HIV reservoir. While a dormant state of HIV provirus can be switched to productive infection in T-cell receptor (TCR)-activated memory CD4 T cells, HSP-cultured naive CD4 T cells are not susceptible to HIV reactivation. This might be due to distinct mechanism of HIV reversal in HSP-cultured cells. This thesis has 3 objectives:

1. To identify differentially expressed genes in HSP-cultured naive CD4 T compared to TCR-activated memory CD4 T cells that may restrict HIV protein production.
2. To characterize the mechanism of action of potentially novel HIV restriction factors.

MATERIALS AND METHODS

1. Cell culture

ACH2 cells (NIH AIDS Reagent Program) were cultured in RPMI medium (Gibco) supplemented with 10% heat-inactivated fetal bovine serum (FBS, Sigma Aldrich) and 1% of penicillin/streptomycin mix (P/S, Gibco). HEK293T cells (ATCC) and TZM-bl cells (NIH AIDS Reagent Program) were maintained in DMEM medium (Gibco) supplemented with 10% heat-inactivated FBS and 1% P/S. All cell types were incubated at 37ºC in presence of 5% CO_2.

2. Naive CD4 T cells isolation and cultivation

Peripheral blood mononuclear cells (PBMC) from three healthy donors (two males and one female) were isolated from blood samples of healthy donors by Histopaque-1077 density centrifugation. Briefly, the blood was diluted 1:1 in PBS (Lonza) and layered over Histopaque solution (Sigma-Aldrich) in a ratio 1:3. Then the 20 minutes centrifugation was performed at 600g and room temperature without break. After centrifugation, PBMCs were washed in PBS twice. From enriched PBMCs, CD4 T naïve cells were isolated using the Naïve CD4 T cell Isolation Kit II (Miltenyi Biotec) following the manufacturer's instruction. Purified naive CD4 T cells were cultured under 4 different conditions for 13 days: HSP condition – cell cultured with IL-15 and 7 (10 µg/ml, PeproTech), HSP+TCR condition – cells cultured with IL-15 and 7 and activated by anti-CD3 (5 µg/ml, BD Biosciences) and CD28 (1 µg/ml, BD Biosciences) on day 12, TCR condition – cells activated with anti-CD3/CD28 on day 0 and cultured with IL-2 (2 ng/ml, PeproTech), TCR+TCR condition – cells activated with anti-CD3/CD28 on day 0, cultured with IL-2 and second time activated with anti-CD3/CD28 at day 12.

3. RNA-sequencing and bioinformatic analysis

Total RNA from cultured cells was isolated according to the manufacturer's instructions using Qiagen RNeasy Micro kit (Qiagen). RNA was submitted for sequencing to Genomics Unit of Centre for Genomic Regulation (CRG, PRBB). The

quality and concentration of RNA were determined by an Agilent Bioanalyzer. Sequencing libraries were obtained after removing ribosomal RNA by a Ribo-Zero kit (Illumina). cDNA was synthesized and tagged by addition of barcoded Truseq adapters. Libraries were quantified using the KAPA Library Quantification Kit (KapaBiosystems) prior to amplification with Illumina's cBot. Four libraries were pooled and sequenced (single strand, 50nts) on an Illumina HiSeq2000 sequencer to obtain 50-60 million reads per sample. RNA-seq reads were mapped against the *Homo sapiens* reference genome (GRCh37.p13) with the GEMtools RNA-seq pipeline (http://gemtools.github.io/docs/rna_pipeline.html). Genes were quantified with the same pipeline with using the Gencode version 19 as an annotation. Normalization was performed with the edgeR TMM method (Robinson and Oshlack 2010). Differential expression analysis was performed with the 'robust' version of the edgeR R package (X. Zhou, Lindsay, and Robinson 2014). Genes with a false discovery rate (FDR)<5% were considered significant. Gene ontology (GO) enrichment analysis was performed with DAVID (http://david.ncifcrf.gov/) (Huang, Sherman, and Lempicki 2009).

4. RNA extraction and quantitative PCR

Total RNA was extracted from cells and treated with DNase I according to the manufacturer's instructions using Qiagen RNeasy Mini Kit (Qiagen). 100 to 1000 ng RNA was reverse-transcribed into cDNA in total volume of 20 µl using SuperScript IV Reverse Transcriptase (ThermoFisher). 2 µl of cDNA was used for quantitative PCR (qPCR) in 10 µl reaction mix with 2 µl of 2 µM forward and reverse primers and 5 µl of 2x SYBR master mix (ThermoFisher). Each reaction was performed in triplicates in 348-well plate (Life Biotechnologies) in a QuantStudio 12K flex (ThermoFisher) using the following parameters: 2 min 50ºC, 95ºC 10 min, 40 cycles of 15 sec at 95ºC and 60 sec at 60ºC. Primers were designed using the program Primer Express 3.0 (Applied Biosystems) and obtained from Biomers. Sequences of the primers used in qPCR reactions can be found in **Table M1.**

Table M1. A list of primers used in qPCR reactions.

Gene	Strand	Sequence
Slfn5	Forward	5′-caa gcc tgt gtg cat tca taa-3′
	Reverse	5′- tct gga gta tat acc act ctg tct gaa-3′
Slfn11	Forward	5′-tgc agt ccc tcg tga ttg tc-3′
	Reverse	5′-atc tca tac tgc tgg gct gtg a-3′
Slfn12	Forward	5′-tgt ttg cta aag agc ctg att cc-3′
	Reverse	5′-ttt ggt tca gcc tcc acc at-3′
Slfn13	Forward	5′-gag aaa atg atg gac gca gat-3′
	Reverse	5′-aga ctc aaa ggc ctc agc aa-3′
Slfn14	Forward	5′-ggt ggt cat gat gct gga ta-3′
	Reverse	5′-tga tga aat cag gca aga gtt g-3′
eGFP	Forward	5′-cag cag aac acc ccc atc-3′
	Reverse	5′-tgg gtg ctc agg tag tgg tt-3′
HIV-gag	Forward	5′-tgc atg ggt aaa agt agt aga aga ga-3′
	Reverse	5′-tga taa tgc tga aaa cat ggg ta-3′
HIV-gag (optimized)	Forward	5′-cat cta caa gcg ctg gat ca-3′
	Reverse	5′-gtc ttg aag aag cgg tcc ac-3′
HIV-RNA (total)	Forward	5′-gcc gcc tag cat ttc atc ac-3′
	Reverse	5′-aaa gct cga tgt cag cag tct t-3′

snoRNA	Forward	5´-cca cga gga aga gag gta gc-3´
	Reverse	5´-cac tca gac cgc gtt ctc tc-3´
18S RNA	Forward	5´-caa gac gga cca gag cga aa-3´
	Reverse	5´-ggc ggg tca tgg gaa taa c-3´

5. Cloning and plasmids

5.1 Construction of pmCherry vector expressing SLFN11/SLFN12

The original vectors encoding SLFN11/12 sequences were acquired from Dharmacon as glycerol stocks, clone MGS: 59997 (SLFN11) and clone MGS: 45076 (SLFN12). They were streaked on the agar plate and left overnight at 37ºC. Single colonies were taken and placed into 5 ml of LB media containing Ampicillin or Chloramphenicol, respectively (50 µg/mL) and cultures were left to grow overnight. Using the Plasmid Miniprep Kit (Qiagen) the plasmid DNA was isolated and used as a template to amplify the coding sequences of SLFN11/12. PCR reaction was performed in a total volume of 50 µl that includes 0.3 µg plasmid DNA, 1 µl of dNTP mix, 5 µl of 10x Pfu Buffer, forward and reverse primers at the concentration of 10 µM, and 0.5 µl of Pfu polymerase. Each reaction was performed in Peltier Thermal Cycler - 100 (BioRad) using the following parameters: Initial denaturation for 1 min at 95ºC, 35 cycles of 30 sec at 95ºC, 30 sec at 65ºC, 5 min at 74ºC, and final extension for 5 min at 74ºC. Sequences of the primers used in PCR reactions can be found in **Table M2**. PCR product was isolated from agarose gel by PureLink, Quick Gel Extraction Kit (Invitrogen) and cloned into pmCherry expression vector (ClonTech) in between NheI and HindIII restriction sites by overnight ligation of insert and vector in ratio 3:1, using T4 DNA Ligase (Promega). 2 µl of ligates was transformed into the 50 µl of DH5α competent E.coli cells (NEB) by heat-shock transformation strategy. Transformants were streaked on Kanamycin agar plates (50 µg/mL) and left overnight at 37ºC. Single colonies were taken and placed into 5 ml of LB media and cultures were left to grow overnight in the presence of Kanamycin (50 µg/mL).

pmCherry vectors encoding SLFN11 or SLFN12 (pmCherry-SLFN11/pmCherry-SLFN12) were prepared according to manufacturer's instructions using the Plasmid Miniprep Kit (Qiagen).

5.2 HIV-gag wild-type and HIV-gag optimized expressing vectors

The vector expressing HIV-1 wild-type gag sequence (pGag-wt) was a kind gift from Yasuko Tsunetsugu-Yokota (Yoshizawa et al. 2001). To generate HIV-1 codon-optimized gag expressing vector (pGag-opt), the plasmid p96ZM651gag-opt was obtained from NIH AIDS Reagent Program. We cut HIV-gag optimized sequence by BamHI and NotI restriction enzymes (NEB) and ligated into pEF-BOS_bsr (a kind gift from Yasuko Tsunetsugu-Yokota), keeping the ratio 3:1 (insert:vector).

5.3 Retrovirus vector expressing shRNA against SLFN11 or SLFN12

The short-hairpin RNA (shRNA) sequence against SLFN12 was designed by using BLOCK-iT™ RNAi Designer online tool (http://rnaidesigner.thermofisher.com/rnaiexpress). The shRNA sequence against SLFN11 was obtained from The RNAi Consortium (shRNA sequence #TRCN0000148990). Retrovirus vectors carrying the shRNA sequences were constructed by inserting annealed oligonucleotides into a pSIN-siU6 vector (Takara) between BamHI and ClaI restriction sites. As a negative control pSIN-siU6 vector expressing shRNA scramble sequences was used (a kind gift from Dr. Yamagishi). Specific shRNA sequences against SLFN11 and SLFN12 can be found in **Table M3**.

6. Transfection of HEK293T cells

In order to overexpress specific genes, HEK293T cells were seeded in 24-well plate (Greiner Bio-One) with density 2.5 x 10^5, and after 24h co-transfected with construct pmCherry-SLFN11/ pmCherry-SLFN12 (500 ng/well) along with vector HIV-pNLE (500 ng/well, a kind gift from Yasuko Tsunetsugu-Yokota), or with pGag-wt/ pGag-opt (250 ng/well) together with construct pmCherry-SLFN11/ pmCherry-SLFN12 (250 ng/well) using Lipofectamine 2000 (2.5 µl/well, Invitrogen). A 6h post

transfection fresh medium was replaced and the cells were kept at 37ºC with 5% CO_2 for 24 or 48 hours.

Table M2: A list of primers used in PCR reactions.

Gene	Strand	Sequence
Slfn11	Forward	5´-gat ccg cta gca tgg agg caa atc agt gcc ccc tgg ttg-3´
	Reverse	5´-att cga agc tta tgg cca ccc cac gga aaa ata tac ag-3´
Slfn12	Forward	5´-atc cgc tag cat gaa cat cag tgt tga ttt gga aac gaa tta tg-3´
	Reverse	5´-ttc gaa gct tgg tga gcc ttc gac aag att taa aca tc-3´

Table M3. A list of shRNA sequences cloned to prepare retrovirus encoding shRNA against SLFN11 and SLFN12.

shRNA	Strand	Sequence
Slfn11	Top	5´-gat ccg ctc aga att tcc gta ctg aac tcg agt tca gta cgg aaa ttc tga gct ttt tta t-3´
	Bottom	5´-cga taa aaa agc tca gaa ttt ccg tac tga act cga gtt cag tac gga aat tct gag cg-3´
Slfn12	Top	5´-gat ccg cag aat ggt aac tac ttt ctc gaa aga aag tag tta cca ttc tgc ttt ttt at-3´
	Bottom	5´-cga taa aaa agc aga atg gta act act ttc ttt cga gaa agt agt tac cat tct gcg-3´

7. DNA Sequencing

Sequences of constructs pmCherry-SLFN11 and pmCherry-SLFN12 were checked by Sanger sequencing in 96-capillary 3730xl DNA Analyzer (Applied Bioscience). The primers were designed using the program Primer Express 3.0 (Applied Biosystems), sequences can be found in **Table M4**. Six primers for pmCherry-SLFN11 and four primers to sequence pmCherry-SLFN12 have been used. The method was performed by Genomics Core Facility, UPF.

Table M4. A list of primers used in DNA sequencing reactions.

Gene	Primer number	Sequence
Slfn11	1	5´-cgc aaa tgg gcg gta ggc gtg-3´
	2	5´-ggt gta tac caa gag ctc cct aac tc-3´
	3	5´-aaa ggc ctg gaa cat aaa aag ga-3´
	4	5´-ctt act cgg ctt cag gtc tct ctt-3´
	5	5´-agg tat ttc ctg aag ccg aat g-3´
	6	6´-aca tgg cca tca tca agg agt t-3´
Slfn12	1	5´-cgc aaa tgg gcg gta ggc gtg-3´
	2	5´-ttg acc ttt act gaa tcc aca cat g-3´
	3	5´-agg gct cac tga tct tct cta gga-3´
	4	5´-atc ttg tcg aag gct cac caa-3´

8. Establishment of SLFN11 and SLFN12 knock-down ACH2 cells

To prepare recombinant retroviruses carrying the shRNAs, HEK293T cells were seeded in 6-well plate (Greiner Bio-One) with density 6 x 10^5 cells/well and co-

transfected with pSIN-siU6 - shSLFN11/ shSLFN12/ shSc (2 µg) along with plasmids pGP(1 µg, Takara) and pPE ampho (1 µg, Takara) using 12 µl of Lipofectamine 2000 per well. At 48h after transfection, the supernatant was harvested and added into ACH2 cells (1 ml of supernatant/10^5 cells). Transduction was done by spinoculation (1200 xg, 25ºC, 2h). Pelleted cells were resuspended in 500µl of RPMI with 10% FBS and placed into 24-well plate. Selection of the transduced cells was done by adding G418 (1 mg/ml, InvivoGen) into the cell at 48h after transduction. Cells were kept in culture for at least two weeks. SLFN11 and SLFN12 knockdown expression was validated by qPCR (as described above).

9. HIV reactivation in SLFN11 or SLFN12 knock-down ACH2 cells

ACH2 cells with blocked expression of SLFN11 and SLFN12 (as described above) were seeded in 24-well plate and treated with DMSO (0.01%, Sigma-Aldrich) or SAHA-Vorinostat (0.5 µM, Sigma-Aldrich). At 48h after treatment, some of the cells were lysed for RNA or protein isolation. At 72h after treatment, supernatants were harvested to test for virus titer by TZM-bl luciferase assay (as described below).

10. TZM-bl luciferase assay

Virus titers in supernatants from transfected HEK293T cells and HIV-reactivated ACH2 cells (as described above) were determined by the TZM-bl assay. The culture supernatants were filtered and pelleted by 4h centrifugation at 4ºC in pellet sucrose buffer (50 mM Tris-HCl (pH=7.4), 100 mM NaCl, 0.5 mM EDTA, 20% sucrose). Pellets were resuspended in 40 µl PBS. In total 11 serial dilutions of supernatants were prepared and added into fresh TZM-bl cells (10^4 cells/well) in 96-well flat-bottom culture plate (Greiner Bio-One). After 72h incubation at 37ºC, 5% CO_2 the luciferase activity was measured on Centro LB 960 Microplate Luminometer (Berthold Technologies) using Britelite Plus™ (PerkinElmer) according to the manufacturer's protocol. Based on the luciferase level $TCID_{50}$ was calculated.

11. Western Blot

The cells were lysed with 1x passive lysis buffer (Promega), fast-frozen in liquid nitrogen and kept at -80ºC overnight. Next day a cell debris was removed by centrifugation at full speed for 5 min and supernatants were mixed with 2x Leammli buffer, heated at 97°C for 5 min, transferred to the nitrocellulose membrane and proceed to immunoblot using specific antibodies. Detection was done by using secondary antibodies conjugated with horseradish peroxidase (HRP). Protein bands were developed on Medical X-Ray Blue Films (AGFA) using Pierce^{TM} ECL Plus Western Blotting Substrate or SuperSignal WestFemto Maximum Sensitivity Substrate (Thermo Scientific) and quantified in Image-J software. List of the antibodies used in the immunoblotting assay can be found in **Table M5.** HIV protein gp160 was detected and developed by using New LAV Blot I HIV diagnosis kit (BioRad), following manufacturer's instructions.

12. Polysome profiling

HEK293T were co-transfected with pmCherry/ pmCherry-SLFN11/ pmCherry-SLFN12 (12 µg) and HIV-pNLE (12 µg) using Lipofectamine 2000 (48 µl) in a T-150 culture dish (Thermo Fisher Scientific). In order to freeze elongation ribosomes, 48h after transfection cells were treated with 10 ml of DMEM containing cycloheximide (CHX, 100 µg/ml) during 2 min at 37ºC and washed with 10 ml of PBS containing CHX (100 µg/ml) using the vacuum system. Cells were lysed with 700µl of lysis buffer (10 mM Tris-HCl (pH=7.4), 10 mM MgCl2, 100 mM NaCl, 1% Triton X100, 2 mM DTT, 100 ug/ml CHX), scraped and immediately frozen in liquid nitrogen and stored at -80ºC. Cell lysates were thawed at 25ºC and centrifuged at 12 000 xg, 5min, 4ºC and the supernatants were transferred to new tubes. After quantification, aliquots of 8 UA_{260} were made and stored at -80ºC. Linear gradients of 10%-50% sucrose were prepared in polysome buffer (20 mM Tris-HCl (pH=7.4), 10 mM MgCl2, 100 mM NH4Cl). The Gradient Master (Biocomp) was used for making the gradients in polyallomer tubes (Beckman Coulter). One aliquot of 8 UA_{260} was loaded on each gradient and centrifuged in Beckman SW41 rotor at 35 000 RPM, 3h, 4ºC. Gradients were fractionated with fraction collector Model 2128 (BioRad). These fractions were

used for phenol: chloroform RNA extraction or TCA-acetone protein precipitation and analyzed by qPCR or Western Blot, respectively.

Table M5. A list of antibodies used for immunoblotting method.

Product Name	Company	Cat. Number
mCherry Polyclonal Antibody	ThermoFisher Scientific	PA5-34974
Anti-Glyceraldehyde-3-Phosphate Dehydrogenase, clone 6C5	Merck	MAB374
anti-HIV-1 p24 Monoclonal (91-5)	NIH	1238
anti-HIV-1 Nef Monoclonal (AG11)	NIH	1124
GFP Antibody (B-2)	Santa Cruz	sc9996
Amersham ECL Anti-Mouse IgG	GE Healthcare	NA931
Amersham ECL Anti-Rabbit IgG	GE Healthcare	NA934
Peroxidase-conjugated AffiniPure Goat Anti-Human IgG	Jackson ImmunoResearch	109-035-003

13. Separation of cytoplasmic and nuclear RNA

HEK293T cells were transfected with pmCherry/ pmCherry-SLFN11/ pmCherry-SLFN12 along with HIV-pNLE (as described above). At 24h after transfection the cells were lysed with lysis buffer (10 mM Tris-HCl (pH=7.5), 10 mM NaCl, 1.5 mM $MgCl_2$, 10 mM Vanadyl complex (NEB), 1% NP-40 (Sigma-Aldrich) and kept on ice

for 5 min. After centrifugation at 3000 RPM for 5 min at 4ºC, supernatant (cytoplasmic fraction) was transferred to a new tube and nuclear pellet was resuspended in the lysis buffer without Vanadyl complex and $MgCl_2$. To extract RNA from each fraction, an equal volume of Roti-Aqua-PCL (Carl Roth) was added and centrifuged at 16000 xg for 5 min at room temperature. The aqueous phase was transferred into a new tube and subjected to a chloroform extraction and ethanol precipitation. The ethanol precipitation was done by adding 0.3 volumes of 3 M Sodium Acetate, 3 volumes of 100% EtOH (Merck) and 1 µl of glycogen (Roche). After 15 min incubation at -80ºC, samples were centrifuged for 15 min at maximum speed at 4ºC. The supernatant was discarded and the pellet was resuspended in 1 ml of 70% EtOH, and proceed to a centrifugation for 5 min at maximum speed at 4ºC. The RNA pellet was dissolved in Diethyl Pyrocarbonate (DEPC)-treated water, and followed by TURBO DNA-free kit (Ambion) for DNA removal. Expression levels of HIV-gag RNA and total HIV RNA were analyzed by qPCR.

14. Calculating and visualizing a gene-wise codon adaptation index (CAI)

For all hg38 RefSeq genes, we used the seqinr (v.3.3-6) and ggplot2 (3.1.0) R-packages and codon weights obtained from CAIcal (http://genomes.urv.es/CAIcal/CU_human_nature).

RESULTS

1. SLFN12 is differentially expressed in naive CD4 T cells under HSP and TCR conditions

HIV latently infected naive and memory CD4 T cells behave differently towards latency reversal (Tsunetsugu-Yokota et al. 2016b). The dormant state of HIV proviruses cannot be switched to productive infection in HSP-cultured naive CD4 T cells, while TCR-stimulated memory CD4 T cells are susceptible to HIV reactivation. One way to decipher the mechanisms that contribute to the HIV refractory state of naive CD4 T cells cultured under homeostatic proliferation (HSP) conditions, is an analysis of their transcriptomic profile. Therefore we aimed to analyze genes that are differentially expressed (DE) in naive (HSP) compared to memory (TCR) CD4 T cells.

Naive CD4 T cells were purified from peripheral blood mononuclear cells (PBMC) of three healthy donors (Purity > 90%), and cultured under four different conditions: cells cultured with IL-7 and IL-15 (HSP-cultured naive CD4 T cells) before and after T-cell receptor (TCR) activation at day 12 (HSP and HSP+TCR cultures), and cells cultured with IL-2 after anti-CD3/CD28 activation (TCR-cultured memory CD4 T cells) before and after second TCR activation at day 12 (TCR and TCR+TCR cultures; **Figure R1 A**). At day 13, RNA was isolated and processed for transcriptome analysis by RNA-seq. From 16.380 genes mapped to the human reference genome database, we were looking for those that are differentially expressed in naive CD4 T cells under HSP condition compared to memory CD4 T cells with or without TCR stimulation. Based on fold change (FC) of these genes in both comparisons we classified them into two main groups (**Figure R1 B**): genes significantly upregulated in TCR-cultured memory CD4 T cells compared to HSP-cultured naïve CD4 T cells before and after TCR activation (Group I, 167 DE genes; **Table S1**), and genes upregulated in HSP-cultured naïve CD4 T cells compared to TCR-cultured memory CD4 T cells before and after TCR activation (Group II, 648 DE genes) (**Table S2**).

Analysis of genes from Group I that were highly upregulated in TCR-cultured memory CD4 T cells compared to HSP-cultured naïve CD4 T cells before and after

TCR activation (FC>2; **Table S3**), showed a significant enrichment on the terms like cell-cell signaling, immune response and regulation of T cell activation (**Table S4**). They contain genes such as *IL12a*, *Ccl17*, *Cxcl10* or *Hla-dqa1* that play roles in T cell regulation and T cell responses (Gately et al. 1991; Henry et al. 2008; Norose et al. 2011; Tree et al. 2004). From 648 DE genes in Group II, 304 were highly upregulated in HSP-cultured naive CD4 T cells compared to TCR-cultured memory CD4 T cells before and after TCR stimulation (FC<-2) (**Table S5**). Most of them are involved in defense and immune responses (**Table S6**). Interestingly, GO enrichment analysis showed an upregulation of 4 genes involved in TLR-signaling (*Tlr4*, *Tlr2*, *Irak2*, *Irak3*; **Figure R1 C**). These results are of particular interest since they indicate that HSP-cultured naive CD4 T cells might quickly induce an innate immune response upon TLR-mediated signaling that might contribute to the suppression of HIV-reactivation on these cells upon TCR stimulation. Further analysis of genes with FC<-2 from group II allowed the identification of 20 genes involved in transcription regulation. Some of them have been previously described to inhibit HIV infection or reactivation such as *RNase2* acting against viral single-stranded RNA (Rugeles et al. 2003; Bedoya et al. 2006), *Irf8* maintaining HIV latency by repressing IRF-1 mediated activation through the HIV-1 promoter (Munier et al. 2005), or *Tle1* and *Uaca* as repressors of NF-κB transcription (L. Liu et al. 2009; Ghosh et al. 2007); **Figure R1 C**). All together, these results show that HSP-cultured naive CD4 T cells have a transcriptional signature refractory to HIV infection and reactivation, even before TCR stimulation.

Restriction factors (RFs) affect different steps of the HIV life cycle (Jia, Zhao, and Xiong 2015), and therefore we focused on the analysis of RFs in our dataset. To note, *Apobec3g*, an HIV RF that induces mutation of viral single strand DNA during the process of reverse transcription (Bishop et al. 2008; Harris and Liddament 2004), was the only known RF significantly upregulated in HSP-cultured naive cells compared to memory CD4 T cells before and also after TCR stimulation. This is in concordance with previous results showing that *Apobec3g* expression is enhanced in presence of IL-7 and IL-15 (Stopak et al. 2007). Since previous results of ours strongly suggested a post-transcriptional block of HIV in HSP-cultured naive CD4 T cells (Tsunetsugu-Yokota et al. 2016b), we aimed to find potentially novel RFs repressing late stages of the HIV life cycle. Therefore we compare genes from Group

II to members of 16 gene families (**Table S7**) which contain HIV restriction factors. From 82 matching genes, only 28 were from the same families as RFs affecting HIV life cycle stages following transcription. Products of 22 of these genes have been previously described to interact with HIV proteins or indirectly influence HIV infection. To identify novel potential RFs suppressing HIV reversal from latency in HSP-cultured naive CD4 T cells, we focused on six genes which have not been previously reported to affect HIV (**Table S8**). *Bcl2l2* and *Spred1* are both from gene family of protein phosphatase 1 regulatory subunits. *Bcl2l2* encodes a protein that belongs to Bcl-2 proteins which are usually involved in apoptosis and cell survival regulation (Tsujimoto 1998). *Spred1* is a member of the family of Sprouty proteins and regulates activation of MAP-kinase signaling (Guy et al. 2009). *Ppp1r26* and *Ppp1r9A* are both regulatory subunits of protein phosphatase 1. *Plxnc1* is from the family of clusters of differentiation (CD) molecules. The protein belongs to plexins, transmembrane receptors that mainly influence cell motility (Roney, Holl, and Ting 2013). The last gene, *Slfn12* (**Figure R1 D**) is a member of a small family containing five genes that express Schlafen proteins (SLFNs). SLFN11 has been classified as RF repressing HIV protein translation (not found in our group II; (M. Li et al. 2012). Moreover, SLFN13 and SLFN14 attenuate production of different viruses (Yang et al. 2018; Seong et al. 2017). Based on this, we hypothesized that SLFN12 might be another member of the Schlafen family with antiviral activity. To verify differential expression of SLFN12 in HSP and TCR cultured CD4 T cells, we isolated naive CD4 T cells from PBMCs of 5 additional healthy donors and cultured them under the four different conditions (described in Figure R1 A). RNA was then extracted and SLFN12 mRNA quantified by qPCR (**Figure R1 E**). Our results were consistent with RNAseq data, therefore we moved to further experiments with a focus on the influence of SLFN12 on HIV production and latency reversal.

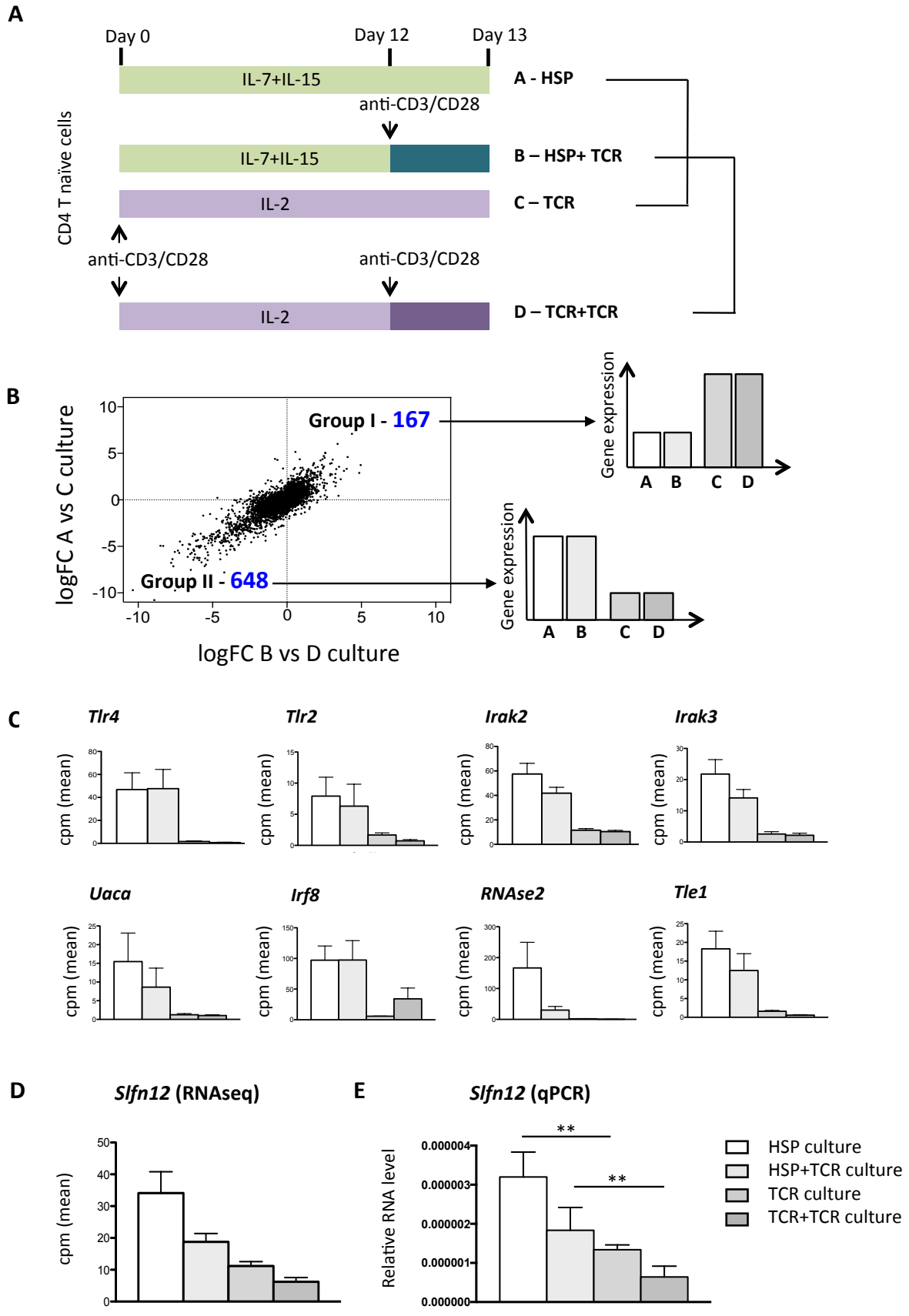

Figure R1. Differentially expressed genes in naive CD4 T cells cultured under HSP and TCR conditions. A - Naive CD4 T cells were cultured under four different conditions for 13 days: In

presence of IL-7 and IL-15 with or without activation by anti-CD3/CD28 at day 12 (A-HSP and B-HSP+TCR cultures). In presence of IL-2 after activation with anti-CD3/CD28 with or without second activation by anti-CD3/CD28 at day 12 (C-TCR and D-TCR+TCR cultures). At day 13 RNA was isolated and processed to transcriptomic analysis to analyze differentially expressed (DE) genes between cultures HSP and TCR and cultures HSP+TCR and TCR+TCR. B - Identification of different gene groups according to fold-change (FC) of DE genes. Group I - 167 DE genes with FC>0 in HSP compared to TCR culture before and after activation by anti-CD3/CD28. Group II - 648 DE genes with FC<0 in HSP compared to TCR culture before and activation by anti-CD3/CD28. The left part of the figure represents theoretical examples of gene expression pattern in each group. C - Genes highly upregulated (FC<-2) in HSP compared to TCR culture before and after activation by anti-CD3/CD28. D - Expression pattern of *Slfn12*. Error bars in figures C and D represent standard error of the mean (SEM; n=3; see Material and Methods section for details in bioinformatics analysis). E - mRNA levels of SLFN12 in naive CD4 T cells under four different conditions validated by qPCR. RNA levels were normalized to 18S rRNA levels. Error bars represent standard deviations (SD) in 5 additional healthy donors. ** $p \leq 0.01$; *** $p \leq 0.001$ (unpaired two-tailed t-test).

2. SLFN12 and SLFN11 inhibit HIV reactivation from latently infected ACH2 cells

The biggest impediment in HIV cure is the HIV reservoir formed by latently infected cells. These cells are resistant to antiretroviral therapy and they have a long half-life *in vivo*. One way to eradicate the latent reservoir is to reactivate the virus from the dormant state to produce viral progeny. Viral antigens will then be recognized by the immune system and CTLs will eliminate infected cells (Shan and Siliciano 2013). However, the efficiency of HIV reactivation *in vivo* is very low. This might be due to so far unknown regulators of HIV latency that have to be targeted in order to make latently infected cells more susceptible to HIV reversal. As the process of HIV latency is controlled by many factors and new ones are still to be discovered, we tested whether SLFN11 and 12 contribute to the maintenance of HIV provirus latent state.

First, we examined SLFN gene expression profiles in different cell lines (**Figure R2 A**). Comparing mRNA levels of different SLFNs in T cells (Jurkat, A3.01 and ACH2 cells) and embryonic kidney HEK 293T cells, we found that HEK 293T cells express only SLFN5 while SLFN13 was found in all tested cells. SLFN11 and 12 were expressed in Jurkat, A3.01 cells and in latent HIV provirus containing ACH2 cells. ACH2 cells have a similar expression pattern of SLFN11 and SLFN12 like naive CD4 T cells under HSP condition. Given that HSP has been suggested to maintain HIV

latent reservoir and that ACH2 cell line is a well-established model for HIV latency, we used these cells to study the effect of SLFN11 and SLFN12 on HIV reactivation from latently infected cells. Expression of SLFN14 was not found in any of the tested cell lines.

In order to establish ACH2 cells with knockdown expression of SLFN11 or SLFN12, we first produced recombinant retroviruses expressing shRNA against SLFN11 (shSLFN11), SLFN12 (shSLFN12-1/ shSLFN12-2) or scramble shRNA (shSc - mock). HEK293T cells were co-transfected with pSIN-siU6 vectors encoding specific shRNA sequences together with a plasmid expressing Gag-Pol and an amphotropic *env* expression vector. Supernatants were harvested and added in ACH2 cells for spinoculation. Transduced ACH2 cells, selected by G418 were then treated with an HDAC inhibitor, SAHA (also known as Vorinostat) to reactivate latent HIV provirus. DMSO treatment was used as a negative control (**Figure R2 B**). Expression of SLFN11 or SLFN12 was sufficiently suppressed by specific shRNA on mRNA level (**Figure R2 C**). After treatment with SAHA or DMSO, we took supernatants from ACH2 cells and titrated them in TZM-bl cells. We observed an enhanced HIV production in reactivated ACH2 cells with knock-down expression of SLFN11 or SLFN12 (**Figure R2 D**). Moreover, the translation efficiency of the HIV-p24 protein increased in ACH2 cells when SLFN11 and SLFN12 expression was diminished by shRNA knock-down (**Figure R2 E**). All together, these results show that SLFN11 and SLFN12 control HIV reversal from latently infected T cells by repressing the translation efficiency of the HIV-p24 protein.

Figure R2. SLFN11 or SLFN12 are involved in HIV latency maintenance. A - mRNA expression of SLFN family members in different cell lines and CD4 T cells under HSP and TCR condition normalized by 18S rRNA levels. B - Latently infected ACH2 cells were transduced with retrovirus expressing specific shRNA against SLFN11 (shSLFN11), SLFN12 (shSLFN12-1/ shSLFN12-2) or scramble shRNA (shSc). HIV was then reactivated with SAHA or DMSO (negative control) treatment in ACH2 cells with knockdown expression of SLFN11 or SLFN12. 72 hours post-reactivation, supernatants were harvested to measure HIV production. C - Knockdown efficiency of SLFN11 or 12 mRNA expression by specific shRNA. D - HIV reactivation from latently infected ACH2 cells with blocked SLFN11 or SLFN12 expression was significantly enhanced. Fold HIV reactivation has been determined by titration of supernatants in TZM-bl cells and normalized to the basal level (DMSO treated samples). Error bars in Figures C and D represent standard deviations (SD, n=3 or 4). Statistical analyses were done by one-way Anova test (*$p \leq 0.1$; ** $p \leq 0.01$; *** $p \leq 0.001$). E - Increased translation efficiency after HIV reactivation with SAHA in ACH2 cells with blocked SLFN11 or SLFN12 expression (representative example). HIV-p24 protein expression after SAHA treatment

was normalized to the basal level (HIV-p24 protein expression after DMSO treatment). Relative HIV-gag mRNA levels from SAHA treated cells were normalized to the basal level (relative HIV-gag mRNA from DMSO treated cells). Translation efficiency was calculated as a ratio of normalized HIV-p24 protein levels to HIV-gag mRNA normalized levels.

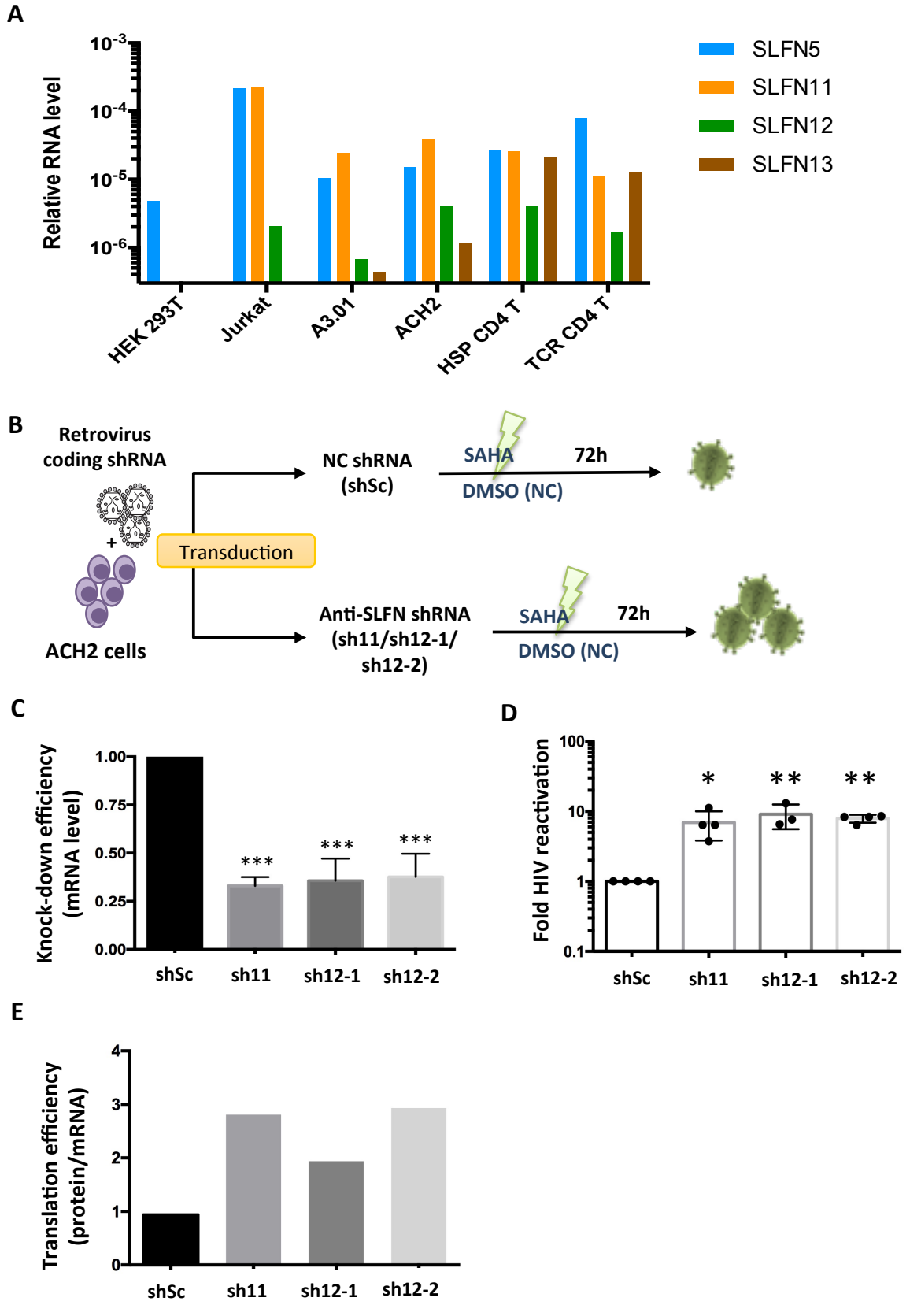

3. SLFN12 inhibits HIV production at the post-transcriptional level

Given that SLFN11 is an HIV restriction factor attenuating viral protein synthesis (M. Li et al. 2012), we aimed to test whether SLFN12 also influences HIV production. First, we constructed pmCherry expressing vectors encoding SLFN11 or SLFN12 (pmCherry-SLFN11/ pmCherry-SLFN12; **Figure R3 A**). E-coli was transformed with original plasmids encoding SLFN11 or SLFN12. DNA was isolated from single colonies and used as a template to amplify SLFN11 or SLFN12 sequence by PCR reaction. The PCR products were purified and cloned between the NheI and HindIII restriction sites of the pmCherry expression vector. SLFN11 and SLFN12 were separately fused into the mCherry protein using a natural linker (the detailed cloning strategy is described under Material and Methods).

In contrast to the knock-down experiment which we used to test the effect of SLFN11 and 12 on HIV latency, we here used an overexpression system. HEK 293T cell line does not express SLFN11 or SLFN12 (**Figure R2 A**). Therefore we co-transfected HEK 293T cells with pmCherry-SLFN11 (positive control), pmCherry-SLFN12 or empty pmCherry vector (mock) together with the HIV-NLE plasmid. 48 hours post-transfection, supernatants and cell lysates were collected and used for further analysis (**Figure R3 B**). Transfection efficiency was determined by mCherry protein levels from cell lysates (**Figure R3 C**). Like SLFN11, SLFN12 also affected HIV production. The HIV titer, as well as the HIV-p24 protein level in the supernatant, were strongly diminished by SLFN12 expression (**Figure R3 D**). Western blot analysis with specific antibodies also revealed that SLFN12, as SLFN11, inhibited expression of the gp160 envelope protein, the p24 Gag protein and the Nef accessory protein (**Figure R3 E**). We did not observe any changes in enhanced green fluorescent protein (eGFP) derived from pHIV-NLE or GAPDH which suggested that SLFN12 does not cause a global protein synthesis shutdown. No significant effect on spliced or unspliced HIV RNA was observed, demonstrating that SLFN12 does not influence HIV RNA processing (**Figure R3 F**). All together these results showed that SLFN12, like SLFN11, selectively inhibits HIV protein synthesis. Moreover, as HIV mRNA levels were not affected by SLFN11 or SLFN12, we suggest that both contribute to an HIV post-transcriptional block.

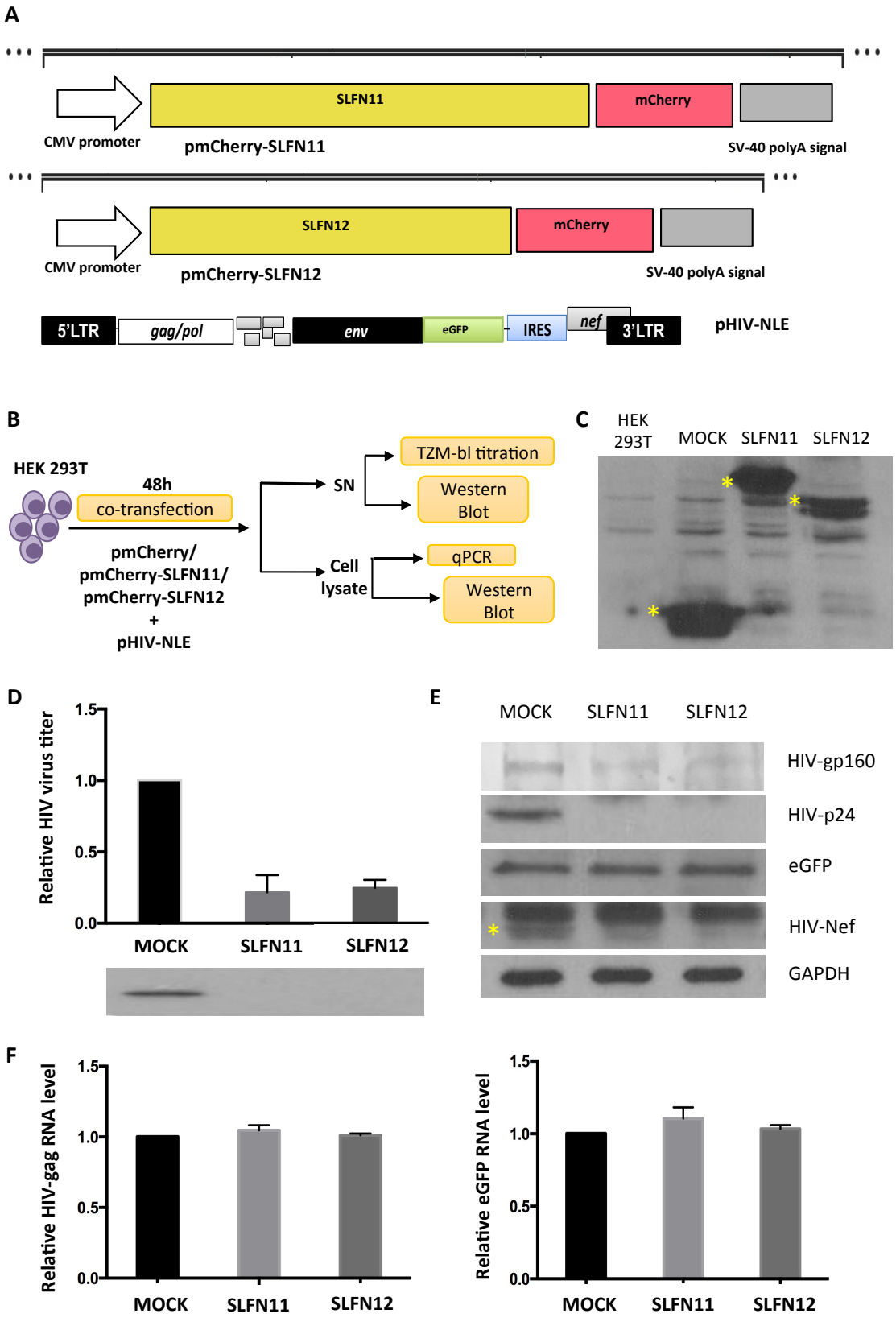

Figure R3. SLFN12 inhibits HIV protein synthesis without affecting HIV mRNA. A - Schematic maps of molecular plasmids used in following experiments. pmCherry vector encoding SLFN11 (pmCherry-SLFN11) or SLFN12 (pmCherry-SLFN12) with specific features (from left): CMV promoter in white, SLFN11/SLFN12 sequence in yellow, mCherry protein sequence in pink and SV-40 polyA

termination signal in grey. pHIV-NLE molecular strain from 5´end: long terminal repetition (LTR), gag/pol open reading frame (ORF), env ORF, eGFP sequence, internal ribosome entry site (IRES), gene nef and 3´LTR. B - HEK 293T cells were co-transfected with pmCherry-SLFN11/ pmCherry-SLFN12 or pmCherry empty vector (mock) along with pHIV-NLE. 48 hours after transfection, supernatants (SN) and cell lysates were collected and processed for further analysis. C - Transfection efficiency in HEK 293T cells. Western blot was from co-transfected HEK 293T cells was performed with a specific antibody against the mCherry protein. mCherry bands are highlighted with the yellow star. D - HIV virus production is attenuated by SLFN12 expression. Supernatants from HEK 293T co-transfected cells were titrated in TZM-bl cells and also analyzed by western blot for HIV-p24 protein levels. HIV titer obtained from mock-transfected HEK 293T cells was assigned to 1. E - Western blot from cell lysates of HEK 293T co-transfected cells. Specific antibodies against HIV-gp160, HIV-p24, eGFP, HIV-Nef (the band of Nef is highlighted with the yellow star, abundant band above is non-specific) and GAPDH were used. F - HIV mRNA levels are not affected by SLFN12 expression. RNA isolated from co-transfected HEK 293T cells was analyzed by qPCR for HIV-gag and eGFP mRNA expression. mRNA levels were normalized to 18S RNA expression in each condition. mRNA levels from mock-transfected HEK 293T cells were assigned to 1. Error bars in Figures E and F represent standard deviations (SD; n=3).

4. SLFN12 and SLFN11 do not affect export of HIV mRNA

HIV generates three different species of mRNA - unspliced, single spliced and double spliced. All of them encode HIV proteins. The unspliced mRNA is also used as genomic RNA. In order to produce viral progeny, all HIV transcripts have to be efficiently exported to the cytoplasm. Normally, the cell does not allow a release of unspliced and incompletely spliced mRNAs from the nucleus. However, to omit nuclear checkpoints of the cell, HIV encodes the regulatory protein Rev that binds nascent viral pre-mRNAs and thus ensures their sufficient export to the cytoplasm (Hope 1997).

To test whether SLFN11 or SLFN12 affect HIV RNA distribution within the cell, we co-transfected HEK 293T cells with SLFN11, SLFN12 or empty pmCherry expressing vector together with pHIV-NLE. 24 hours post-transfection, cells were lysed using NP-40 lysis buffer to separate cytoplasmic (supernatant) and nuclear (cell pellet) fractions. Next, we isolated RNA from both fractions and measured mRNA levels of specific genes by qPCR (**Figure R4 A**). The efficiency of RNA separation was verified by the levels of cytoplasmic 18S rRNA and nuclear U3 snoRNA (**Figure R4 B**). 18S rRNA was enriched in the cytoplasm by 79% and U3 snoRNA by 75% in the nucleus. We didn't observe significant differences of HIV-gag

or total HIV RNAs in the presence of SLFN12 or SLFN11 (**Figure R4 C**). Thus, the inhibitory effect of SLFN12 on HIV production is not a consequence of altered HIV RNA export within the cell.

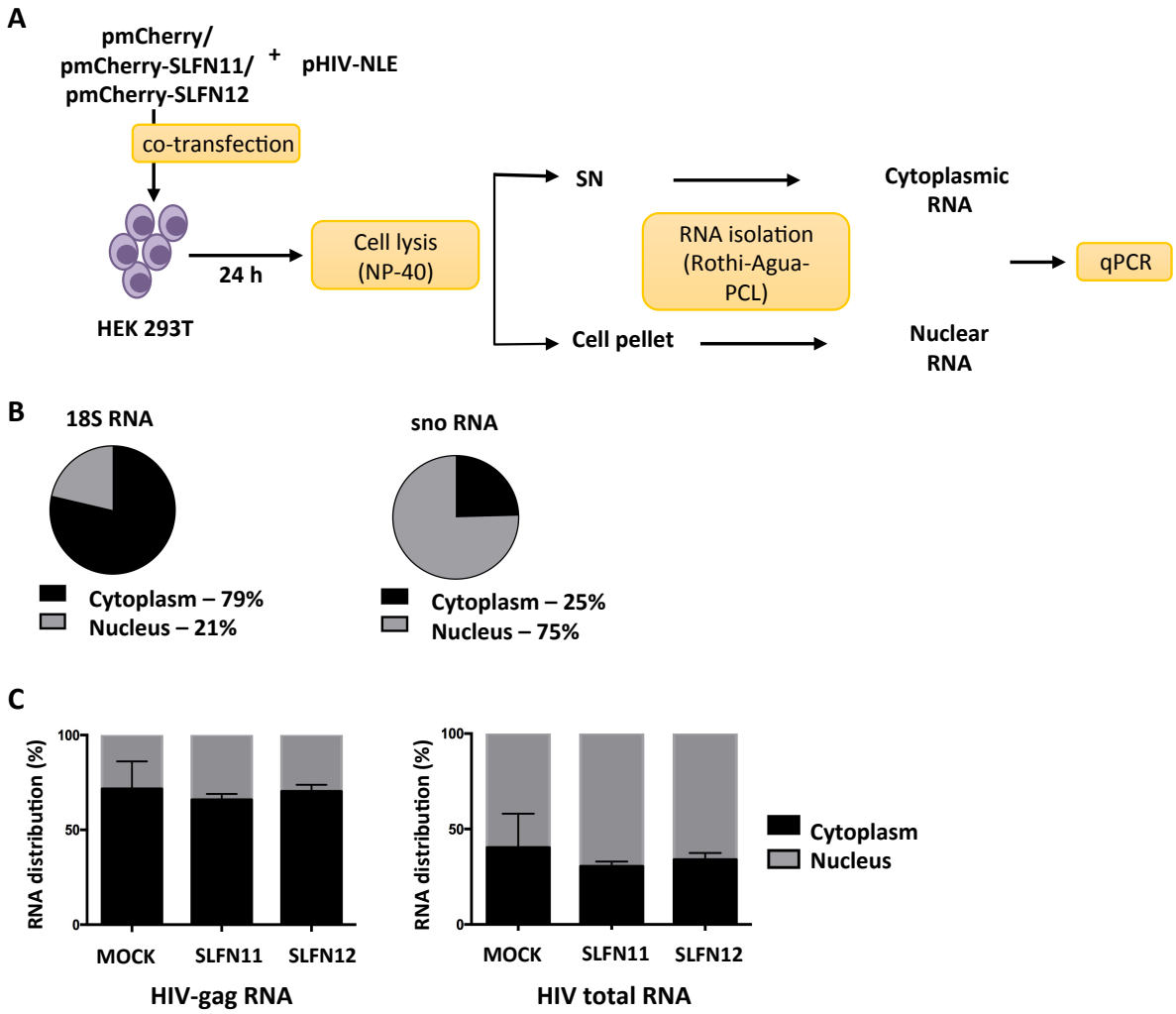

Figure R4. SLFN12 does not affect HIV RNA export from the nucleus. A - HEK 293T cells were co-transfected with pmCherry-SLFN11/ pmCherry-SLFN12 or pmCherry empty vector (mock) along with pHIV-NLE and lysed at 24 hours post-transfection. RNA was isolated from both, supernatant (cytoplasmic RNA) and cell pellet fraction (nuclear RNA) and analyzed by qPCR. B - Efficiency of separation of cytoplasmic and nuclear RNA. 18S RNA was used as a control for cytoplasmic RNA. U3 sno RNA was used as a control for nuclear RNA. Cytoplasmic and nuclear RNA distribution shown in percentage is calculated as an average of independent triplicates from mock-transfected HEK 293T cells. C - Distribution of HIV-gag RNA and HIV total RNA in transfected HEK 293T cells. The total amount of HIV-gag or HIV total RNA in both fractions (cytoplasmic and nuclear) was set to 100%. Error bars represent standard deviations of three independent samples. Statistical analyses were done by unpaired two-tailed t-test (not significant - ns).

5. SLFN12 selectively inhibits HIV-p24 expression in a codon-usage-dependent manner

The degeneracy of the genetic code allows that several synonymous codons can code for the same amino acid. However, some of these codons are more abundant than the others. The Codon Adaptation Index (CAI) is a general metric to analyze codon usage bias, based on codon frequency within the genome (P. M. Sharp and Li 1987). Genes enriched in highly frequent codons have generally higher CAI values (codon optimized genes) than genes with rare codons (non-optimized genes). When comparing the codon usage of wild-type HIV-1 proteins to RefSeq-based human coding sequences, it is apparent that all viral sequences harbour less optimal codons compared to most human transcripts as indicated by a lower CAI value (**Figure R5 A**). This is in concordance with the differences found in nucleotide sequences of human and HIV transcripts. While human genes are GC-rich, the HIV-1 genome has an unusual frequent use of adenosine in the third position of a codon (Keating et al. 2009; J.-P. Vartanian, Henry, and Wain-Hobson 2002). The A-rich codon-usage bias is mediated by G-to-A hypermutation which most probably occurs during the process of reverse transcription (Martinez, Vartanian, and Wain-Hobson 1994; J. P. Vartanian et al. 1997).

SLFN11 has been previously described to inhibit HIV translation in a codon-usage-dependent manner (M. Li et al. 2012). Therefore we compared the effect of SLFN12 on HIV-p24 protein production from wild-type (wt) and codon-optimized HIV-*gag* transcripts. HEK 293T cells were co-transfected with SLFN11 (positive control), SLFN12 or empty pmCherry vector along with a vector expressing HIV-*gag* wild-type sequence (pGag-wt) or HIV-*gag* sequence optimized to human codon usage (pGag-opt). Vector pGag-wt was a gift from Yasuko Tsunetsugu-Yokota, and pGag-opt was prepared by cloning the codon-optimized HIV-*gag* into the pEF-BOS_bsr vector. At 48 hours post-transfection, we analyzed protein and mRNA levels (**Figure R5 B**). Comparing to mock, SLFN12 strongly diminished translation of HIV-p24 protein transcribed from HIV-*gag* wt, however, protein expression in cells transfected with pGag-opt remained the same. We did not observe significant changes in HIV-gag wt or HIV-gag optimized mRNA transcripts caused by SLFN12 (**Figure R5 C and D**),

which confirms our earlier observation suggesting that SLFN12 inhibits HIV at the post-transcriptional level (Figure R3 E and F). Altogether these results demonstrated that attenuation of HIV protein production by SLFN12 is codon-usage dependent. The translation of mRNA transcripts with low CAI values is inhibited.

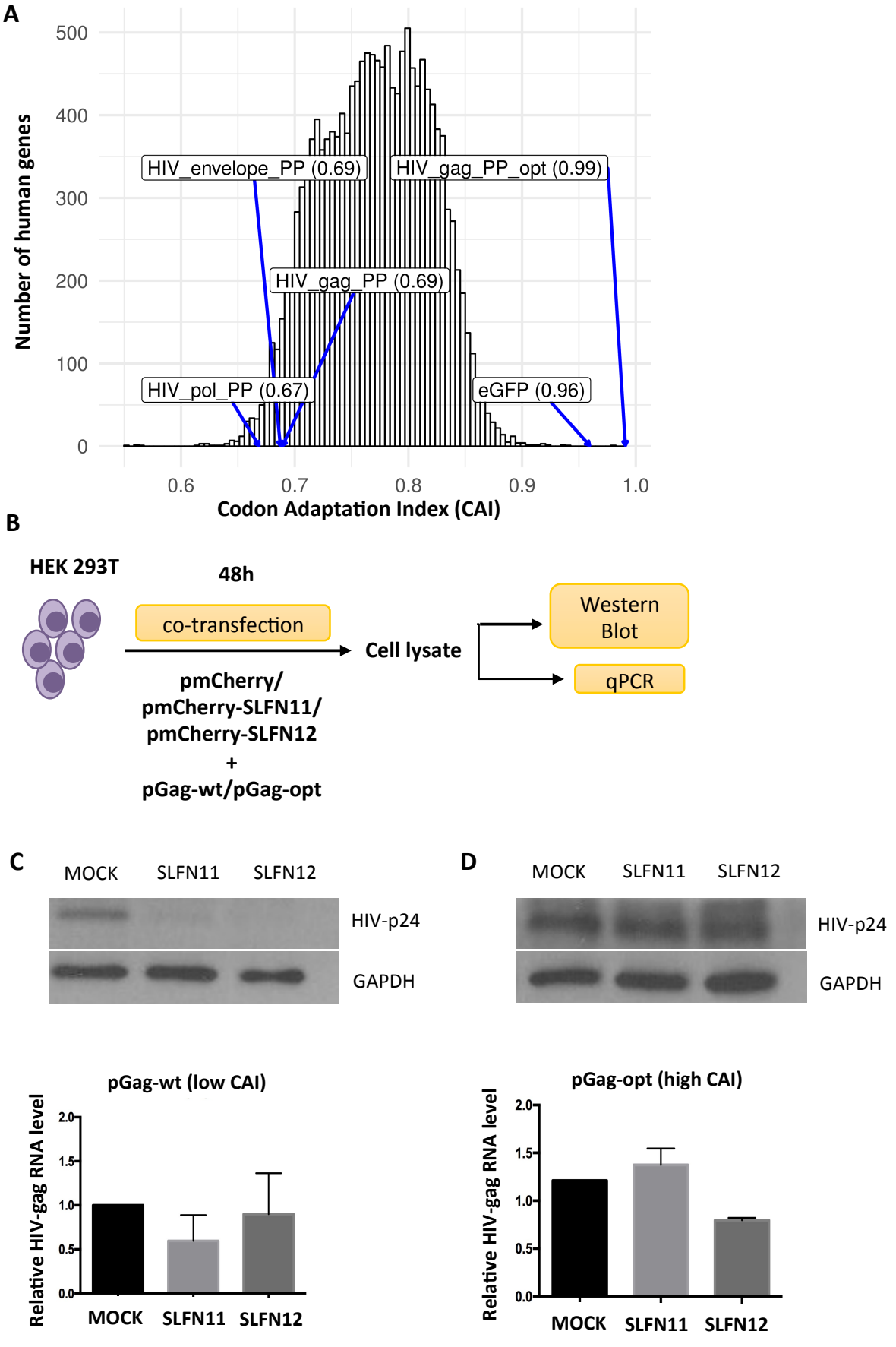
A
Number of human genes
500
400
300
200
100
0
HIV_envelope_PP (0.69)
HIV_gag_PP_opt (0.99)
HIV_gag_PP (0.69)
HIV_pol_PP (0.67)
eGFP (0.96)
0.6
0.7
0.8
0.9
1.0
Codon Adaptation Index (CAI)
B
HEK 293T
48h
co-transfection
pmCherry/
pmCherry-SLFN11/
pmCherry-SLFN12
+
pGag-wt/pGag-opt
Cell lysate
Western Blot
qPCR
C
MOCK
SLFN11
SLFN12
HIV-p24
GAPDH
D
MOCK
SLFN11
SLFN12
HIV-p24
GAPDH
pGag-wt (low CAI)
Relative HIV-gag RNA level
2.0
1.5
1.0
0.5
0.0
MOCK
SLFN11
SLFN12
pGag-opt (high CAI)
Relative HIV-gag RNA level
2.0
1.5
1.0
0.5
0.0
MOCK
SLFN11
SLFN12

Figure R5. SLFN12 preferentially inhibits translation of HIV-p24 from transcripts with low CAI value. A - Histogram of codon adaptation indices (CAIs) of hg38 RefSeq transcripts. CAIs of HIV sequences and eGFP are highlighted for comparison. PP - polyprotein; opt – codon optimized sequence. Mean CAI for RefSeq transcripts: 0.77. B - SLFN11, SLFN12 or empty vector pmCherry (mock) were expressed in HEK293T cells together with HIV vector expressing HIV-gag wild-type sequence (pGag-wt) or HIV vector expressing HIV-gag optimized sequence (pGag-opt). 48 hours post-transfection cells were lysed and analyzed by western blot and qPCR. C - SLFN12 inhibits HIV-p24 wt protein expression. Upper panel - Western blot detection of HIV-p24 protein from HEK 293T cells expressing HIV-gag wt sequence. Down panel - Relative HIV-gag wt mRNA levels. D - SLFN12 does not affect HIV-p24 opt protein expression. Upper panel - Western blot detection of HIV-p24 protein from HEK 293T cells expressing HIV-gag optimized sequence. Down panel - Relative HIV-gag optimized mRNA levels. In Figures B and C: GAPDH was used as endogenous control in the immunoblotting analysis. mRNA levels of HIV-gag wt/optimized were normalized to 18S RNA. Error bars represent standard deviations of three independent samples. Statistical analysis was done by one-way Anova test (not significant - ns).

6. SLFN12 and SLFN11 do not affect initiation of HIV translation

Our previous results showed that both, SLFN11 and SLFN12 preferentially inhibited HIV translation whose RNAs are enriched in non-optimal codons. Codon usage bias has been described to regulate protein translation and protein folding efficiency (M. Li et al. 2012; Akashi 1994; Gingold and Pilpel 2011; Spencer et al. 2012). Recent studies suggest that the elongation rate is increased by using optimal codons and decreased by rare non-optimal codons (Qian et al. 2012; G.-W. Li, Oh, and Weissman 2012; Yu et al. 2015). To determine which step of HIV translation is affected by SLFN11 or SLFN12, we performed polysome profiling analysis in HEK 293T cells overexpressing SLFN11 or SLFN12 together with the pHIV-NLE vector. Cells were then lysed, centrifuged on a sucrose gradient, fractionated and analyzed by qPCR and western blot (**Figure R6 A**). UV absorbance profiles showed no significant differences comparing mock- to SLFN11/SLFN12-transfected cells. Moreover, the monosomes to polysomes ratio (M/P) was also similar (**Figure R6 B and C**). These results indicated that SLFN11 and SLFN12 do not affect global translation. Analysis of HIV-gag RNA distribution in the different fractions showed a shift of HIV-gag RNA from light polysomes towards heavy polysomes upon SLFN11 or SLFN12 expression (**Figure R6 D**). These results suggested that SLFN11 and

SLFN12 do not affect HIV translation initiation but function in translation elongation. The increase of ribosomes per HIV RNA upon SLFN11 and SLFN12 expression could be explained with slow or stuck ribosomes which is in agreement with the enrichment of rare codons inside the HIV RNA. Western blot analysis revealed a different distribution of SLFN11 and SLFN12 proteins within the fractions (**Figure R6 E**). With this result, we concluded that both SLFNs bind to ribosomal subunits and complete ribosomes.

Figure R6. SLFN11 and SLFN12 do not affect initiation of HIV translation. A - SLFN11, SLFN12 or empty vector pmCherry (mock) were expressed in HEK 293T cells together with pHIV-NLE. 48 hours post-transfection cells were lysed and centrifuged on a sucrose gradient. Gradients were then fractionated and processed by qPCR and western blot, respectively. B - UV absorbance profiles at 260 nm of lysed HEK 293T transfected cells after centrifugation on a 10-50% sucrose gradient. C - Ratio between monosomes and polysomes calculated for each sample shows no effect of SLFN11 or SLFN12 on global translation. D - Sucrose gradient analysis of HIV-gag RNA in HEK 293T cells expressing SLFN11 or SLFN12. Distribution of normalized HIV-gag RNA levels in different fractions. Fractions were pooled in free proteins (mRNP) (1-7), single ribosomal subunits (40S+60S) (8-12), 80S monosome (13-17), light (18-23) and heavy polysomes (24-29). The total amount of HIV-gag RNA in all fractions was set to 100%. Error bars in Figures C and D represent standard deviations (SD; n=3). E - Western blot of SLFN11 and SLFN12 protein distribution among different fractions. Specific bands of SLFN11 and SLFN12 are highlighted with the yellow star. RLP 11 ribosomal protein has been used as a control in the immunoblotting analysis.

A

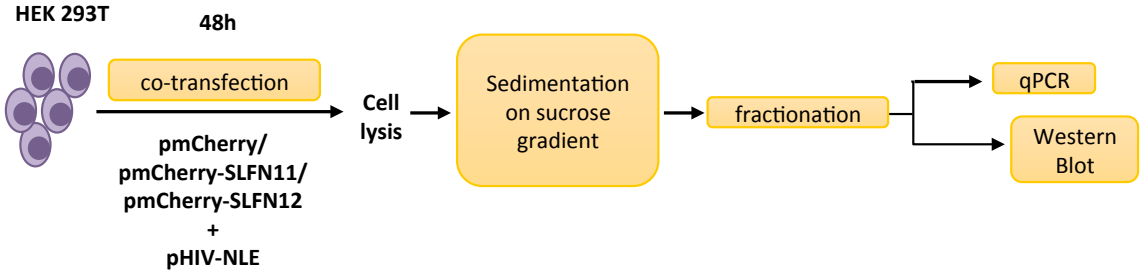

B

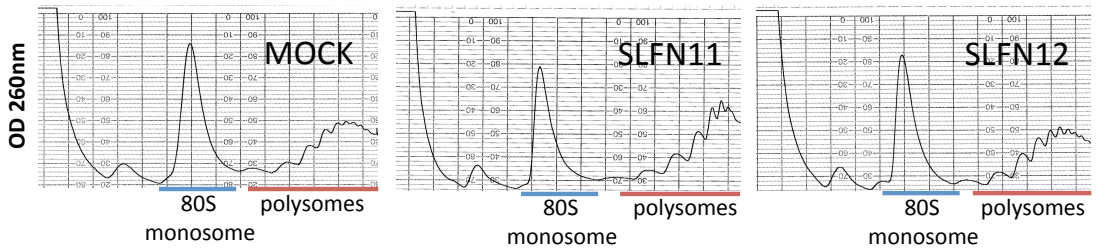

C

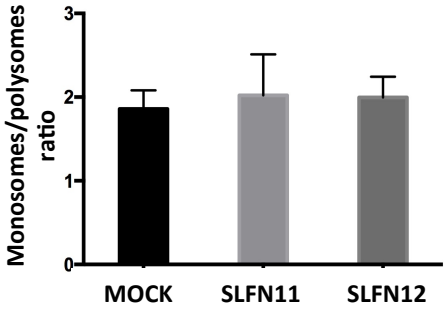

D

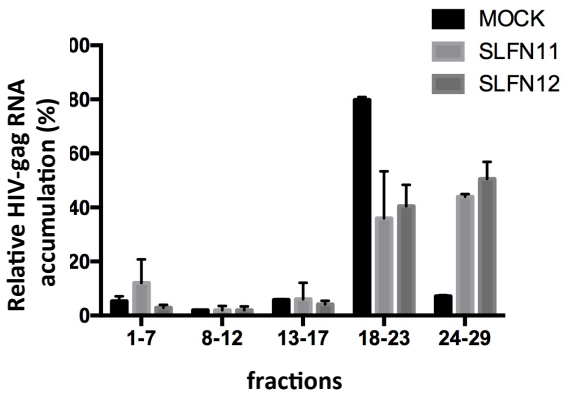

E

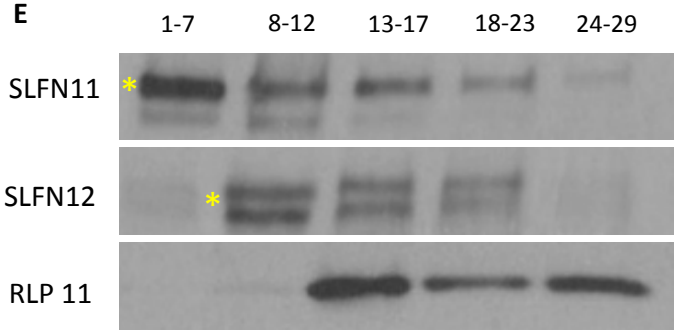

1-7 – free proteins (mRNP)

8-12 – single ribosomal subunits

13-17 – 80S monosome

18-23 – light polysomes

24-29 – heavy polysomes

SUPPLEMENTARY TABLES

Supplementary Table S1. List of differentially expressed genes significantly upregulated in TCR-cultured memory CD4 T cells compared to HSP-cultured naïve CD4 T cells before (A versus C) and after (B versus D) TCR activation (Group I).

Gene ID	Gene symbol	logFC A vs C	logFC B vs D	Gene ID	Gene symbol	logFC A vs C	logFC B vs D	Gene ID	Gene symbol	logFC A vs C	logFC B vs D
ENSG00000162772	ATF3	0,798906575	0,918786332	ENSG00000116761	CTH	2,077513469	1,489514819	ENSG00000178146	RP1-232L22__B.1	1,51018832	1,350864724
ENSG00000123685	BATF3	2,196744814	1,670354395	ENSG00000118402	ELOVL4	3,040990756	2,0881996	ENSG00000178445	GLDC	2,692154011	1,842020716
ENSG00000145386	CCNA2	0,769160287	1,067403082	ENSG00000121742	GJB6	3,96467389	1,814381803	ENSG00000178999	AURKB	0,71834185	1,12817753
ENSG00000144354	CDCA7	0,939029048	0,956880505	ENSG00000122786	CALD1	2,167280725	2,489589715	ENSG00000182054	IDH2	0,69299392	0,768426642
ENSG00000049768	FOXP3	2,342295436	0,919232552	ENSG00000123416	TUBA1B	0,695597128	0,727330071	ENSG00000183780	SLC35F3	3,450181622	1,040689178
ENSG00000198502	HLA-DRB5	2,940275493	1,741024148	ENSG00000123975	CKS2	0,711663104	0,940569859	ENSG00000183813	CCR4	2,765296845	1,58543929
ENSG00000137309	HMGA1	1,38643403	0,888816615	ENSG00000125454	SLC25A19	0,769115328	0,726233175	ENSG00000184524	CEND1	2,833633775	1,852568872
ENSG00000164104	HMGB2	0,640184853	0,811437505	ENSG00000126878	AIF1L	2,043713071	1,752236008	ENSG00000184584	TMEM173	1,292489237	0,907642854
ENSG00000050405	LIMA1	1,845812142	2,405820751	ENSG00000128050	PAICS	0,904396073	0,678253953	ENSG00000185433	LINC00158	2,385921999	1,765429669
ENSG00000166508	MCM7	0,690009015	0,721192825	ENSG00000128683	GAD1	3,345804765	4,013649214	ENSG00000189221	MAOA	7,09436472	4,374067053
ENSG00000118513	MYB	1,432447985	1,188732469	ENSG00000130005	GAMT	1,143348727	1,292289726	ENSG00000196126	HLA-DRB1	2,958608487	1,695518057
ENSG00000109674	NEIL3	0,974664381	1,39030174	ENSG00000133131	MORC4	0,822044288	0,931165439	ENSG00000196735	HLA-DQA1	4,540858546	2,541517235
ENSG00000145506	NKD2	3,895824291	2,906351563	ENSG00000137078	SIT1	2,054017679	1,456582396	ENSG00000198814	GK	1,418138198	1,32240884
ENSG00000181163	NPM1	0,497008124	0,471619183	ENSG00000141076	CIRH1A	0,58665264	0,669683488	ENSG00000204252	HLA-DOA	3,939524632	3,005956468
ENSG00000119403	PHF19	0,759473073	0,570646203	ENSG00000143061	IGSF3	1,46773583	2,492090814	ENSG00000204257	HLA-DMA	1,487469593	1,158563361
ENSG00000164754	RAD21	0,501228105	0,508679002	ENSG00000143079	CTTNBP2NL	1,125831914	1,093338245	ENSG00000204264	PSMB8	0,66693763	0,551451151
ENSG00000159216	RUNX1	0,744634519	0,692045109	ENSG00000143195	ILDR2	1,550325223	2,503514621	ENSG00000204287	HLA-DRA	2,560442008	1,597485084
ENSG00000087077	TRIP6	2,327153101	1,104843723	ENSG00000143344	RGL1	1,207827453	1,470305878	ENSG00000204472	AIF1	2,048206925	1,314346093
ENSG00000002587	HS3ST1	2,633431026	2,029115955	ENSG00000143891	GALM	1,986674504	1,215303033	ENSG00000204856	FAM216A	0,725215251	0,821666028
ENSG00000038210	PI4K2B	0,58833888	0,883299969	ENSG00000144381	HSPD1	0,822448099	0,717604872	ENSG00000205002	AARD	3,562364617	3,501544652
ENSG00000039068	CDH1	2,374770256	3,240438183	ENSG00000146216	TTBK1	2,716044599	2,213968416	ENSG00000205089	CCNI2	1,976209504	1,190225319
ENSG00000065923	SLC9A7	1,276191871	1,012577143	ENSG00000146410	MTFR2	0,776241795	0,938425161	ENSG00000205639	MFSD2B	1,072868208	0,948920926
ENSG00000071909	MYO3B	3,127552477	3,834383649	ENSG00000147434	CHRNA6	3,769076214	2,351248971	ENSG00000211784	TRAV10	2,38160505	1,914061969
ENSG00000077782	FGFR1	1,022181069	0,986472168	ENSG00000148090	AUH	0,845635466	0,98079111	ENSG00000211789	TRAV12-2	2,056200904	1,230212696
ENSG00000079156	OSBPL6	1,675911401	2,018202042	ENSG00000148468	FAM171A1	1,558628722	0,937495195	ENSG00000211795	TRAV8-6	1,725484263	1,132034524
ENSG00000080819	CPOX	0,696318578	0,858121095	ENSG00000151948	GLT1D1	2,795934707	3,25257683	ENSG00000211805	TRAV24	2,988796454	1,611336053
ENSG00000080824	HSP90AA1	0,509338553	0,699172269	ENSG00000153044	CENPH	0,807059462	0,822424893	ENSG00000211806	TRAV25	2,554629616	1,317774649
ENSG00000081026	MAGI3	0,907113523	1,115415459	ENSG00000153563	CD8A	2,010506894	1,399726227	ENSG00000211807	TRAV26-1	2,351420415	1,338555237
ENSG00000090104	RGS1	1,328443302	0,871834589	ENSG00000154096	THY1	6,010397244	3,409913431	ENSG00000211897	IGHG3	3,518193354	2,452326883
ENSG00000092621	PHGDH	1,558192247	1,454435435	ENSG00000157654	PALM2-AKAP2	1,218590121	1,275405357	ENSG00000213430	HSPD1P1	0,867897016	0,68195031
ENSG00000095203	EPB41L4B	1,460090645	1,714854047	ENSG00000159164	SV2A	2,297384656	2,285964008	ENSG00000213694	S1PR3	4,716192546	2,476463604
ENSG00000099194	SCD	1,387048841	1,466541706	ENSG00000160013	PTGIR	1,788318819	1,147613351	ENSG00000214391	RP11-121L10.3	0,73979043	0,756666745
ENSG00000099250	NRP1	2,63000307	2,907231213	ENSG00000160014	CALM3	0,615324815	0,420165507	ENSG00000215246	RP11-43F13.3	4,609328562	4,072311622
ENSG00000099284	H2AFY2	1,008454288	1,230773757	ENSG00000160200	CBS	1,671842033	1,784590297	ENSG00000223865	HLA-DPB1	2,825842465	1,78943668
ENSG00000100077	ADRBK2	0,765692283	0,854526464	ENSG00000160654	CD3G	1,24137665	0,659454119	ENSG00000226549	SCDP1	1,266898955	1,471868572
ENSG00000100167	SEPT3	2,592308292	2,259230376	ENSG00000163568	AIM2	1,539889076	1,520964136	ENSG00000227028	SLC8A1-AS1	3,310459782	3,31919302
ENSG00000100351	GRAP2	1,183416581	0,685830918	ENSG00000164032	H2AFZ	0,630174848	0,99854533	ENSG00000229391	HLA-DRB6	2,32883325	1,664721176
ENSG00000100867	DHRS2	2,730480731	1,290117918	ENSG00000164649	CDCA7L	1,023082834	0,851063723	ENSG00000229894	GK3P	1,336541994	1,28973786
ENSG00000100889	PCK2	0,607990852	0,606879437	ENSG00000165474	GJB2	4,364398617	2,39065388	ENSG00000230067	HSPD1P6	0,878005556	0,711789921
ENSG00000102970	CCL17	5,020880473	2,568487407	ENSG00000166803	KIAA0101	0,8001745	1,154238039	ENSG00000230537	RP11-305L7.1	1,876699998	1,312754698
ENSG00000103187	COTL1	1,074726907	0,617560978	ENSG00000166813	KIF7	1,217596038	1,223028794	ENSG00000231389	HLA-DPA1	2,915184393	1,87274979
ENSG00000103966	EHD4	0,757453856	0,63009804	ENSG00000167552	TUBA1A	0,706115977	0,710318176	ENSG00000231434	RP11-144L1.8	0,522134682	0,68493551
ENSG00000104427	ZC2HC1A	1,000021302	0,873805772	ENSG00000167553	TUBA1C	0,680890942	0,684149146	ENSG00000235831	BHLHE40-AS1	2,149961503	1,752491441
ENSG00000104833	TUBB4A	1,281395343	1,205422381	ENSG00000167747	C19orf48	0,767600344	0,763580798	ENSG00000236683	HMGA1P1	1,155008284	0,91810043
ENSG00000108176	DNAJC12	3,725222076	1,748760168	ENSG00000168280	KIF5C	1,646861058	1,558381313	ENSG00000236703	MYB-AS1	1,395163705	1,031529429
ENSG00000108424	KPNB1	0,509097438	0,662895557	ENSG00000168405	CMAHP	0,678217053	0,66443837	ENSG00000237541	HLA-DQA2	4,236652144	2,259355335
ENSG00000109452	INPP4B	0,991872562	0,881847495	ENSG00000168811	IL12A	2,786929245	2,932772775	ENSG00000241978	AKAP2	1,223005733	1,275534064
ENSG00000111674	ENO2	0,848092663	0,824631098	ENSG00000169245	CXCL10	2,448361228	2,018675595	ENSG00000244734	HBB	3,734210042	4,951349244
ENSG00000111716	LDHB	0,725864263	0,564252416	ENSG00000170017	ALCAM	0,837827554	0,969361357	ENSG00000249193	HSPD1P5	0,867068195	0,692590609
ENSG00000112655	PTK7	1,515778956	1,169493071	ENSG00000170989	S1PR1	1,065800934	0,809712634	ENSG00000249244	RP11-548H18.2	1,41562405	1,364057807
ENSG00000113739	STC2	2,739220761	3,026480139	ENSG00000171792	RHNO1	0,57130416	0,681891767	ENSG00000254126	CD8BP	3,54375816	2,077039492
ENSG00000115457	IGFBP2	1,756247917	2,678027694	ENSG00000171848	RRM2	1,062350011	1,396320219	ENSG00000256039	RP11-291B21.2	2,112269938	1,600081441
ENSG00000115541	HSPE1	0,624015105	0,554551263	ENSG00000172116	CD8B	3,458379602	1,917679561	ENSG00000256545	AL139819.1	1,412792444	1,446069092
ENSG00000269292	CTB-12A17.3	0,631490272	0,505695353	ENSG00000172673	THEMIS	1,030245197	0,710783739	ENSG00000256553	TRAV1-2	2,500543181	1,240670054
ENSG00000269968	RP5-940J5.9	0,574489308	0,585701769	ENSG00000172725	CORO1B	0,783380104	0,737862251	ENSG00000257576	RP11-153M3.1	0,90076119	0,712723139
ENSG00000258232	RP11-161H23.5	0,708769636	0,688262937	ENSG00000258017	RP11-386G11.10	0,734282277	0,758321174				

Supplementary Table S2. List of differentially expressed genes significantly downregulated in TCR-cultured memory CD4 T cells compared to HSP-cultured naïve CD4 T cells before (A versus C) and after (B versus D) TCR activation (Group II).

Gene ID	Gene symbol	logFC A vs C	logFC B vs D	Gene ID	Gene symbol	logFC A vs C	logFC B vs D	Gene ID	Gene symbol	logFC A vs C	logFC B vs D
ENSG00000000938	FGR	-4,117155726	-5,535520969	ENSG00000079112	CDH17	-6,946613909	-5,446915823	ENSG00000105501	SIGLEC5	-6,282642048	-6,013971191
ENSG00000000971	CFH	-2,611061674	-3,743953029	ENSG00000079215	SLC1A3	-7,800067487	-4,205818979	ENSG00000105514	RAB3D	-1,836243387	-1,303709142
ENSG00000001036	FUCA2	-1,230677275	-0,926806155	ENSG00000079482	OPHN1	-6,381427694	-4,477266884	ENSG00000105699	LSR	-1,203464341	-1,249089312
ENSG00000001084	GCLC	-0,537308135	-0,498544309	ENSG00000080493	SLC4A4	-2,546047944	-2,436870379	ENSG00000106546	AHR	-1,463666272	-1,110698347
ENSG00000004799	PDK4	-7,51457914	-6,458264292	ENSG00000080845	DLGAP4	-1,098123556	-1,320150445	ENSG00000106665	CLIP2	-2,286233622	-1,944095361
ENSG00000005020	SKAP2	-1,812012261	-1,457812472	ENSG00000081052	COL4A4	-4,310774732	-5,976763071	ENSG00000106683	LIMK1	-1,31065311	-1,046422656
ENSG00000005238	FAM214B	-0,678169256	-1,212214291	ENSG00000081320	STK17B	-0,510009847	-0,678939801	ENSG00000106799	TGFBR1	-0,818671071	-0,967969835
ENSG00000005379	BZRAP1	-0,898576582	-1,865986315	ENSG00000084764	MAPRE3	-1,114647379	-1,091732691	ENSG00000107140	TESK1	-0,663113641	-0,551504731
ENSG00000006534	ALDH3B1	-3,08786693	-2,977341854	ENSG00000085063	CD59	-1,098248076	-0,782575706	ENSG00000107331	ABCA2	-1,383147801	-1,806412954
ENSG00000007237	GAS7	-3,567461618	-4,121680327	ENSG00000085563	ABCB1	-1,758039945	-2,369557727	ENSG00000107719	PALD1	-3,48134165	-1,736605242
ENSG00000007264	MATK	-2,478558021	-2,173955762	ENSG00000085741	WNT11	-4,232821382	-5,642684341	ENSG00000107968	MAP3K8	-1,223068889	-1,070946241
ENSG00000007402	CACNA2D2	-1,289827902	-2,212053408	ENSG00000086289	EPDR1	-1,605886984	-1,441857625	ENSG00000108018	SORCS1	-7,117094361	-5,535271343
ENSG00000008256	CYTH3	-1,720659628	-3,202336478	ENSG00000086730	LAT2	-2,774512006	-2,717454356	ENSG00000108370	RGS9	-1,283584577	-3,187434456
ENSG00000008394	MGST1	-4,984790604	-3,651249541	ENSG00000088179	PTPN4	-0,722951559	-1,827859987	ENSG00000108511	HOXB6	-2,814737117	-1,922196412
ENSG00000008516	MMP25	-1,126939117	-2,31792759	ENSG00000089159	PXN	-0,764990293	-1,039928084	ENSG00000108582	CPD	-1,014843125	-0,661469709
ENSG00000008853	RHOBTB2	-1,162843113	-1,009838633	ENSG00000089505	CMTM1	-1,289404882	-1,151006154	ENSG00000109107	ALDOC	-2,679182033	-3,041992043
ENSG00000011600	TYROBP	-5,026124721	-5,947316074	ENSG00000090376	IRAK3	-3,196687412	-2,854081793	ENSG00000109458	GAB1	-1,675511728	-1,483400519
ENSG00000019144	PHLDB1	-2,523110279	-1,832165824	ENSG00000090975	PITPNM2	-0,771064907	-0,829212991	ENSG00000109684	CLNK	-3,412803051	-3,658591149
ENSG00000019485	PRDM11	-1,124348138	-1,19917893	ENSG00000092067	CEBPE	-2,82282593	-2,759310037	ENSG00000109906	ZBTB16	-1,638787136	-2,093524829
ENSG00000021762	OSBPL5	-2,108526817	-2,491392064	ENSG00000095303	PTGS1	-1,851935424	-2,101734204	ENSG00000109943	CRTAM	-1,943829301	-1,04618073
ENSG00000030419	IKZF2	-1,433303886	-1,126726349	ENSG00000096264	NCR2	-5,390561015	-6,265509019	ENSG00000110057	UNC93B1	-1,519381592	-1,475690878
ENSG00000031081	ARHGAP31	-1,57546229	-0,842091889	ENSG00000099219	ERMP1	-1,153795384	-1,559469617	ENSG00000110090	CPT1A	-1,179799923	-0,832845578
ENSG00000035664	DAPK2	-1,999754955	-3,802715233	ENSG00000099282	TSPAN15	-1,994284	-2,330865542	ENSG00000110092	CCND1	-1,89522429	-2,232113562
ENSG00000038382	TRIO	-2,420590232	-1,516889139	ENSG00000099889	ARVCF	-1,313028216	-1,140816349	ENSG00000110719	TCIRG1	-1,15616454	-1,212931832
ENSG00000038427	VCAN	-3,77944307	-3,495646369	ENSG00000099994	SUSD2	-1,529947597	-1,738977528	ENSG00000110852	CLEC2B	-1,060011523	-1,792621707
ENSG00000042493	CAPG	-1,168420484	-1,863079752	ENSG00000100228	RAB36	-2,348518399	-1,984338618	ENSG00000111670	GNPTAB	-1,032335664	-0,828715091
ENSG00000042980	ADAM28	-4,989989686	-5,849499427	ENSG00000100302	RASD2	-3,296280975	-2,635068311	ENSG00000111727	HCFC2	-0,712212267	-0,723541005
ENSG00000047648	ARHGAP6	-3,634238424	-5,801219175	ENSG00000100336	APOL4	-3,684107366	-4,921383409	ENSG00000111796	KLRB1	-2,126006015	-4,026589976
ENSG00000048052	HDAC9	-3,617438967	-4,085333973	ENSG00000100364	KIAA0930	-1,323712354	-0,757743441	ENSG00000112137	PHACTR1	-3,029455392	-2,877699296
ENSG00000049089	COL9A2	-1,888532156	-1,752134285	ENSG00000100368	CSF2RB	-2,072509748	-2,842784119	ENSG00000112773	FAM46A	-1,889891485	-1,879693423
ENSG00000050628	PTGER3	-3,945728686	-5,023897855	ENSG00000100385	IL2RB	-1,825279414	-0,93190936	ENSG00000113269	RNF130	-1,657267697	-1,146500295
ENSG00000050767	COL23A1	-2,81891578	-2,541182913	ENSG00000100427	MLC1	-3,521950684	-4,116441524	ENSG00000113369	ARRDC3	-1,017232931	-1,280813501
ENSG00000057704	TMCC3	-2,173682227	-2,946957051	ENSG00000100485	SOS2	-0,762107412	-0,910257979	ENSG00000114554	PLXNA1	-0,869873568	-1,016339872
ENSG00000059377	TBXAS1	-1,349050516	-1,444021384	ENSG00000100599	RIN3	-1,074382837	-1,684415394	ENSG00000114805	PLCH1	-4,198483298	-3,238983898
ENSG00000059728	MXD1	-1,073916915	-1,026442375	ENSG00000100647	KIAA0247	-0,881563175	-0,563882174	ENSG00000114853	ZBTB47	-2,380334033	-2,887442494
ENSG00000061918	GUCY1B3	-1,656727569	-1,404300382	ENSG00000101439	CST3	-3,044775527	-3,238292108	ENSG00000114993	RTKN	-2,260819277	-1,756646683
ENSG00000064393	HIPK2	-1,198885415	-0,879616512	ENSG00000101474	APMAP	-0,78786344	-0,691893557	ENSG00000115295	CLIP4	-0,694524684	-0,876735983
ENSG00000064601	CTSA	-0,569205981	-0,514769746	ENSG00000101493	ZNF516	-1,713037551	-1,824941534	ENSG00000115594	IL1R1	-4,844626931	-3,260985046
ENSG00000064687	ABCA7	-0,954799489	-2,339101215	ENSG00000101955	SRPX	-4,475301841	-7,192544449	ENSG00000115602	IL1RL1	-3,986201933	-1,954539558
ENSG00000064787	BCAS1	-2,280218656	-2,306773305	ENSG00000102595	UGGT2	-3,0935402	-2,264462021	ENSG00000115604	IL18R1	-1,598789192	-0,876449638
ENSG00000065308	TRAM2	-1,286048137	-1,662907889	ENSG00000102996	MMP15	-2,261723407	-1,477900547	ENSG00000115607	IL18RAP	-2,437769942	-1,743821855
ENSG00000065833	ME1	-2,292546346	-1,752299906	ENSG00000103254	FAM173A	-1,300703939	-0,927394408	ENSG00000115738	ID2	-1,00031884	-0,999405817
ENSG00000066056	TIE1	-3,392696856	-2,428050162	ENSG00000103489	XYLT1	-0,621451376	-1,333227872	ENSG00000116005	PCYOX1	-0,597313413	-0,573072384
ENSG00000066336	SPI1	-2,560832871	-2,039646278	ENSG00000103855	CD276	-2,80602012	-2,010331579	ENSG00000116661	FBXO2	-2,279583196	-2,355213402
ENSG00000070610	GBA2	-0,508057325	-0,542579296	ENSG00000104043	ATP8B4	-1,332067223	-1,061425302	ENSG00000116663	FBXO6	-0,908512274	-0,93851453
ENSG00000073792	IGF2BP2	-4,255867345	-3,316811195	ENSG00000104205	SGK3	-1,11485042	-1,470368423	ENSG00000116985	BMP8B	-1,570422694	-1,795633765
ENSG00000073861	TBX21	-0,893493609	-0,793092514	ENSG00000104312	RIPK2	-1,270753694	-1,474366412	ENSG00000117114	LPHN2	-4,056086322	-4,238023567
ENSG00000074660	SCARF1	-3,190464793	-3,094204594	ENSG00000104763	ASAH1	-0,647954417	-0,564880093	ENSG00000117139	KDM5B	-0,651045806	-0,95595341
ENSG00000074966	TXK	-2,539976074	-3,941436635	ENSG00000104970	KIR3DX1	-2,326570304	-2,305888143	ENSG00000117586	TNFSF4	-1,263476571	-1,315494011
ENSG00000075234	TTC38	-0,665979017	-0,592730676	ENSG00000105205	CLC	-4,426496767	-3,959144672	ENSG00000117984	CTSD	-1,121847096	-1,368116776
ENSG00000075420	FNDC3B	-1,742955857	-1,168063091	ENSG00000105278	ZFR2	-2,64591617	-3,177228922	ENSG00000118276	B4GALT6	-2,742787637	-1,36734865
ENSG00000075643	MOCOS	-2,909766581	-1,448885358	ENSG00000105339	DENND3	-1,247695574	-1,361352436	ENSG00000118508	RAB32	-3,883841147	-2,792925999
ENSG00000075651	PLD1	-2,270187797	-2,994323976	ENSG00000105370	LIM2	-2,339528851	-2,499545152	ENSG00000118804	FAM47E-STBD1	-1,160994485	-1,720911216
ENSG00000076826	CAMSAP3	-2,288773889	-1,556591561	ENSG00000105374	NKG7	-1,403048489	-1,517171165	ENSG00000120075	HOXB5	-3,04142721	-2,437949736
ENSG00000078399	HOXA9	-5,092019085	-5,872943053	ENSG00000105472	CLEC11A	-2,365940372	-1,843839793	ENSG00000120093	HOXB3	-1,558747825	-2,260797043
ENSG00000120594	PLXDC2	-3,81809103	-4,660354567	ENSG00000134539	KLRD1	-1,678100384	-1,427909567	ENSG00000143622	RIT1	-0,627991824	-0,715326322
ENSG00000120659	TNFSF11	-1,167542815	-1,738947223	ENSG00000134545	KLRC1	-4,43195442	-4,096751888	ENSG00000143995	MEIS1	-4,010417935	-4,806542354
ENSG00000120833	SOCS2	-0,79925714	-0,87901499	ENSG00000134897	BIVM	-0,671620718	-0,643104069	ENSG00000144290	SLC4A10	-1,470407934	-2,163414134
ENSG00000121005	CRISPLD1	-4,17563365	-2,834847235	ENSG00000134955	SLC37A2	-2,235125113	-2,112025351	ENSG00000144648	ACKR2	-3,614510963	-2,015979226
ENSG00000121053	FAX	-5,900898113	-6,470960306	ENSG00000135063	FAM189A2	-6,77141933	-7,776284677	ENSG00000145246	ATP10D	-1,65709647	-1,959055207
ENSG00000121064	SCPEP1	-1,329836399	-0,656930168	ENSG00000135083	CCNJL	-5,694584902	-6,403939752	ENSG00000145685	LHFPL2	-3,620275463	-3,121479431
ENSG00000121068	TBX2	-5,878818501	-4,034079142	ENSG00000135093	USP30	-0,913346684	-0,92660027	ENSG00000145730	PAM	-0,945110441	-0,867336177
ENSG00000122068	FYTTD1	-0,830013821	-0,704244466	ENSG00000135362	PRR5L	-1,215458235	-1,372035294	ENSG00000145757	SPATA9	-1,882572671	-1,698700637
ENSG00000122223	CD244	-1,427031188	-2,718875194	ENSG00000135404	CD63	-1,294265633	-1,288749009	ENSG00000145990	GFOD1	-2,320768708	-1,071369088
ENSG00000122642	FKBP9	-2,248744941	-1,848666743	ENSG00000135443	KRT85	-5,113412094	-5,868813604	ENSG00000146054	TRIM7	-2,541741838	-2,436605908
ENSG00000122870	BICC1	-2,400918291	-1,999734276	ENSG00000135477	KRT121P	-4,462285798	-4,27598115	ENSG00000146094	DOK3	-2,706231432	-1,752165612
ENSG00000123094	RASSF8	-4,361701134	-4,387324808	ENSG00000135503	ACVR1B	-1,380263848	-1,698778784	ENSG00000147036	LANCL3	-1,917752208	-2,245309179
ENSG00000123146	CD97	-0,819986242	-1,116111513	ENSG00000135605	TEC	-2,209302453	-2,031589057	ENSG00000147459	DOCK5	-3,283391964	-3,346594508
ENSG00000123329	ARHGAP9	-1,380065646	-1,758689627	ENSG00000135686	KLHL36	-0,645512055	-0,719219007	ENSG00000147883	CDKN2B	-1,848039468	-3,151640073
ENSG00000123384	LRP1	-2,181448604	-2,065362684	ENSG00000135925	WNT10A	-3,01684805	-2,541497557	ENSG00000147889	CDKN2A	-0,96945453	-1,23661238
ENSG00000124126	PREX1	-1,414700962	-1,763256612	ENSG00000136040	PLXNC1	-1,450614774	-0,973386714	ENSG00000148154	UGCG	-0,852276504	-0,591977069
ENSG00000124191	TOX2	-3,164299495	-2,647553093	ENSG00000136158	SPRY2	-4,457005915	-4,068280235	ENSG00000148175	STOM	-1,049812514	-1,279275641
ENSG00000124313	IQSEC2	-1,451902191	-1,953396357	ENSG00000136161	RCBTB2	-1,101048108	-2,186285414	ENSG00000148180	GSN	-4,181815828	-5,047972114
ENSG00000124491	F13A1	-4,660816157	-5,283156128	ENSG00000136193	SCRN1	-3,208057919	-3,589392736	ENSG00000148400	NOTCH1	-0,904226035	-0,563714453
ENSG00000125089	SH3TC1	-1,450615646	-1,584011597	ENSG00000136315	RP11-84C10.2	-6,468093311	-5,334018284	ENSG00000148848	ADAM12	-2,651828721	-3,897053471
ENSG00000125498	KIR2DL1	-3,802376286	-3,453755208	ENSG00000136404	TM6SF1	-1,046825541	-0,801902613	ENSG00000149294	NCAM1	-4,98906861	-6,092032656
ENSG00000125730	C3	-4,568928093	-3,871435444	ENSG00000136869	TLR4	-4,813895853	-6,505025098	ENSG00000149403	GRIK4	-3,241977455	-2,857984916
ENSG00000125734	GPR108	-0,505568741	-0,527879459	ENSG00000137166	FOXP4	-1,12354729	-1,731156224	ENSG00000149527	PLCH2	-1,109727906	-1,928917801
ENSG00000125844	RRBP1	-0,817053083	-0,599986207	ENSG00000137177	KIF13A	-3,382615126	-2,447717603	ENSG00000149557	FEZ1	-2,775985099	-3,240869567
ENSG00000125875	TBC1D20	-0,547646952	-0,675700155	ENSG00000137364	TPMT	-0,960131501	-0,642694135	ENSG00000150045	KLRF1	-4,850029257	-7,027407091
ENSG00000125967	NECAB3	-1,107339733	-0,75709067	ENSG00000137462	TLR2	-2,186240902	-2,549915002	ENSG00000150457	LATS2	-1,894790611	-2,039676951
ENSG00000126217	MCF2L	-1,545464505	-1,645806869	ENSG00000137801	THBS1	-2,893386635	-3,357854738	ENSG00000150681	RGS18	-2,869178788	-3,244519077
ENSG00000126262	FFAR2	-6,197344491	-6,015716425	ENSG00000137821	LRRC49	-3,512771917	-3,619168411	ENSG00000150782	IL18	-5,344232361	-3,804231709
ENSG00000126705	AHDC1	-1,356382521	-1,253024516	ENSG00000137831	UACA	-3,3669108	-2,572955282	ENSG00000150938	CRIM1	-2,250113767	-1,580171901
ENSG00000127507	EMR2	-0,80751727	-1,022435982	ENSG00000137834	SMAD6	-5,248198028	-3,556015389	ENSG00000151117	TMEM86A	-1,318623908	-1,579144802
ENSG00000127533	F2RL3	-2,217363594	-4,297210413	ENSG00000138758	SEPT11	-1,207094611	-0,834545092	ENSG00000151458	ANKRD50	-3,738031276	-3,42013796
ENSG00000127946	HIP1	-1,430648759	-1,270891871	ENSG00000138814	PPP3CA	-0,745839073	-0,894698901	ENSG00000151632	AKR1C2	-1,916770933	-1,823535301
ENSG00000128040	SPINK2	-2,392664525	-3,74016904	ENSG00000138835	RGS3	-1,437683613	-0,655353061	ENSG00000151718	WWC2	-2,563291442	-2,094869182
ENSG00000128268	MGAT3	-2,094862262	-2,793075331	ENSG00000139112	GABARAPL1	-1,424447493	-1,796330515	ENSG00000151778	SERP2	-3,067703552	-2,366074774
ENSG00000128294	TPST2	-0,714293804	-1,098979745	ENSG00000139132	FGD4	-3,6563968	-3,107356876	ENSG00000151914	DST	-1,862494541	-1,221089646
ENSG00000128311	TST	-1,418255868	-1,347906189	ENSG00000139182	CLSTN3	-1,024891316	-1,617915731	ENSG00000152076	CCDC74B	-2,174157921	-1,40966905
ENSG00000128487	SPECC1	-2,477314921	-1,32357238	ENSG00000139354	GAS2L3	-1,908582646	-2,707759118	ENSG00000152127	MGAT5	-0,870996365	-0,87777068
ENSG00000128604	IRF5	-1,404823192	-0,860980544	ENSG00000139410	SDSL	-2,769921426	-2,485118042	ENSG00000152128	TMEM163	-2,246919195	-3,135923596
ENSG00000129028	THAP10	-2,378080948	-2,049836239	ENSG00000139572	GPR84	-4,544674528	-2,407006565	ENSG00000152229	PSTPIP2	-1,650085147	-1,125099513
ENSG00000129473	BCL2L2	-1,607941336	-1,04757376	ENSG00000139668	WDFY2	-0,908122939	-0,679582583	ENSG00000152409	IMY	-0,801800942	-0,742423578
ENSG00000129474	AJUBA	-1,289042374	-1,274472867	ENSG00000140398	NEIL1	-2,994508856	-2,663608335	ENSG00000152492	CCDC50	-0,817468637	-0,920352722
ENSG00000129667	RHBDF2	-0,693920571	-0,88937075	ENSG00000140465	CYP1A1	-3,118385363	-3,404955458	ENSG00000152804	HHEX	-3,179159598	-2,711370703
ENSG00000130202	PVRL2	-3,421427714	-3,65677357	ENSG00000140678	ITGAX	-2,58041231	-3,554028226	ENSG00000153064	BANK1	-3,173378849	-3,859442905
ENSG00000130787	HIP1R	-0,743487759	-0,847476134	ENSG00000140691	ARMC5	-0,850729112	-0,801904734	ENSG00000153666	GOLGA8I	-2,026761437	-2,589300312
ENSG00000131037	EPS8L1	-1,02880879	-1,619662322	ENSG00000140836	ZFHX3	-2,44151419	-1,37188153	ENSG00000153707	PTPRD	-4,261105833	-4,131427742
ENSG00000131149	GSE1	-0,92881345	-0,91427015	ENSG00000140859	KIFC3	-4,502057472	-4,201991329	ENSG00000153814	JAZF1	-1,747148047	-1,598435231
ENSG00000131183	SLC34A1	-3,937399409	-4,533877433	ENSG00000140968	IRF8	-4,05907736	-2,221629307	ENSG00000154127	UBASH3B	-1,60456692	-0,899061985
ENSG00000132003	ZSWIM4	-0,773183225	-0,838088118	ENSG00000141526	SLC16A3	-1,333809727	-0,994813458	ENSG00000154188	ANGPT1	-3,89241672	-3,387025114
ENSG00000132334	PTPRE	-0,832033547	-0,993826227	ENSG00000141576	RNF157	-0,688842555	-1,104174782	ENSG00000154734	ADAMTS1	-4,099218082	-3,992684917
ENSG00000132561	MATN2	-3,955136894	-5,567553198	ENSG00000141622	RNF165	-4,218021396	-4,254614357	ENSG00000154760	SLFN13	-1,033513802	-0,957159818
ENSG00000133246	PRAM1	-4,100071113	-5,389566407	ENSG00000141696	LEPREL4	-0,977131197	-0,84356279	ENSG00000154914	USP43	-3,718088946	-3,260928784
ENSG00000133401	PDZD2	-2,428199537	-2,200598778	ENSG00000143013	LMO4	-0,657435184	-0,623668385	ENSG00000155366	RHOC	-1,206269348	-1,618913494
ENSG00000134070	IRAK2	-2,310473704	-2,000520323	ENSG00000143226	FCGR2A	-2,898413205	-3,258637639	ENSG00000155629	PIK3AP1	-3,285342349	-3,434381216

ENSG00000134215	VAV3	-2,652410642	-2,054208359	ENSG00000143365	RORC	-3,463627935	-4,751623335	ENSG00000155926	SLA	-1,061390952	-0,690548473
ENSG00000134243	SORT1	-2,94668663	-2,653300061	ENSG00000143434	SEMA6C	-1,156229803	-1,585099986	ENSG00000156273	BACH1	-0,796790479	-0,652241097
ENSG00000156299	TIAM1	-1,312839723	-0,763351765	ENSG00000172216	CEBPB	-1,452804911	-0,802034583	ENSG00000197122	SRC	-1,833079984	-1,286411344
ENSG00000156575	PRG3	-9,737648227	-7,522712574	ENSG00000172322	CLEC12A	-3,630916112	-6,286636015	ENSG00000197183	C20orf112	-0,990265235	-1,775777215
ENSG00000156966	B3GNT7	-4,962189317	-5,770693272	ENSG00000172380	GNG12	-3,259691219	-2,481640192	ENSG00000197872	FAM49A	-1,972051369	-2,33625343
ENSG00000156968	MPV17L	-2,404423854	-2,723072363	ENSG00000172508	CARNS1	-1,406855789	-1,699331507	ENSG00000197903	HIST1H2BK	-1,058152306	-1,494755074
ENSG00000157227	MMP14	-4,007760023	-4,592629161	ENSG00000172543	CTSW	-2,241564251	-2,736671043	ENSG00000197928	ZNF677	-1,493114368	-1,284643126
ENSG00000157404	KIT	-3,871348507	-5,148339776	ENSG00000172667	ZMAT3	-0,8404205	-1,206711796	ENSG00000197943	PLCG2	-2,691902273	-2,861520852
ENSG00000157510	AFAP1L1	-6,708900643	-5,738306368	ENSG00000172830	SSH3	-1,243886043	-1,364548376	ENSG00000198113	TOR4A	-0,981093514	-0,894072926
ENSG00000158186	MRAS	-4,067519509	-4,176201964	ENSG00000173064	HECTD4	-0,619856616	-0,635570666	ENSG00000198121	LPAR1	-4,961875298	-5,957089559
ENSG00000158517	NCF1	-2,004940435	-2,696257515	ENSG00000173110	HSPA6	-2,672582707	-2,757024588	ENSG00000198125	MB	-3,589271074	-1,867150377
ENSG00000158528	PPP1R9A	-5,624181146	-5,339011722	ENSG00000173530	TNFRSF10D	-1,11790873	-1,708597284	ENSG00000198286	CARD11	-0,703867721	-0,628947683
ENSG00000158856	DMTN	-0,806353587	-1,054453074	ENSG00000173801	JUP	-2,066340412	-2,449174254	ENSG00000198324	FAM109A	-1,518844397	-0,9927767
ENSG00000158869	FCER1G	-4,613681079	-5,086702795	ENSG00000173917	HOXB2	-1,139001765	-1,152670434	ENSG00000198561	CTNND1	-1,438518003	-1,465317958
ENSG00000159388	BTG2	-1,024281324	-0,980030622	ENSG00000173930	SLCO4C1	-2,838543989	-3,483268012	ENSG00000198574	SH2D1B	-5,269950127	-5,459238537
ENSG00000159433	STARD9	-1,10547107	-1,598542921	ENSG00000174083	PIK3R6	-1,761772514	-1,132514568	ENSG00000198719	DLL1	-3,979720795	-4,226999868
ENSG00000160111	CPAMD8	-1,850592256	-4,095630203	ENSG00000174233	ADCY6	-2,796842693	-3,111288707	ENSG00000198829	SUCNR1	-3,854820466	-3,251390743
ENSG00000160190	SLC37A1	-1,284117054	-0,952017886	ENSG00000175029	CTBP2	-3,253926728	-2,70311597	ENSG00000198846	TOX	-1,624154927	-0,979752767
ENSG00000160255	ITGB2	-0,593334257	-0,932953304	ENSG00000175048	ZDHHC14	-0,777236952	-0,939149236	ENSG00000198853	RUSC2	-2,274855639	-1,455066642
ENSG00000160325	CACFD1	-2,701782787	-3,05953205	ENSG00000175294	CATSPER1	-3,404255618	-3,789011592	ENSG00000198879	SFMBT2	-1,004706381	-0,664622679
ENSG00000160781	PAQR6	-1,068192218	-1,246182818	ENSG00000175489	LRRC25	-5,284158551	-6,646801969	ENSG00000198959	TGM2	-6,126061976	-6,669878362
ENSG00000160991	ORAI2	-0,617071375	-0,63584874	ENSG00000175556	LONRF3	-3,247229955	-3,449263295	ENSG00000203288	RP11-98D18.9	-1,815908644	-1,455009671
ENSG00000161010	C5orf45	-0,595344566	-0,608181486	ENSG00000175866	BAIAP2	-1,168024724	-1,475854106	ENSG00000203709	C1orf132	-1,38911923	-1,860527442
ENSG00000161011	SQSTM1	-0,695903167	-0,591330936	ENSG00000175920	DOK7	-4,19053219	-4,840411375	ENSG00000203747	FCGR3A	-3,128614743	-3,219001804
ENSG00000161642	ZNF385A	-3,112485273	-2,018176718	ENSG00000177191	B3GNT8	-1,256795046	-1,892690826	ENSG00000204475	NCR3	-1,275588479	-1,435451462
ENSG00000161681	SHANK1	-4,940628569	-8,50469731	ENSG00000177426	TGIF1	-0,842833459	-1,230201679	ENSG00000204482	LST1	-1,358070334	-1,89566023
ENSG00000161791	FMNL3	-0,790879542	-0,866485839	ENSG00000177465	ACOT4	-1,559121266	-1,173177762	ENSG00000204764	RANBP17	-4,888496615	-5,01833915
ENSG00000162004	CCDC78	-1,460660173	-1,237710011	ENSG00000177570	SAMD12	-1,630823736	-1,92104768	ENSG00000205189	ZBTB10	-1,283028057	-1,159457177
ENSG00000162490	DRAXIN	-4,914142388	-5,802808823	ENSG00000177663	IL17RA	-0,845259012	-1,266722824	ENSG00000205426	KRT81	-5,445551473	-7,322843202
ENSG00000162594	IL23R	-3,021378449	-1,832805426	ENSG00000177674	AGTRAP	-0,880510975	-1,722546152	ENSG00000205683	DPF3	-2,332761827	-2,590730342
ENSG00000162711	NLRP3	-2,709567672	-2,107772111	ENSG00000177685	EFCAB4A	-1,573543537	-2,301621233	ENSG00000205809	KLRC2	-3,741043372	-3,710156192
ENSG00000162722	TRIM58	-2,423707086	-2,22702199	ENSG00000178026	FAM211B	-2,669210726	-2,887024949	ENSG00000205810	KLRC3	-2,914342427	-3,058013328
ENSG00000162746	FCRLB	-1,676998977	-3,953168787	ENSG00000178115	GOLGA8Q	-2,912692167	-3,897675143	ENSG00000206127	GOLGA8O	-2,899104075	-3,856376012
ENSG00000162747	FCGR3B	-3,215654976	-3,324554975	ENSG00000178386	ZNF223	-2,204368718	-2,238855781	ENSG00000206190	ATP10A	-1,425257105	-1,550103856
ENSG00000163235	TGFA	-3,037963404	-3,340677118	ENSG00000178538	CA8	-3,762161198	-4,239029772	ENSG00000211689	TRGC1	-1,775938656	-2,440007974
ENSG00000163362	C1orf106	-3,230483852	-3,764126257	ENSG00000178719	GRINA	-0,565650303	-0,528531477	ENSG00000211696	TRGV8	-2,031297595	-2,232780333
ENSG00000163393	SLC22A15	-1,593644996	-1,623720835	ENSG00000178789	CD300LB	-4,395041801	-6,121639373	ENSG00000211698	TRGV4	-0,969963816	-1,58287119
ENSG00000163491	NEK10	-2,300718174	-2,757961008	ENSG00000179163	FUCA1	-2,709376224	-2,947111586	ENSG00000211829	TRDC	-2,798546414	-3,429635992
ENSG00000163577	EIF5A2	-0,723000188	-0,831832289	ENSG00000179241	LDLRAD3	-4,540446816	-3,153179572	ENSG00000213073	RP11-288H12.3	-1,153252304	-0,885702238
ENSG00000163701	IL17RE	-2,162920885	-3,124749033	ENSG00000179630	LACC1	-3,277211689	-3,009261788	ENSG00000213171	LINGO4	-5,854576095	-6,182497854
ENSG00000163751	CPA3	-2,111327674	-3,277764857	ENSG00000179841	AKAP5	-1,832732583	-1,549865468	ENSG00000213316	LTC4S	-3,691458301	-5,007619368
ENSG00000163754	GYG1	-0,982157229	-1,328659111	ENSG00000180155	LYNX1	-1,727435326	-2,251074577	ENSG00000213614	HEXA	-0,666016781	-0,625475146
ENSG00000163755	HPS3	-0,825024168	-0,928766162	ENSG00000180530	NRIP1	-1,260873555	-0,884424625	ENSG00000213699	SLC35F6	-1,051665566	-1,023699903
ENSG00000163814	CDCP1	-2,045800675	-2,033555322	ENSG00000180644	PRF1	-2,202621341	-2,279798229	ENSG00000213722	DDAH2	-0,934105162	-1,461674468
ENSG00000163818	LZTFL1	-1,24886733	-1,269006406	ENSG00000180730	SHISA2	-5,005351978	-5,514570023	ENSG00000213859	KCTD11	-0,910572425	-1,086417706
ENSG00000163820	FYCO1	-0,75835438	-0,613013502	ENSG00000180921	FAM83H	-0,804720712	-0,732255289	ENSG00000214022	REPIN1	-0,752383697	-0,91472258
ENSG00000163823	CCR1	-1,86305511	-2,125154561	ENSG00000180938	ZNF572	-1,519967957	-1,632771976	ENSG00000214530	STARD10	-1,000329683	-1,032999322
ENSG00000163874	ZC3H12A	-0,821119426	-1,02957217	ENSG00000181019	NQO1	-1,155554042	-0,950575354	ENSG00000215187	FAM166B	-4,084929133	-3,294548934
ENSG00000164023	SGMS2	-1,700662705	-1,725099412	ENSG00000181409	AATK	-4,454929192	-4,831485905	ENSG00000221866	PLXNA4	-1,917427577	-3,959337342
ENSG00000164050	PLXNB1	-1,742091663	-1,519445737	ENSG00000182472	CAPN12	-1,195981132	-1,775242991	ENSG00000221869	CEBPD	-3,86130127	-5,173400467
ENSG00000164116	GUCY1A3	-3,035111472	-1,729524009	ENSG00000182487	NCF1B	-2,027318861	-2,593452106	ENSG00000221957	KIR2DS4	-3,591100263	-3,723964217
ENSG00000164292	RHOBTB3	-3,627855745	-3,965970162	ENSG00000182511	FES	-3,029601339	-3,225363811	ENSG00000223547	ZNF844	-1,675883634	-1,794537755
ENSG00000164695	CHMP4C	-4,462847457	-4,199005764	ENSG00000182621	PLCB1	-2,681597943	-2,55230866	ENSG00000224376	AC017104.6	-2,549777565	-3,814993806
ENSG00000164949	GEM	-5,749629542	-4,481768629	ENSG00000182732	RGS6	-3,132119484	-2,196694753	ENSG00000225217	HSPA7	-2,614953607	-3,390305052
ENSG00000165025	SYK	-3,545028187	-3,211814073	ENSG00000182742	HOXB4	-0,949031612	-1,02011481	ENSG00000225614	ZNF469	-1,518922228	-1,40534048
ENSG00000165140	FBP1	-1,904391326	-2,980677108	ENSG00000182885	GPR97	-8,47126228	-7,743636536	ENSG00000227487	NCAM1-AS1	-4,757822889	-6,581888497
ENSG00000165178	NCF1C	-2,111327902	-2,840976707	ENSG00000183579	ZNRF3	-2,747367048	-1,794317008	ENSG00000227777	RP4-738P11.3	-4,997137958	-3,792650274
ENSG00000165424	ZCCHC24	-1,763095875	-1,673700698	ENSG00000183742	MACC1	-4,665337548	-4,413358167	ENSG00000229757	RP4-738P11.4	-3,059713524	-3,493689364
ENSG00000165801	ARHGEF40	-2,91657146	-3,209769171	ENSG00000183778	B3GALT5	-7,131738048	-7,634366936	ENSG00000231560	AC091814.3	-3,950381631	-5,632297804
ENSG00000166068	SPRED1	-4,885125157	-3,746177787	ENSG00000183828	NUDT14	-1,263841925	-1,875479598	ENSG00000232653	GOLGA8N	-2,976624343	-3,85662221
ENSG00000166900	STX3	-0,952913123	-1,415850051	ENSG00000184226	PCDH9	-3,491882695	-2,137402868	ENSG00000232907	RP5-977B1.7	-0,998186119	-1,173669545
ENSG00000166920	C15orf48	-3,439912134	-2,34941429	ENSG00000184254	ALDH1A3	-9,701269094	-10,35445343	ENSG00000233057	EEF1A1P14	-1,757162135	-1,387380599
ENSG00000167236	CCL23	-2,459157681	-2,48148263	ENSG00000184730	APOBR	-1,150785757	-2,183698405	ENSG00000233093	LINC00892	-0,754019345	-1,016993317
ENSG00000167633	KIR3DL1	-3,254551672	-2,89114634	ENSG00000184809	C21orf88	-6,368074497	-7,698024191	ENSG00000233101	HOXB-AS3	-2,699100633	-2,115083937
ENSG00000167634	NLRP7	-1,990171938	-1,977667567	ENSG00000184916	JAG2	-2,73267161	-2,83411581	ENSG00000234383	CTBP2P8	-1,891206615	-1,696313283
ENSG00000167664	TMIGD2	-1,491357132	-2,271977084	ENSG00000185015	CA13	-3,441216757	-3,382119978	ENSG00000235027	AC068580.6	-1,296656697	-1,742017561
ENSG00000167703	SLC43A2	-1,90770059	-1,784422728	ENSG00000185022	MAFF	-1,558935429	-1,10039336	ENSG00000235609	AF127936.7	-1,391806475	-2,545474828
ENSG00000167850	CD300C	-3,999443307	-4,75239545	ENSG00000185052	SLC24A3	-4,363361575	-5,24740298	ENSG00000236790	LINC00299	-3,975466367	-4,609257293
ENSG00000167851	CD300A	-2,427039458	-3,982105329	ENSG00000185198	PRSS57	-3,270408997	-3,705496523	ENSG00000237484	AP000476.1	-1,675676824	-1,333864729
ENSG00000168229	PTGDR	-3,898094584	-6,346368044	ENSG00000185650	ZFP36L1	-1,247729182	-1,074942135	ENSG00000237854	LINC00674	-1,41058105	-1,424931135
ENSG00000168502	SOGA2	-3,195986513	-3,034732258	ENSG00000186111	PIP5K1C	-1,055335783	-0,9015903	ENSG00000238243	OR2W3	-2,460532763	-2,862614453
ENSG00000168792	ABHD15	-0,755998683	-0,733714759	ENSG00000186350	RXRA	-2,063633305	-0,853171183	ENSG00000238244	GABARAPL3	-1,46120002	-1,740709247
ENSG00000168874	ATOH8	-4,147555797	-5,156734085	ENSG00000186399	GOLGA8R	-2,969985148	-4,058363319	ENSG00000239713	APOBEC3G	-0,727266577	-0,972241024
ENSG00000168916	ZNF608	-5,481623729	-6,236953535	ENSG00000186594	MIR22HG	-1,117989346	-1,952989883	ENSG00000239998	LILRA2	-3,769408444	-4,625057921
ENSG00000168995	SIGLEC7	-5,587285021	-7,539310035	ENSG00000186652	PRG2	-5,950501364	-5,294920031	ENSG00000241839	PLEKHO2	-0,719038865	-0,875699808
ENSG00000169026	MFSD7	-3,11899746	-2,931604651	ENSG00000186891	TNFRSF18	-1,932156393	-1,048195526	ENSG00000242258	LINC00996	-2,539844904	-3,149268027
ENSG00000169129	AFAP1L2	-2,104637266	-1,726596865	ENSG00000186994	KANK3	-1,247551139	-1,582655297	ENSG00000242473	KIR2DP1	-3,42047862	-2,982066068
ENSG00000169385	RNASE2	-6,434770135	-6,291563158	ENSG00000187037	GPR141	-3,02004569	-3,587504002	ENSG00000243772	KIR2DL3	-3,671304614	-3,660429936
ENSG00000169397	RNASE3	-6,287997923	-5,499367295	ENSG00000187134	AKR1C1	-1,921580676	-1,910263414	ENSG00000244242	IFITM10	-2,072298137	-2,281520597
ENSG00000169403	PTAFR	-3,566874237	-2,108183078	ENSG00000187583	PLEKHN1	-1,215172896	-1,90282593	ENSG00000244405	ETV5	-4,833617794	-3,235307965
ENSG00000169583	CLIC3	-2,040840881	-4,737355398	ENSG00000187678	SPRY4	-4,376650576	-1,436323915	ENSG00000244414	CFHR1	-2,778674267	-3,727065986
ENSG00000169744	LDB2	-5,715146757	-7,238696551	ENSG00000188305	C19orf35	-2,453832303	-3,798257915	ENSG00000246082	NUDT16P	-2,869778054	-3,199798933
ENSG00000169896	ITGAM	-1,728563528	-2,897831167	ENSG00000188559	RALGAPA2	-0,813437229	-0,690386438	ENSG00000246695	RASSF8-AS1	-4,35584916	-5,030840409
ENSG00000170442	KRT86	-5,319286135	-6,277225325	ENSG00000188626	GOLGA8M	-2,809436658	-3,678982283	ENSG00000248254	AC092597.3	-1,567133771	-2,089938423
ENSG00000170522	ELOVL6	-1,952361831	-2,293434915	ENSG00000188822	CNR2	-4,389426401	-6,060842923	ENSG00000248323	LUCAT1	-1,374751357	-1,427217827
ENSG00000170523	KRT83	-5,822488125	-6,495655831	ENSG00000188906	LRRK2	-2,447381	-4,327988195	ENSG00000248360	LINC00504	-5,396642321	-4,554570794
ENSG00000170545	SMAGP	-1,475093542	-1,045940781	ENSG00000189013	KIR2DL4	-6,232509698	-5,875432955	ENSG00000249978	TRGV7	-1,822511951	-2,631386189
ENSG00000170558	CDH2	-4,352281343	-3,400646051	ENSG00000189350	FAM179A	-1,488169953	-1,734076952	ENSG00000250091	DNAH10OS	-2,036321117	-2,143131167
ENSG00000170858	LILRP2	-3,667163513	-5,069311178	ENSG00000189430	NCR1	-4,533706447	-4,50189562	ENSG00000250240	CTD-2154I11.2	-4,291343696	-3,738058412
ENSG00000170962	PDGFD	-2,317341315	-4,365382131	ENSG00000196139	AKR1C3	-2,562132626	-2,792580541	ENSG00000250644	RP11-295K3.1	-1,118469532	-1,393464843
ENSG00000171476	HOPX	-0,813555099	-1,149515384	ENSG00000196220	SRGAP3	-3,582220608	-4,518324096	ENSG00000251002	AE000661.37	-2,763793338	-3,404687897
ENSG00000171604	CXXC5	-3,860113976	-3,883754671	ENSG00000196422	PPP1R26	-1,732637593	-1,523855567	ENSG00000253210	RP11-809O17.1	-1,381161414	-1,244514361
ENSG00000171657	GPR82	-5,387040962	-3,510238906	ENSG00000196542	SPTSSB	-10,77958667	-8,912803375	ENSG00000253230	LINC00599	-3,263466917	-4,547755824
ENSG00000171658	RP11-443P15.2	-3,63586029	-2,91828308	ENSG00000196684	HSH2D	-1,063160489	-1,012410789	ENSG00000253293	HOXA10	-4,166961925	-4,787145142
ENSG00000171659	GPR34	-3,132702542	-2,170384365	ENSG00000196781	TLE1	-3,491017442	-4,535805466	ENSG00000254087	LYN	-2,427635661	-2,171000362
ENSG00000171813	PWWP2B	-1,012855672	-1,370214802	ENSG00000196782	MAML3	-1,945732294	-2,281724405	ENSG00000254415	SIGLEC14	-4,943421095	-4,289694461
ENSG00000171840	NINJ2	-1,089779423	-1,292553606	ENSG00000196914	ARHGEF12	-0,71623819	-0,542111588	ENSG00000255031	RP11-802E16.3	-0,872048736	-1,054586115
ENSG00000172123	SLFN12	-1,609691269	-1,614437601	ENSG00000196937	FAM3C	-1,220309819	-0,554927655	ENSG00000255587	RAB44	-3,005464114	-3,485086758
ENSG00000255641	NKG2-E	-2,746722661	-3,088109246	ENSG00000260916	CCPG1	-0,713917495	-0,854114324	ENSG00000267648	RP11-686D22.3	-1,709558713	-1,642944746
ENSG00000255857	PXN-AS1	-0,703475401	-0,73192584	ENSG00000261064	RP11-1000B6.3	-2,616402117	-3,444291109	ENSG00000267745	RP11-686D22.8	-1,698265145	-1,596173487
ENSG00000256667	KLRAP1	-2,15414276	-1,928137235	ENSG00000261602	CTD-2033A16.1	-1,345303647	-1,014160059	ENSG00000268424	AC008948.1	-2,567015353	-4,100235574
ENSG00000256797	KLRF2	-4,580062703	-4,36198647	ENSG00000261739	GOLGA8S	-2,266621211	-2,536229324	ENSG00000268500	SIGLEC5	-6,209501197	-6,217416889
ENSG00000259583	RP11-66B24.4	-5,442701584	-4,084101323	ENSG00000261771	DYX1C1-CCPG1	-0,711634749	-0,820066339	ENSG00000269072	CTD-3187F8.14	-4,962322222	-8,321586755
ENSG00000260244	RP11-588K22.2	-3,47765152	-2,460535998	ENSG00000262728	AC123768.4	-2,331042523	-2,746060548	ENSG00000269930	RP11-932O9.9	-3,335797278	-4,635809223
ENSG00000260682	7SK	-2,801048147	-2,717420012	ENSG00000265168	RP11-192H23.5	-2,68319635	-3,014223822	ENSG00000271810	RP11-426L16.10	-1,249632002	-1,563300768
ENSG00000260693	AC026150.8	-2,220490769	-2,937752728	ENSG00000267102	RP11-686D22.7	-1,640859614	-1,653494885	ENSG00000272211	RP11-347P5.1	-1,514456537	-1,589786035
ENSG00000260810	CTD-2547L24.4	-1,282209115	-2,510826049	ENSG00000267379	CTC-548K16.5	-0,906809499	-1,042042289	ENSG00000272414	FAM47E	-1,137666122	-1,706353631
ENSG00000260828	HMGB3P32	-2,08814589	-1,401446684	ENSG00000267547	RP11-686D22.4	-1,751301805	-1,503468357	ENSG00000272908	RP11-121A8.1	-3,209709065	-3,858379975

Supplementary Table S3. List of differentially expressed genes highly upregulated (fold-change FC>2) in TCR-cultured memory CD4 T cells compared to HSP-cultured naïve CD4 T cells before (A versus C) and after (B versus D) TCR activation.

Gene ID	Gene symbol	logFC A vs C	logFC B vs D
ENSG00000244734	HBB	3,734210042	4,951349244
ENSG00000189221	MAOA	7,09436472	4,374067053
ENSG00000215246	RP11-43F13.3	4,609328562	4,072311622
ENSG00000128683	GAD1	3,345804765	4,013649214
ENSG00000071909	MYO3B	3,127552477	3,834383649
ENSG00000205002	AARD	3,562364617	3,501544652
ENSG00000154096	THY1	6,010397244	3,409913431
ENSG00000227028	SLC8A1-AS1	3,310459782	3,31919302
ENSG00000151948	GLT1D1	2,795934707	3,25257683
ENSG00000039068	CDH1	2,374770256	3,240438183
ENSG00000113739	STC2	2,739220761	3,026480139
ENSG00000204252	HLA-DOA	3,939524632	3,005956468
ENSG00000168811	IL12A	2,786929245	2,932772775
ENSG00000099250	NRP1	2,63000307	2,907231213
ENSG00000145506	NKD2	3,895824291	2,906351563
ENSG00000102970	CCL17	5,020880473	2,568487407
ENSG00000196735	HLA-DQA1	4,540858546	2,541517235
ENSG00000122786	CALD1	2,167280725	2,489589715
ENSG00000213694	S1PR3	4,716192546	2,476463604
ENSG00000211897	IGHG3	3,518193354	2,452326883
ENSG00000165474	GJB2	4,364398617	2,39065388
ENSG00000147434	CHRNA6	3,769076214	2,351248971
ENSG00000159164	SV2A	2,297384656	2,285964008
ENSG00000237541	HLA-DQA2	4,236652144	2,259355335
ENSG00000100167	37865	2,592308292	2,259230376
ENSG00000146216	TTBK1	2,716044599	2,213968416
ENSG00000118402	ELOVL4	3,040990756	2,0881996
ENSG00000254126	CD8BP	3,54375816	2,077039492
ENSG00000002587	HS3ST1	2,633431026	2,029115955
ENSG00000169245	CXCL10	2,448361228	2,018675595

Supplementary Table S4. List of geneontology (GO) enriched terms from genes in Group I with fold change (FC)>2. Enrichment analysis was performed using DAVID (http://david.ncifcrf.gov/).

GO Term	PValue	Gene ID
GO:0007267~cell-cell signaling	3,10E-05	ENSG00000128683, ENSG00000099250, ENSG00000102970, ENSG00000165474, ENSG00000189221, ENSG00000147434, ENSG00000169245, ENSG00000113739
GO:0006955~immune response	4,34E-03	ENSG00000168811, ENSG00000102970, ENSG00000204252, ENSG00000196735, ENSG00000211897, ENSG00000169245
GO:0050863~regulation of T cell activation	1,53E-02	ENSG00000168811, ENSG00000204252, ENSG00000154096
GO:0051249~regulation of lymphocyte activation	2,38E-02	ENSG00000168811, ENSG00000204252, ENSG00000154096
GO:0008284~positive regulation of cell proliferation	2,85E-02	ENSG00000168811, ENSG00000099250, ENSG00000213694, ENSG00000169245
GO:0002694~regulation of leukocyte activation	2,94E-02	ENSG00000168811, ENSG00000204252, ENSG00000154096
GO:0050865~regulation of cell activation	3,24E-02	ENSG00000168811, ENSG00000204252, ENSG00000154096
GO:0042133~neurotransmitter metabolic process	3,52E-02	ENSG00000128683, ENSG00000189221
GO:0051270~regulation of cell motion	3,88E-02	ENSG00000099250, ENSG00000169245, ENSG00000154096
GO:0050771~negative regulation of axonogenesis	3,99E-02	ENSG00000099250, ENSG00000154096
GO:0050877~neurological system process	4,14E-02	ENSG00000118402, ENSG00000128683, ENSG00000165474, ENSG00000189221, ENSG00000147434, ENSG00000071909
GO:0031345~negative regulation of cell projection organization	4,46E-02	ENSG00000099250, ENSG00000154096
GO:0009611~response to wounding	5,30E-02	ENSG00000099250, ENSG00000102970, ENSG00000213694, ENSG00000169245
GO:0007166~cell surface receptor linked signal transduction	7,05E-02	ENSG00000099250, ENSG00000102970, ENSG00000213694, ENSG00000145506, ENSG00000169245, ENSG00000113739, ENSG00000154096
GO:0050768~negative regulation of neurogenesis	7,07E-02	ENSG00000099250, ENSG00000154096
GO:0010721~negative regulation of cell development	7,53E-02	ENSG00000099250, ENSG00000154096
GO:0006952~defense response	0,07581433	ENSG00000168811, ENSG00000102970, ENSG00000213694, ENSG00000169245
GO:0007268~synaptic transmission	0,08370113	ENSG00000128683, ENSG00000189221, ENSG00000147434
GO:0050770~regulation of axonogenesis	0,08877442	ENSG00000099250, ENSG00000154096
GO:0006954~inflammatory response	0,09702717	ENSG00000102970, ENSG00000213694, ENSG00000169245

Supplementary Table S5. List of genes highly downregulated (fold-change FC<-2) in TCR-cultured memory CD4 T cells compared to HSP-cultured naïve CD4 T cells before (A versus C) and after (B versus D) TCR activation.

Gene ID	Gene symbol	logFC A vs C	logFC B vs D	Gene ID	Gene symbol	logFC A vs C	logFC B vs D	Gene ID	Gene symbol	logFC A vs C	logFC B vs D
ENSG00000196542	SPTSSB	-10,77958667	-8,912803375	ENSG00000158186	MRAS	-4,067519509	-4,176201964	ENSG00000186399	GOLGA8R	-2,969985148	-4,058363319
ENSG00000156575	PRG3	-9,737648227	-7,522712574	ENSG00000140968	IRF8	-4,05907736	-2,221629307	ENSG00000134243	SORT1	-2,94668663	-2,653300061
ENSG00000184254	ALDH1A3	-9,701269094	-10,35445343	ENSG00000117114	LPHN2	-4,056086322	-4,238023567	ENSG00000165801	ARHGEF40	-2,91657146	-3,209769171
ENSG00000182885	GPR97	-8,47126228	-7,743636536	ENSG00000143995	MEIS1	-4,010417935	-4,806542354	ENSG00000205810	KLRC3	-2,914342427	-3,058013328
ENSG00000079215	SLC1A3	-7,800067487	-4,205818979	ENSG00000157227	MMP14	-4,007760023	-4,592629161	ENSG00000178115	GOLGA8Q	-2,912692167	-3,897675143
ENSG00000004799	PDK4	-7,51457914	-6,458264292	ENSG00000167850	CD300C	-3,999443307	-4,75239545	ENSG00000206127	GOLGA8O	-2,899104075	-3,856376012
ENSG00000183778	B3GALT5	-7,131738048	-7,634366936	ENSG00000198719	DLL1	-3,979720795	-4,226999868	ENSG00000143226	FCGR2A	-2,898413205	-3,258637639
ENSG00000108018	SORCS1	-7,117094361	-5,535271343	ENSG00000236790	LINC00299	-3,975466367	-4,609257293	ENSG00000137801	THBS1	-2,893386635	-3,357854738
ENSG00000079112	CDH17	-6,946613909	-5,446915823	ENSG00000132561	MATN2	-3,955136894	-5,567553198	ENSG00000246082	NUDT16P	-2,869778054	-3,199798933
ENSG00000135063	FAM189A2	-6,77141933	-7,776284677	ENSG00000231560	AC091814.3	-3,950381631	-5,632297804	ENSG00000150681	RGS18	-2,869178788	-3,244519077
ENSG00000157510	AFAP1L1	-6,708900643	-5,738306368	ENSG00000050628	PTGER3	-3,945728686	-5,023897855	ENSG00000173930	SLCO4C1	-2,838543989	-3,483268012
ENSG00000121053	EPX	-6,470960306	-5,900898113	ENSG00000131183	SLC34A1	-3,937399409	-4,533877433	ENSG00000092067	CEBPE	-2,82282593	-2,759310037
ENSG00000136315	RP11-84C10.2	-6,468093311	-5,334018284	ENSG00000168229	PTGDR	-3,898094584	-6,346068044	ENSG00000050767	COL23A1	-2,81891578	-2,541182913
ENSG00000169385	RNASE2	-6,434770135	-6,291563158	ENSG00000154188	ANGPT1	-3,89241672	-3,387025114	ENSG00000188626	GOLGA8M	-2,809436658	-3,678982283
ENSG00000079482	OPHN1	-6,381427694	-4,477266884	ENSG00000118508	RAB32	-3,883841147	-2,792925999	ENSG00000103855	CD276	-2,80602012	-2,010331579
ENSG00000184809	C21orf88	-6,368074497	-7,698024191	ENSG00000157404	KIT	-3,871348507	-5,148339776	ENSG00000260682	7SK	-2,801048147	-2,717420012
ENSG00000169397	RNASE3	-6,287997923	-5,499367295	ENSG00000221869	CEBPD	-3,86130127	-5,173400467	ENSG00000211829	TRDC	-2,798546414	-3,429635992
ENSG00000105501	SIGLEC5	-6,282642048	-6,013971191	ENSG00000171604	CXXC5	-3,860113976	-3,883754671	ENSG00000174233	ADCY6	-2,796842693	-3,111288707
ENSG00000189013	KIR2DL4	-6,232509698	-5,875432955	ENSG00000198829	SUCNR1	-3,854820466	-3,251390743	ENSG00000244414	CFHR1	-2,778674267	-3,727065986
ENSG00000268500	SIGLEC5	-6,209501197	-6,217416889	ENSG00000120594	PLXDC2	-3,81809103	-4,660354567	ENSG00000149557	FEZ1	-2,775985099	-3,240869567
ENSG00000126262	FFAR2	-6,197344491	-6,015716425	ENSG00000125498	KIR2DL1	-3,802376286	-3,453755208	ENSG00000086730	LAT2	-2,774512006	-2,717454356
ENSG00000198959	TGM2	-6,126061976	-6,669878362	ENSG00000038427	VCAN	-3,77994307	-3,495646369	ENSG00000139410	SDSL	-2,769921426	-2,485118042
ENSG00000186652	PRG2	-5,950501364	-5,294920031	ENSG00000239998	LILRA2	-3,769408444	-4,625057921	ENSG00000251002	AE000661.37	-2,763793338	-3,404687897
ENSG00000121068	TBX2	-5,878818501	-4,034079142	ENSG00000178538	CA8	-3,762161198	-4,239029772	ENSG00000255641	NKG2-E	-2,746722661	-3,088109246
ENSG00000213171	LINGO4	-5,854576095	-6,182497854	ENSG00000205809	KLRC2	-3,741043372	-3,710156192	ENSG00000184916	JAG2	-2,73267161	-2,83411581
ENSG00000170523	KRT83	-5,822488125	-6,495655831	ENSG00000151458	ANKRD50	-3,738031276	-3,42013796	ENSG00000162711	NLRP3	-2,709567672	-2,107772111
ENSG00000164949	GEM	-5,749629542	-4,481768629	ENSG00000154914	USP43	-3,718088946	-3,260928784	ENSG00000179163	FUCA1	-2,709376224	-2,947111586
ENSG00000169744	LDB2	-5,715146757	-7,238696551	ENSG00000213316	LTC4S	-3,691458301	-5,007619368	ENSG00000160325	CACFD1	-2,701782787	-3,05953205
ENSG00000135083	CCNJL	-5,694584902	-6,403939752	ENSG00000100336	APOL4	-3,684107366	-4,921383409	ENSG00000233101	HOXB-AS3	-2,699100633	-2,115083937
ENSG00000158528	PPP1R9A	-5,624181146	-5,339011722	ENSG00000243772	KIR2DL3	-3,671304614	-3,660429936	ENSG00000197943	PLCG2	-2,691902273	-2,861520852
ENSG00000168995	SIGLEC7	-5,587285021	-7,539310035	ENSG00000170858	LILRP2	-3,667163513	-5,069311178	ENSG00000265168	RP11-192H23.5	-2,68319635	-3,014223822
ENSG00000168916	ZNF608	-5,481623729	-6,236953535	ENSG00000139132	FGD4	-3,6563968	-3,107356876	ENSG00000182621	PLCB1	-2,681597943	-2,55230866
ENSG00000205426	KRT81	-5,445551473	-7,322843202	ENSG00000171658	RP11-443P15.2	-3,63586029	-2,91828308	ENSG00000109107	ALDOC	-2,679182033	-3,041992043
ENSG00000259583	RP11-66B24.4	-5,442701584	-4,084101323	ENSG00000047648	ARHGAP6	-3,634238424	-5,801219175	ENSG00000173110	HSPA6	-2,672582707	-2,757024588
ENSG00000248360	LINC00504	-5,396642321	-4,554570794	ENSG00000172322	CLEC12A	-3,630916112	-6,286636015	ENSG00000178026	FAM211B	-2,669210726	-2,887024949
ENSG00000096264	NCR2	-5,390561015	-6,265509019	ENSG00000164292	RHOBTB3	-3,627855745	-3,965970162	ENSG00000134215	VAV3	-2,652410642	-2,054208359
ENSG00000171657	GPR82	-5,387040962	-3,510238906	ENSG00000145685	LHFPL2	-3,620275463	-3,121479431	ENSG00000148848	ADAM12	-2,651828721	-3,897053471
ENSG00000150782	IL18	-5,344232361	-3,804231709	ENSG00000048052	HDAC9	-3,617438967	-4,085333973	ENSG00000105278	ZFR2	-2,64591617	-3,177228922
ENSG00000170442	KRT86	-5,319286135	-6,277225325	ENSG00000144648	ACKR2	-3,614510963	-2,015979226	ENSG00000261064	RP11-1000B6.3	-2,616402117	-3,444291109
ENSG00000175489	LRRC25	-5,284158551	-6,646801969	ENSG00000221957	KIR2DS4	-3,591100263	-3,723964217	ENSG00000225217	HSPA7	-2,614953607	-3,390305052
ENSG00000198574	SH2D1B	-5,269950127	-5,459238537	ENSG00000196220	SRGAP3	-3,582220608	-4,518324096	ENSG00000000971	CFH	-2,611061674	-3,743953029
ENSG00000137834	SMAD6	-5,248198028	-3,556015389	ENSG00000007237	GAS7	-3,567461618	-4,121680327	ENSG00000140678	ITGAX	-2,58041231	-3,554028226
ENSG00000135443	KRT85	-5,113412094	-5,868813604	ENSG00000169403	PTAFR	-3,566874237	-2,108183078	ENSG00000268424	AC008948.1	-2,567015353	-4,100235574
ENSG00000078399	HOXA9	-5,092019085	-5,872943053	ENSG00000165025	SYK	-3,545028187	-3,211814073	ENSG00000151718	WWC2	-2,563291442	-2,094869182
ENSG00000011600	TYROBP	-5,026124721	-5,947316074	ENSG00000100427	MLC1	-3,521950684	-4,116441524	ENSG00000196139	AKR1C3	-2,562132626	-2,792580541
ENSG00000180730	SHISA2	-5,005351978	-5,514570023	ENSG00000137821	LRRC49	-3,512771917	-3,619168411	ENSG00000066336	SPI1	-2,560832871	-2,039646278
ENSG00000227777	RP4-738P11.3	-4,997137958	-3,792650274	ENSG00000184226	PCDH9	-3,491882695	-2,137402868	ENSG00000224376	AC017104.6	-2,549777565	-3,814993806
ENSG00000042980	ADAM28	-4,989989686	-5,849499427	ENSG00000196781	TLE1	-3,491017442	-4,535805466	ENSG00000080493	SLC4A4	-2,546047944	-2,436870379
ENSG00000149294	NCAM1	-4,98906861	-6,092032656	ENSG00000260244	RP11-588K22.2	-3,47765152	-2,460535998	ENSG00000146054	TRIM7	-2,541741838	-2,436605908
ENSG00000008394	MGST1	-4,984790604	-3,651249541	ENSG00000143365	RORC	-3,463627935	-4,751623335	ENSG00000074966	TXK	-2,539976074	-3,941436635
ENSG00000269072	CTD-3187F8.14	-4,962322222	-8,321586755	ENSG00000185015	CA13	-3,441216757	-3,382119978	ENSG00000242258	LINC00996	-2,539844904	-3,149268027
ENSG00000156966	B3GNT7	-4,962189317	-5,770693272	ENSG00000166920	C15orf48	-3,439912134	-2,34941429	ENSG00000007264	MATK	-2,478558021	-2,173955762
ENSG00000198121	LPAR1	-4,961875298	-5,957089559	ENSG00000130202	PVRL2	-3,421427714	-3,65677357	ENSG00000238243	OR2W3	-2,460532763	-2,862614453
ENSG00000254415	SIGLEC14	-4,943421095	-4,289694461	ENSG00000242473	KIR2DP1	-3,42047862	-2,982066068	ENSG00000167236	CCL23	-2,459157681	-2,48148263
ENSG00000161681	SHANK1	-4,940628569	-8,50469731	ENSG00000109684	CLNK	-3,412803051	-3,658591149	ENSG00000188305	C19orf35	-2,453832303	-3,798257915
ENSG00000162490	DRAXIN	-4,914142388	-5,802808823	ENSG00000175294	CATSPER1	-3,404255618	-3,789011592	ENSG00000188906	LRRK2	-2,447381	-4,327988195
ENSG00000204764	RANBP17	-4,888496615	-5,01833915	ENSG00000066056	TIE1	-3,392696856	-2,428050162	ENSG00000133401	PDZD2	-2,428199537	-2,200598778
ENSG00000166068	SPRED1	-4,885125157	-3,746177787	ENSG00000137177	KIF13A	-3,382615126	-2,447717603	ENSG00000254087	LYN	-2,427635661	-2,171000362
ENSG00000150045	KLRF1	-4,850029257	-7,027407091	ENSG00000137831	UACA	-3,3669108	-2,572955282	ENSG00000167851	CD300A	-2,427039458	-3,982105329
ENSG00000115594	IL1R1	-4,844626931	-3,260985046	ENSG00000269930	RP11-932O9.9	-3,335797278	-4,635809223	ENSG00000162722	TRIM58	-2,423707086	-2,22702199
ENSG00000244405	ETV5	-4,833617794	-3,235307965	ENSG00000100302	RASD2	-3,296280975	-2,635068311	ENSG00000156968	MPV17L	-2,404423854	-2,723072363
ENSG00000136869	TLR4	-4,813895853	-6,505025098	ENSG00000155629	PIK3AP1	-3,285342349	-3,434381216	ENSG00000128040	SPINK2	-2,392664525	-3,74016904
ENSG00000227487	NCAM1-AS1	-4,757822889	-6,581888497	ENSG00000147459	DOCK5	-3,283391964	-3,346594508	ENSG00000114853	ZBTB47	-2,380334033	-2,887442494
ENSG00000183742	MACC1	-4,665337548	-4,413358167	ENSG00000179630	LACC1	-3,277211689	-3,009261788	ENSG00000129028	THAP10	-2,378080948	-2,049836239
ENSG00000124491	F13A1	-4,660816157	-5,283156128	ENSG00000185198	PRSS57	-3,270408997	-3,705496523	ENSG00000105370	LIM2	-2,339528851	-2,499545152
ENSG00000158869	FCER1G	-4,613681079	-5,086702795	ENSG00000253230	LINC00599	-3,263466917	-4,547755824	ENSG00000205683	DPF3	-2,332761827	-2,590730342
ENSG00000256797	KLRF2	-4,580062703	-4,36198647	ENSG00000172380	GNG12	-3,259691219	-2,481640192	ENSG00000262728	AC123768.4	-2,331042523	-2,746060548
ENSG00000125730	C3	-4,568928093	-3,871435444	ENSG00000167633	KIR3DL1	-3,254551672	-2,89114634	ENSG00000104970	KIR3DX1	-2,326570304	-2,305888143
ENSG00000139572	GPR84	-4,544674528	-2,407006565	ENSG00000175029	CTBP2	-3,253926728	-2,70311597	ENSG00000170962	PDGFD	-2,317341315	-4,365382131
ENSG00000179241	LDLRAD3	-4,540446816	-3,153179572	ENSG00000175556	LONRF3	-3,247229955	-3,449263295	ENSG00000134070	IRAK2	-2,310473704	-2,000520323
ENSG00000189430	NCR1	-4,533706447	-4,50189562	ENSG00000149403	GRIK4	-3,241977455	-2,857984916	ENSG00000163491	NEK10	-2,300718174	-2,757961008
ENSG00000140859	KIFC3	-4,502057472	-4,201991329	ENSG00000163362	C1orf106	-3,230483852	-3,764126257	ENSG00000064787	BCAS1	-2,280218656	-2,306773305
ENSG00000101955	SRPX	-4,475301841	-7,192544449	ENSG00000162747	FCGR3B	-3,215654976	-3,324554975	ENSG00000116661	FBXO2	-2,279583196	-2,355213402
ENSG00000164695	CHMP4C	-4,462847457	-4,199005764	ENSG00000272908	RP11-121A8.1	-3,209709065	-3,858379975	ENSG00000075651	PLD1	-2,270187797	-2,994323976
ENSG00000135477	KRT121P	-4,462285798	-4,27598115	ENSG00000136193	SCRN1	-3,208057919	-3,589392736	ENSG00000261739	GOLGA8S	-2,266621211	-2,536229324
ENSG00000136158	SPRY2	-4,457005915	-4,068280235	ENSG00000090376	IRAK3	-3,196687412	-2,854081793	ENSG00000152128	TMEM163	-2,246919195	-3,135923596
ENSG00000181409	AATK	-4,454929192	-4,831485905	ENSG00000168502	SOGA2	-3,195986513	-3,034732258	ENSG00000172543	CTSW	-2,241564251	-2,736671043
ENSG00000134545	KLRC1	-4,43195442	-4,096751888	ENSG00000074660	SCARF1	-3,190464793	-3,094204594	ENSG00000134955	SLC37A2	-2,235125113	-2,112025351
ENSG00000105205	CLC	-4,426496767	-3,959144672	ENSG00000152804	HHEX	-3,179159598	-2,711370703	ENSG00000260693	AC026150.8	-2,220490769	-2,937752728
ENSG00000178789	CD300LB	-4,395041801	-6,121639373	ENSG00000153064	BANK1	-3,173378849	-3,859442905	ENSG00000127533	F2RL3	-2,217363594	-4,297210413
ENSG00000188822	CNR2	-4,389426401	-6,060842923	ENSG00000124191	TOX2	-3,164299495	-2,647553093	ENSG00000135605	TEC	-2,209302453	-2,031589057
ENSG00000185052	SLC24A3	-4,363361575	-5,24740298	ENSG00000171659	GPR34	-3,132702542	-2,170384365	ENSG00000178386	ZNF223	-2,204368718	-2,238855781
ENSG00000123094	RASSF8	-4,361701134	-4,387324808	ENSG00000182732	RGS6	-3,132119484	-2,196694753	ENSG00000180644	PRF1	-2,202621341	-2,279798229
ENSG00000246695	RASSF8-AS1	-4,35584916	-5,030840409	ENSG00000203747	FCGR3A	-3,128614743	-3,219001804	ENSG00000137462	TLR2	-2,186240902	-2,549915002
ENSG00000170558	CDH2	-4,352281343	-3,400646051	ENSG00000169026	MFSD7	-3,11899746	-2,931604651	ENSG00000123384	LRP1	-2,181448604	-2,065362684
ENSG00000081052	COL4A4	-4,310774732	-5,976763071	ENSG00000140465	CYP1A1	-3,118385363	-3,404955458	ENSG00000057704	TMCC3	-2,173682227	-2,946957051
ENSG00000250240	CTD-2154I11.2	-4,291343696	-3,738058412	ENSG00000161642	ZNF385A	-3,112485273	-2,018176718	ENSG00000163701	IL17RE	-2,162920885	-3,124749033
ENSG00000153707	PTPRD	-4,261105833	-4,131427742	ENSG00000102595	UGGT2	-3,0935402	-2,264462021	ENSG00000111796	KLRB1	-2,126006015	-4,026589976
ENSG00000073792	IGF2BP2	-4,255867345	-3,316811195	ENSG00000006534	ALDH3B1	-3,08786693	-2,977341854	ENSG00000165178	NCF1C	-2,111327902	-2,840976707
ENSG00000085741	WNT11	-4,232821382	-5,642684341	ENSG00000151778	SERP2	-3,067703552	-2,366074774	ENSG00000163751	CPA3	-2,111327674	-3,277764857
ENSG00000141622	RNF165	-4,218021396	-4,254614357	ENSG00000229757	RP4-738P11.4	-3,059713524	-3,493689364	ENSG00000021762	OSBPL5	-2,108526817	-2,491392064
ENSG00000114805	PLCH1	-4,198483298	-3,238983898	ENSG00000101439	CST3	-3,044775527	-3,238292108	ENSG00000128268	MGAT3	-2,094862262	-2,793075331
ENSG00000175920	DOK7	-4,19053219	-4,840411375	ENSG00000120075	HOXB5	-3,04142721	-2,437949736	ENSG00000100368	CSF2RB	-2,072509748	-2,842784119
ENSG00000148180	GSN	-4,181815828	-5,047972114	ENSG00000163235	TGFA	-3,037963404	-3,340677118	ENSG00000244242	IFITM10	-2,072298137	-2,281520597
ENSG00000121005	CRISPLD1	-4,17563365	-2,834847235	ENSG00000182511	FES	-3,029601339	-3,225363811	ENSG00000173801	JUP	-2,066340412	-2,449174254
ENSG00000253293	HOXA10	-4,166961925	-4,787145142	ENSG00000112137	PHACTR1	-3,029455392	-2,877699296	ENSG00000163814	CDCP1	-2,045800675	-2,033555322
ENSG00000168874	ATOH8	-4,147555797	-5,156734085	ENSG00000187037	GPR141	-3,02004569	-3,587504002	ENSG00000169583	CLIC3	-2,040840881	-4,737355398
ENSG00000000938	FGR	-4,117155726	-5,535520969	ENSG00000135925	WNT10A	-3,01684805	-2,541497557	ENSG00000250091	DNAH10OS	-2,036321117	-2,143131167
ENSG00000133246	PRAM1	-4,100071113	-5,389566407	ENSG00000255587	RAB44	-3,005464114	-3,485086758	ENSG00000211696	TRGV8	-2,031297595	-2,232780333
ENSG00000154734	ADAMTS1	-4,099218082	-3,992684917	ENSG00000140398	NEIL1	-2,994508856	-2,663608335	ENSG00000182487	NCF1B	-2,027318861	-2,593452106
ENSG00000215187	FAM166B	-4,084929133	-3,294548934	ENSG00000232653	GOLGA8N	-2,976624343	-3,85662221				
ENSG00000158517	NCF1	-2,004940435	-2,696257515	ENSG00000153666	GOLGA8I	-2,026761437	-2,589300312				

Supplementary Table S6. List of geneontology (GO) enriched terms from genes in Group II with fold change (FC)<-2. Enrichment analysis was performed using DAVID (http://david.ncifcrf.gov/).

GO Term	PValue	Gene ID
GO:0006955~immune response	6,66E-09	ENSG00000178789, ENSG00000221957, ENSG00000109684, ENSG00000140968, ENSG00000086730, ENSG00000164949, ENSG00000137462, ENSG00000137801, ENSG00000115594, ENSG00000170858, ENSG00000167633, ENSG00000172543, ENSG00000158869, ENSG00000203747, ENSG00000000971, ENSG00000156575, ENSG00000188822, ENSG00000150782, ENSG00000158517, ENSG00000197943, ENSG00000125498, ENSG00000103855, ENSG00000167236, ENSG00000167851, ENSG00000167850, ENSG00000125730, ENSG00000162711, ENSG00000137834, ENSG00000165178, ENSG00000136869, ENSG00000162747, ENSG00000186652, ENSG00000144648, ENSG00000169403
GO:0006952~defense response	9,67E-08	ENSG00000189430, ENSG00000075651, ENSG00000205810, ENSG00000011600, ENSG00000211829, ENSG00000137462, ENSG00000092067, ENSG00000137801, ENSG00000115594, ENSG00000134070, ENSG00000050628, ENSG00000101439, ENSG00000000971, ENSG00000188822, ENSG00000205809, ENSG00000158517, ENSG00000000938, ENSG00000167236, ENSG00000167850, ENSG00000048052, ENSG00000125730, ENSG00000162711, ENSG00000180644, ENSG00000165178, ENSG00000169397, ENSG00000136869, ENSG00000096264, ENSG00000186652, ENSG00000189013, ENSG00000169403
GO:0006968~cellular defense response	2,41E-07	ENSG00000180644, ENSG00000189430, ENSG00000165178, ENSG00000205809, ENSG00000205810, ENSG00000158517, ENSG00000011600, ENSG00000096264, ENSG00000189013, ENSG00000211829, ENSG00000167850
GO:0007166~cell surface receptor linked signal transduction	9,23E-07	ENSG00000109684, ENSG00000085741, ENSG00000066056, ENSG00000134215, ENSG00000152804, ENSG00000126262, ENSG00000137462, ENSG00000115594, ENSG00000134070, ENSG00000139572, ENSG00000182732, ENSG00000158869, ENSG00000187037, ENSG00000150681, ENSG00000188822, ENSG00000111796, ENSG00000117114, ENSG00000197943, ENSG00000167236, ENSG00000198959, ENSG00000182885, ENSG00000137834, ENSG00000172380, ENSG00000108018, ENSG00000171659, ENSG00000144648, ENSG00000198719, ENSG00000171657, ENSG00000153707, ENSG00000198829, ENSG00000149403, ENSG00000134545, ENSG00000196781, ENSG00000086730, ENSG00000164949, ENSG00000154734, ENSG00000168229, ENSG00000184916, ENSG00000050628, ENSG00000127533, ENSG00000165025, ENSG00000135925, ENSG00000134243, ENSG00000133246, ENSG00000198121, ENSG00000140678, ENSG00000125730, ENSG00000154188, ENSG00000149294, ENSG00000150045, ENSG00000174233, ENSG00000123384, ENSG00000157404, ENSG00000169403
GO:0031349~positive regulation of defense response	9,62E-05	ENSG00000137462, ENSG00000134070, ENSG00000090376, ENSG00000158869, ENSG00000136869, ENSG00000130202, ENSG00000198959, ENSG00000125730
GO:0002757~immune response-activating signal transduction	1,09E-04	ENSG00000137462, ENSG00000134070, ENSG00000197943, ENSG00000090376, ENSG00000136869, ENSG00000086730, ENSG00000165025
GO:0009617~response to bacterium	1,34E-04	ENSG00000137462, ENSG00000075651, ENSG00000092067, ENSG00000140465, ENSG00000197943, ENSG00000090376, ENSG00000169397, ENSG00000136869, ENSG00000008394, ENSG00000186652, ENSG00000000938, ENSG00000169403
GO:0002764~immune response-regulating signal transduction	1,65E-04	ENSG00000137462, ENSG00000134070, ENSG00000197943, ENSG00000090376, ENSG00000136869, ENSG00000086730, ENSG00000165025
GO:0001775~cell activation	0,00112095	ENSG00000156575, ENSG00000221957, ENSG00000189430, ENSG00000197943, ENSG00000086730, ENSG00000103855, ENSG00000048052, ENSG00000137462, ENSG00000184916, ENSG00000167633, ENSG00000136869, ENSG00000153064, ENSG00000165025
GO:0043405~regulation of MAP kinase activity	0,00113708	ENSG00000163235, ENSG00000139132, ENSG00000166068, ENSG00000137801, ENSG00000136158, ENSG00000090376, ENSG00000157404, ENSG00000198121, ENSG00000165025
GO:0045088~regulation of innate immune response	0,00115441	ENSG00000189430, ENSG00000137462, ENSG00000134070, ENSG00000090376, ENSG00000136869, ENSG00000130202
GO:0070498~interleukin-1-mediated signaling pathway	0,00126696	ENSG00000115594, ENSG00000134070, ENSG00000090376
GO:0002237~response to molecule of bacterial origin	0,00166465	ENSG00000137462, ENSG00000140465, ENSG00000197943, ENSG00000090376, ENSG00000136869, ENSG00000008394, ENSG00000169403
GO:0002221~pattern recognition receptor signaling pathway	0,00183122	ENSG00000137462, ENSG00000134070, ENSG00000090376, ENSG00000136869
GO:0002218~activation of innate immune response	0,00255363	ENSG00000137462, ENSG00000134070, ENSG00000090376, ENSG00000136869
GO:0002758~innate immune response-activating signal transduction	0,00255363	ENSG00000137462, ENSG00000134070, ENSG00000090376, ENSG00000136869

GO Term	PValue	Gene ID
GO:0002684~positive regulation of immune system process	5,10E-05	ENSG00000150782, ENSG00000090376, ENSG00000197943, ENSG00000130202, ENSG00000086730, ENSG00000103855, ENSG00000125730, ENSG00000137462, ENSG00000137801, ENSG00000134070, ENSG00000136869, ENSG00000158869, ENSG00000000971, ENSG00000165025
GO:0050778~positive regulation of immune response	5,58E-05	ENSG00000137462, ENSG00000134070, ENSG00000197943, ENSG00000090376, ENSG00000158869, ENSG00000136869, ENSG00000000971, ENSG00000086730, ENSG00000130202, ENSG00000125730, ENSG00000165025
GO:0002253~activation of immune response	7,19E-05	ENSG00000137462, ENSG00000134070, ENSG00000197943, ENSG00000090376, ENSG00000136869, ENSG00000000971, ENSG00000086730, ENSG00000125730, ENSG00000165025
GO:0007242~intracellular signaling cascade	7,21E-05	ENSG00000109684, ENSG00000075651, ENSG00000011600, ENSG00000114805, ENSG00000134215, ENSG00000086730, ENSG00000164949, ENSG00000188906, ENSG00000163235, ENSG00000158186, ENSG00000135605, ENSG00000166068, ENSG00000137462, ENSG00000118508, ENSG00000137801, ENSG00000134070, ENSG00000182732, ENSG00000127533, ENSG00000050628, ENSG00000165025, ENSG00000188822, ENSG00000074966, ENSG00000197943, ENSG00000047648, ENSG00000198121, ENSG00000198959, ENSG00000178538, ENSG00000139132, ENSG00000182621, ENSG00000172380, ENSG00000148180, ENSG00000137831, ENSG00000100302, ENSG00000174233, ENSG00000136869, ENSG00000157404, ENSG00000169403
GO:0048584~positive regulation of response to stimulus	1,96E-04	ENSG00000090376, ENSG00000197943, ENSG00000130202, ENSG00000086730, ENSG00000198959, ENSG00000125730, ENSG00000137462, ENSG00000137801, ENSG00000134070, ENSG00000158869, ENSG00000136869, ENSG00000000971, ENSG00000165025
GO:0045321~leukocyte activation	2,46E-04	ENSG00000156575, ENSG00000221957, ENSG00000189430, ENSG00000197943, ENSG00000086730, ENSG00000103855, ENSG00000048052, ENSG00000137462, ENSG00000184916, ENSG00000167633, ENSG00000136869, ENSG00000153064, ENSG00000165025
GO:0001817~regulation of cytokine production	3,46E-04	ENSG00000156575, ENSG00000073792, ENSG00000150782, ENSG00000137462, ENSG00000137801, ENSG00000090376, ENSG00000158869, ENSG00000136869, ENSG00000103855, ENSG00000165025, ENSG00000162711
GO:0002886~regulation of myeloid leukocyte mediated immunity	3,49E-04	ENSG00000158869, ENSG00000133246, ENSG00000125730, ENSG00000165025
GO:0030155~regulation of cell adhesion	9,44E-04	ENSG00000150782, ENSG00000148180, ENSG00000184916, ENSG00000137801, ENSG00000047648, ENSG00000134215, ENSG00000157227, ENSG00000198959, ENSG00000198719
GO:0002224~toll-like receptor signaling pathway	0,00101263	ENSG00000137462, ENSG00000134070, ENSG00000090376, ENSG00000136869
GO:0044093~positive regulation of molecular function	0,00104644	ENSG00000090376, ENSG00000197943, ENSG00000047648, ENSG00000198121, ENSG00000134215, ENSG00000198959, ENSG00000162711, ENSG00000163235, ENSG00000139132, ENSG00000137831, ENSG00000137462, ENSG00000137801, ENSG00000174233, ENSG00000134070, ENSG00000123384, ENSG00000157404, ENSG00000136869, ENSG00000050628, ENSG00000127533, ENSG00000165025
GO:0002703~regulation of leukocyte mediated immunity	0,00199898	ENSG00000189430, ENSG00000158869, ENSG00000133246, ENSG00000130202, ENSG00000125730, ENSG00000165025
GO:0051895~negative regulation of focal adhesion formation	0,00209115	ENSG00000137801, ENSG00000047648, ENSG00000157227
GO:0009611~response to wounding	0,00214799	ENSG00000188822, ENSG00000167236, ENSG00000048052, ENSG00000079215, ENSG00000125730, ENSG00000162711, ENSG00000124491, ENSG00000148180, ENSG00000137462, ENSG00000137801, ENSG00000140465, ENSG00000134070, ENSG00000038427, ENSG00000136869, ENSG00000050628, ENSG00000127533, ENSG00000000971, ENSG00000169403
GO:0002366~leukocyte activation during immune response	0,01567497	ENSG00000137462, ENSG00000197943, ENSG00000136869, ENSG00000086730
GO:0002263~cell activation during immune response	0,01567497	ENSG00000137462, ENSG00000197943, ENSG00000136869, ENSG00000086730

GO:0046649~lymphocyte activation	0,00275661	ENSG00000189430, ENSG00000221957, ENSG00000184916, ENSG00000197943, ENSG00000167633, ENSG00000103855, ENSG00000086730, ENSG00000048052, ENSG00000153064, ENSG00000165025
GO:0002755~MyD88-dependent toll-like receptor signaling pathway	0,00310638	ENSG00000137462, ENSG00000134070, ENSG00000090376
GO:0019221~cytokine-mediated signaling pathway	0,00365697	ENSG00000115594, ENSG00000134070, ENSG00000090376, ENSG00000157404, ENSG00000100368, ENSG00000198959
GO:0002697~regulation of immune effector process	0,00374422	ENSG00000189430, ENSG00000090376, ENSG00000158869, ENSG00000133246, ENSG00000130202, ENSG00000125730, ENSG00000165025
GO:0051336~regulation of hydrolase activity	0,00421744	ENSG00000047648, ENSG00000134243, ENSG00000198121, ENSG00000134215, ENSG00000198959, ENSG00000162711, ENSG00000140398, ENSG00000137834, ENSG00000139132, ENSG00000137831, ENSG00000101439, ENSG00000127533, ENSG00000050628
GO:0001816~cytokine production	0,004576	ENSG00000150782, ENSG00000092067, ENSG00000136869, ENSG00000169403, ENSG00000162711
GO:0045089~positive regulation of innate immune response	0,004576	ENSG00000137462, ENSG00000134070, ENSG00000090376, ENSG00000136869, ENSG00000130202
GO:0010033~response to organic substance	0,00477707	ENSG00000075651, ENSG00000090376, ENSG00000197943, ENSG00000134243, ENSG00000157227, ENSG00000048052, ENSG00000109107, ENSG00000154188, ENSG00000180644, ENSG00000172380, ENSG00000148180, ENSG00000173110, ENSG00000137462, ENSG00000137801, ENSG00000115594, ENSG00000140465, ENSG00000174233, ENSG00000134070, ENSG00000136869, ENSG00000008394, ENSG00000169403
GO:0050727~regulation of inflammatory response	0,00520164	ENSG00000137831, ENSG00000158869, ENSG00000136869, ENSG00000103855, ENSG00000198959, ENSG00000125730
GO:0032496~response to lipopolysaccharide	0,00549786	ENSG00000140465, ENSG00000197943, ENSG00000090376, ENSG00000136869, ENSG00000008394, ENSG00000169403
GO:0051893~regulation of focal adhesion formation	0,00568711	ENSG00000137801, ENSG00000047648, ENSG00000157227
GO:0042742~defense response to bacterium	0,00619236	ENSG00000137462, ENSG00000075651, ENSG00000092067, ENSG00000169397, ENSG00000136869, ENSG00000186652, ENSG00000000938
GO:0022610~biological adhesion	0,00751472	ENSG00000101955, ENSG00000074660, ENSG00000149557, ENSG00000139410, ENSG00000047648, ENSG00000133401, ENSG00000130202, ENSG00000140678, ENSG00000079112, ENSG00000173801, ENSG00000167851, ENSG00000105501, ENSG00000149294, ENSG00000184226, ENSG00000137801, ENSG00000168995, ENSG00000038427, ENSG00000148848, ENSG00000170558, ENSG00000165025
GO:0006954~inflammatory response	0,00867435	ENSG00000188822, ENSG00000137462, ENSG00000137801, ENSG00000134070, ENSG00000136869, ENSG00000050628, ENSG00000000971, ENSG00000167236, ENSG00000048052, ENSG00000125730, ENSG00000169403, ENSG00000162711
GO:0007243~protein kinase cascade	0,00868097	ENSG00000163235, ENSG00000139132, ENSG00000135605, ENSG00000166068, ENSG00000137462, ENSG00000074966, ENSG00000137801, ENSG00000134070, ENSG00000157404, ENSG00000136869, ENSG00000198121, ENSG00000188906, ENSG00000165025
GO:0001953~negative regulation of cell-matrix adhesion	0,00896471	ENSG00000137801, ENSG00000047648, ENSG00000157227
GO:0042325~regulation of phosphorylation	0,00906929	ENSG00000090376, ENSG00000136158, ENSG00000198121, ENSG00000134215, ENSG00000137834, ENSG00000139132, ENSG00000163235, ENSG00000166068, ENSG00000170962, ENSG00000137801, ENSG00000174233, ENSG00000123384, ENSG00000157404, ENSG00000136869, ENSG00000165025
GO:0043549~regulation of kinase activity	0,01664594	ENSG00000163235, ENSG00000139132, ENSG00000166068, ENSG00000137801, ENSG00000174233, ENSG00000136158, ENSG00000123384, ENSG00000090376, ENSG00000157404, ENSG00000198121, ENSG00000134215, ENSG00000165025
GO:0006800~oxygen and reactive oxygen species metabolic process	0,01694512	ENSG00000156575, ENSG00000182621, ENSG00000165178, ENSG00000140465, ENSG00000158517, ENSG00000121053
GO:0043406~positive regulation of MAP kinase activity	0,01730031	ENSG00000163235, ENSG00000139132, ENSG00000137801, ENSG00000157404, ENSG00000198121, ENSG00000165025
GO:0070482~response to oxygen levels	0,01793107	ENSG00000150782, ENSG00000184916, ENSG00000137801, ENSG00000140465, ENSG00000157227, ENSG00000109107, ENSG00000154188
GO:0051129~negative regulation of cellular component organization	0,01850063	ENSG00000137834, ENSG00000148180, ENSG00000137801, ENSG00000090376, ENSG00000047648, ENSG00000101439, ENSG00000157227
GO:0044087~regulation of cellular component biogenesis	0,01850063	ENSG00000137834, ENSG00000148180, ENSG00000137801, ENSG00000157404, ENSG00000047648, ENSG00000081052, ENSG00000157227
GO:0010518~positive regulation of phospholipase activity	0,01868673	ENSG00000047648, ENSG00000127533, ENSG00000198121, ENSG00000050628, ENSG00000198959
GO:0002429~immune response-activating cell surface receptor signaling pathway	0,01943179	ENSG00000137462, ENSG00000197943, ENSG00000086730, ENSG00000165025
GO:0006468~protein amino acid phosphorylation	0,01945152	ENSG00000182511, ENSG00000181409, ENSG00000163491, ENSG00000066056, ENSG00000074966, ENSG00000090376, ENSG00000198121, ENSG00000000938, ENSG00000004799, ENSG00000188906, ENSG00000139132, ENSG00000163235, ENSG00000135605, ENSG00000137801, ENSG00000134070, ENSG00000157404, ENSG00000007264, ENSG00000165025
GO:0007229~integrin-mediated signaling pathway	0,01959763	ENSG00000133246, ENSG00000134215, ENSG00000140678, ENSG00000154734, ENSG00000165025
GO:0032760~positive regulation of tumor necrosis factor production	0,01993321	ENSG00000137462, ENSG00000158869, ENSG00000136869
GO:0010517~regulation of phospholipase activity	0,02053552	ENSG00000047648, ENSG00000127533, ENSG00000198121, ENSG00000050628, ENSG00000198959
GO:0033674~positive regulation of kinase activity	0,02112284	ENSG00000163235, ENSG00000139132, ENSG00000137801, ENSG00000174233, ENSG00000123384, ENSG00000157404, ENSG00000198121, ENSG00000134215, ENSG00000165025
GO:0043085~positive regulation of catalytic activity	0,02161926	ENSG00000047648, ENSG00000198121, ENSG00000134215, ENSG00000198959, ENSG00000162711, ENSG00000139132, ENSG00000163235, ENSG00000137831, ENSG00000137801, ENSG00000174233, ENSG00000123384, ENSG00000157404, ENSG00000127533, ENSG00000050628, ENSG00000165025
GO:0051338~regulation of transferase activity	0,02197573	ENSG00000163235, ENSG00000139132, ENSG00000166068, ENSG00000137801, ENSG00000174233, ENSG00000136158, ENSG00000123384, ENSG00000090376, ENSG00000157404, ENSG00000198121, ENSG00000134215, ENSG00000165025
GO:0051092~positive regulation of NF-kappaB transcription factor activity	0,0221884	ENSG00000137462, ENSG00000134070, ENSG00000090376, ENSG00000136869
GO:0032088~negative regulation of NF-kappaB transcription factor activity	0,02256303	ENSG00000134070, ENSG00000090376, ENSG00000162711

GO:0060191~regulation of lipase activity	0,00914369	ENSG00000134243, ENSG00000047648, ENSG00000127533, ENSG00000198121, ENSG00000050628, ENSG00000198959
GO:0050729~positive regulation of inflammatory response	0,00950425	ENSG00000158869, ENSG00000136869, ENSG00000198959, ENSG00000125730
GO:0048015~phosphoinositide-mediated signaling	0,00958169	ENSG00000178538, ENSG00000148180, ENSG00000127533, ENSG00000050628, ENSG00000198959, ENSG00000169403
GO:0032680~regulation of tumor necrosis factor production	0,01041036	ENSG00000137462, ENSG00000090376, ENSG00000158869, ENSG00000136869
GO:0001819~positive regulation of cytokine production	0,0105006	ENSG00000150782, ENSG00000137462, ENSG00000137801, ENSG00000158869, ENSG00000136869, ENSG00000162711
GO:0030041~actin filament polymerization	0,01085148	ENSG00000007237, ENSG00000148180, ENSG00000047648
GO:0002714~positive regulation of B cell mediated immunity	0,01085148	ENSG00000158869, ENSG00000130202, ENSG00000125730
GO:0010812~negative regulation of cell-substrate adhesion	0,01085148	ENSG00000137801, ENSG00000047648, ENSG00000157227
GO:0002891~positive regulation of immunoglobulin mediated immune response	0,01085148	ENSG00000158869, ENSG00000130202, ENSG00000125730
GO:0019220~regulation of phosphate metabolic process	0,01255559	ENSG00000090376, ENSG00000136158, ENSG00000198121, ENSG00000134215, ENSG00000137834, ENSG00000139132, ENSG00000163235, ENSG00000166068, ENSG00000170962, ENSG00000137801, ENSG00000174233, ENSG00000123384, ENSG00000157404, ENSG00000136869, ENSG00000165025
GO:0051174~regulation of phosphorus metabolic process	0,01255559	ENSG00000090376, ENSG00000136158, ENSG00000198121, ENSG00000134215, ENSG00000137834, ENSG00000139132, ENSG00000163235, ENSG00000166068, ENSG00000170962, ENSG00000137801, ENSG00000174233, ENSG00000123384, ENSG00000157404, ENSG00000136869, ENSG00000165025
GO:0001666~response to hypoxia	0,01427804	ENSG00000150782, ENSG00000184916, ENSG00000137801, ENSG00000140465, ENSG00000157227, ENSG00000109107, ENSG00000154188
GO:0032103~positive regulation of response to external stimulus	0,01452974	ENSG00000137801, ENSG00000158869, ENSG00000136869, ENSG00000198959, ENSG00000125730
GO:0007155~cell adhesion	0,01512673	ENSG00000101955, ENSG00000074660, ENSG00000149557, ENSG00000047648, ENSG00000133401, ENSG00000130202, ENSG00000140678, ENSG00000079112, ENSG00000173801, ENSG00000167851, ENSG00000105501, ENSG00000149294, ENSG00000184226, ENSG00000137801, ENSG00000168995, ENSG00000038427, ENSG00000148848, ENSG00000170558, ENSG00000165025
GO:0010863~positive regulation of phospholipase C activity	0,01530891	ENSG00000047648, ENSG00000127533, ENSG00000198121, ENSG00000050628, ENSG00000198959
GO:0007202~activation of phospholipase C activity	0,01530891	ENSG00000047648, ENSG00000127533, ENSG00000198121, ENSG00000050628, ENSG00000198959
GO:0019932~second-messenger-mediated signaling	0,02283101	ENSG00000188822, ENSG00000178538, ENSG00000148180, ENSG00000174233, ENSG00000127533, ENSG00000050628, ENSG00000086730, ENSG00000198959, ENSG00000169403
GO:0042035~regulation of cytokine biosynthetic process	0,02351302	ENSG00000156575, ENSG00000073792, ENSG00000136869, ENSG00000103855, ENSG00000165025
GO:0002768~immune response-regulating cell surface receptor signaling pathway	0,02364251	ENSG00000137462, ENSG00000197943, ENSG00000086730, ENSG00000165025
GO:0030097~hemopoiesis	0,02364327	ENSG00000092067, ENSG00000184916, ENSG00000078399, ENSG00000140968, ENSG00000197943, ENSG00000157404, ENSG00000048052, ENSG00000198719, ENSG00000165025
GO:0010647~positive regulation of cell communication	0,0238142	ENSG00000163235, ENSG00000149294, ENSG00000137801, ENSG00000157404, ENSG00000136869, ENSG00000081052, ENSG00000198121, ENSG00000198959, ENSG00000079215, ENSG00000152804, ENSG00000165025
GO:0050867~positive regulation of cell activation	0,02397742	ENSG00000150782, ENSG00000137801, ENSG00000136869, ENSG00000103855, ENSG00000130202, ENSG00000165025
GO:0060193~positive regulation of lipase activity	0,02456069	ENSG00000047648, ENSG00000127533, ENSG00000198121, ENSG00000050628, ENSG00000198959
GO:0032655~regulation of interleukin-12 production	0,02532727	ENSG00000137801, ENSG00000090376, ENSG00000136869
GO:0070555~response to interleukin-1	0,02532727	ENSG00000115594, ENSG00000134070, ENSG00000090376
GO:0051347~positive regulation of transferase activity	0,02566403	ENSG00000163235, ENSG00000139132, ENSG00000137801, ENSG00000174233, ENSG00000123384, ENSG00000157404, ENSG00000198121, ENSG00000134215, ENSG00000165025
GO:0002699~positive regulation of immune effector process	0,0267022	ENSG00000158869, ENSG00000130202, ENSG00000125730, ENSG00000165025
GO:0051240~positive regulation of multicellular organismal process	0,02762689	ENSG00000150782, ENSG00000137462, ENSG00000137801, ENSG00000158869, ENSG00000136869, ENSG00000081052, ENSG00000103855, ENSG00000079215, ENSG00000162711
GO:0002275~myeloid cell activation during immune response	0,02822146	ENSG00000137462, ENSG00000136869, ENSG00000086730
GO:0032958~inositol phosphate biosynthetic process	0,02920514	ENSG00000197943, ENSG00000169403
GO:0002888~positive regulation of myeloid leukocyte mediated immunity	0,02920514	ENSG00000158869, ENSG00000125730
GO:0032959~inositol trisphosphate biosynthetic process	0,02920514	ENSG00000197943, ENSG00000169403

Supplementary Table S7. List of 16 gene families and their members, including HIV restriction factors (RFs; in bold letters). The list of RFs was obtained from (Abdel-Mohsen et al 2013). RFs that do not belong to any gene family: CDKN1A, HERC5, ISG15, RSAD2. RFs that restricts late stages of HIV life cycle: BST2, EIF2AK2, MOV10, ISG15, RSAD2 and SLFN11.

Gene family	Gene symbol											
Ankyrin repeat domain containing	ABTB1	ANKFY1	ANKRD13D	SLF1	ANKRD53	ARAP2	ASB16	DGKI	IBTK	NFKB2	POTEJ	SOWAHB
	ABTB2	ANKHD1	ANKRD16	ANKRD33	ANKRD54	ARAP3	ASB17	DZANK1	ILK	NOTCH1	POTEM	SOWAHC
	ACAP1	ANKIB1	ANKRD17	ANKRD33B	ANKRD55	ASAP1	ASB18	EHMT1	INVS	NOTCH2	PPP1R12A	SOWAHD
	ACAP2	ANKK1	ANKRD18A	ANKRD34A	ANKRD60	ASAP2	ASPG	EHMT2	KANK1	NOTCH3	PPP1R12B	TANC1
	ACAP3	ANKLE1	ANKRD18B	ANKRD34B	ANKRD61	ASAP3	ASZ1	ESPN	KANK2	NOTCH4	PPP1R12C	TANC2
	ACBD6	ANKLE2	ANKRD20A1	ANKRD34C	ANKRD62	ASB1	BANK1	ESPNL	KANK3	NRARP	PPP1R13B	TNKS
	AGAP1	ANKMY1	ANKRD20A2	ANKRD35	ANKRD63	ASB2	BARD1	FANK1	KANK4	NUDT12	PPP1R13L	TNKS2
	AGAP2	ANKMY2	ANKRD20A3	ANKRD36	ANKRD65	ASB3	BCL3	FEM1A	KIDINS220	OSBPL1A	PPP1R16A	TONSL
	AGAP3	ANKRA2	ANKRD20A4	ANKRD36B	ANKRD66	ASB4	BCOR	FEM1B	KRIT1	OSTF1	PPP1R16B	TP53BP2
	AGAP4	ANKRD1	ANKRD22	ANKRD36C	ANKS1A	ASB5	BCORL1	FEM1C	MIB1	PLA2G6	PPP1R27	TRANK1
	AGAP5	ANKRD2	ANKRD23	ANKRD37	ANKS1B	ASB6	BTBD11	FPGT-TNNI3K	MIB2	POTEA	PSMD10	TRPA1
	AGAP6	ANKRD6	ANKRD24	ANKRD39	ANKS3	ASB7	CASKIN1	GABPB1	MPHOSPH8	POTEB	RAI14	
	AGAP7P	ANKRD7	ANKRD26	ANKRD40	ANKS4B	ASB8	CASKIN2	GABPB2	MTPN	POTEB2	RFXANK	
	AGAP9	ANKRD9	ANKRD27	ANKRD42	ANKS6	ASB9	CDKN2C	GIT1	MYO16	POTEC	RIPK4	
	AGAP11	ANKRD10	ANKRD28	ANKRD44	ANKUB1	ASB10	CDKN2D	GIT2	NFKBIA	POTED	**RNASEL**	
	ANKAR	ANKRD11	ANKRD29	ANKRD45	ANKZF1	ASB11	CLIP3	GLS	NFKBIB	POTEE	SHANK1	
	ANKDD1A	ANKRD12	ANKRD30A	ANKRD46	ANK1	ASB12	CLIP4	GLS2	NFKBID	POTEF	SHANK2	
	ANKDD1B	ANKRD13A	ANKRD30B	ANKRD49	ANK2	ASB13	CLPB	GPANK1	NFKBIE	POTEG	SHANK3	
	ANKEF1	ANKRD13B	ANKRD30BL	ANKRD50	ANK3	ASB14	CTTNBP2	HACE1	NFKBIZ	POTEH	SNCAIP	
	ANKFN1	ANKRD13C	ANKRD31	ANKRD52	ARAP1	ASB15	DAPK1	HECTD1	NFKB1	POTEI	SOWAHA	
	ZDHHC13	ZDHHC17	USH1G	UACA	TRPV6	TRPV5	TRPV4	TRPV3	TRPV2	TRPV1	TRPC4	
Gene family	**Gene symbol**											
CD molecules	CD1A	CD24	ITGA2	NT5E	CD96	IL5RA	KIR2DL2	IGLL1	IL15RA	CD248	TLR6	CDCP1
	CD1B	IL2RA	ITGA3	CD74	ADGRE5	IL6R	KIR2DL3	CD180	IL17RA	ENPEP	TLR8	SLAMF7
	CD1C	DPP4	ITGA4	CD79A	SLC7A5	IL7R	KIR3DP1	CXCR1	IL18R1	TNFSF4	TLR9	CD320
	CD1D	CD27	ITGA5	CD79B	CD99	IL9R	KIR2DL4	CXCR2	IL18RAP	TNFSF10	TLR10	F11R
	CD1E	CD28	ITGA6	CD80	SEMA4D	IL6ST	KIR3DL1	CXCR3	INSR	TNFSF11	BMPR1A	JAM2
	CD2	CTLA4	ICAM3	CD81	CD101	CSF2RB	KIR2DL5A	CXCR4	IGF1R	TNFSF13	BMPR1B	CDH1
	CD3D	ITGB1	ITGAV	CD82	ICAM2	IL2RG	KIR2DS5	CXCR5	IGF2R	TNFSF13B	PTGDR2	CDH2
	CD3E	TNFRSF8	CD52	CD83	ITGAE	PROM1	KIR2DS1	CXCR6	LAG3	TNFSF14	LEPR	EPCAM
	CD3G	PECAM1	CD53	CD84	ITGB4	TNFRSF4	KIR2DS4	CCR1	GGT1	TNFRSF10A	ART1	SIGLEC6
	CD4	FCGR2A	ICAM1	LILRB3	ENG	FLT3	KIR2DS2	CCR2	IFITM1	TNFRSF10B	ART4	SIGLEC7
	CD5	FCGR2B	CD55	LILRA6	VCAM1	MST1R	KIR3DL2	CCR3	CD226	TNFRSF10C	ATP1B3	SIGLEC9
	CD6	FCGR2C	NCAM1	LILRB5	LAMP1	TNFRSF9	KIR3DL3	CCR4	MUC1	TNFRSF10D	CLEC4M	FGFR1
	CD7	CD33	B3GAT1	LILRB2	LAMP2	SDC1	KLRC1	CCR5	MELTF	TNFRSF11A	CD300A	FGFR2
	CD8A	CD34	CD58	LILRA3	SEMA7A	PDGFRA	KLRC2	CCR6	LY9	TNFRSF12A	CD300C	FGFR3
	CD8B	CR1	CD59	LILRA5	CD109	PDGFRB	CD160	CCR7	PRNP	TNFRSF13B	CD300E	FGFR4
	CD9	CD36	ITGB3	LILRA4	MPL	THBD	KLRB1	CCR8	TSPAN7	TNFRSF13C	CLEC10A	NCR1
	MME	CD37	SELE	LILRA2	NECTIN1	F3	SELPLG	CCR9	PLXNC1	TNFRSF17	CD302	NCR2
	ITGAL	CD38	SELL	LILRA1	NECTIN2	ACE	CD163	CD200	SLC4A1	TNFRSF14	CLEC4C	NCR3
	ITGAM	ENTPD1	SELP	LILRB1	NECTIN3	CDH5	CD164	PROCR	ACKR1	NGFR	NRP1	ABCG2
	ITGAX	CD40	CD63	LILRB4	CSF3R	MCAM	ALCAM	TEK	GYPA	BTLA	LAIR1	JAG1
	ITGAD	ITGA2B	FCGR1A	LILRP1	CSF1R	BSG	DDR1	ENPP3	GYPB	PDCD1LG2	LAIR2	ERBB2
	ANPEP	GP9	CEACAM1	LILRP2	CSF2RA	PTPRJ	HMMR	MSR1	GYPC	CD274	FCRL1	FZD4
	CD14	GP1BA	CEACAM8	CD86	KIT	SLAMF1	SIGLEC1	LY75	KEL	ICOSLG	FCRL2	FZD9
	FUT4	GP1BB	CEACAM6	PLAUR	LIFR	CD151	SIGLEC5	MRC1	BCAM	CD276	FCRL3	FZD10
	FCGR3A	GP5	CEACAM3	C5AR1	IFNGR1	TNFSF8	L1CAM	CD207	RHCE	BTN3A1	FCRL4	FCAMR
	FCGR3B	SPN	CEACAM5	FCAR	TNFRSF1A	CD40LG	SIRPA	LAMP3	RHD	ICOS	FCRL5	SLAMF6
	ITGB2	CD44	PSG1	THY1	TNFRSF1B	PVR	SIRPB1	CD209	RHAG	PDCD1	KDR	SLAMF8
	CD19	PTPRC	CD68	LRP1	IL1R1	ADAM10	SIRPG	IL10RA	ICAM4	MRC2	ADGRE2	TREM1
	MS4A1	CD46	CD69	SLC44A1	IL1R2	ADAM8	FUT3	IL10RB	ABCB1	TLR1	KLRK1	CRTAM
	CR2	CD47	CD70	CD93	IL2RB	ADAM17	CD177	IL12RB1	CD244	TLR2	PTGFRN	TNFRSF18
	CD22	CD48	TFRC	KLRD1	IL3RA	BST1	FASLG	IL13RA1	ALK	TLR3	IGSF8	TNFRSF21
	FCER2	ITGA1	CD72	FAS	IL4R	KIR2DL1	VPREB1	IL13RA2	CD247	TLR4	**BST2**	IL21R
	EVI2B	SDC2	PI16	S1PR1	HAVCR1	CLEC4A	CLEC4D	CLEC7A	CLEC9A	CLEC12A		
Gene family	**Gene symbol**											
Ring finger proteins	ANAPC11	NSMCE1	RNF19A	ZNRF1	CBL	TRIM9	TRAF2	RNF133	LTN1	TRIM43	RFWD3	RNF224
	BARD1	PCGF7P	RNF19B	RNF43	CBLB	**TRIM11**	TRAF3	PCGF6	MEX3A	TRIM43B	ZNRF2	RNF225
	CCNB1IP1	PDZRN3	RNF20	RNF44	CBLC	TRIM15	TRAF7	RNF135	CNBP	TRIM44	ZNRF3	RNF227
	CNOT4	PDZRN4	TRIM34	AMFR	DTX2	TRIM22	RFPL3	BIRC8	RC3H2	TRIM46	ZNRF4	RSPRY1
	CYHR1	RBBP6	TRIM3	TRIM23	MID1	TRIM26	RNF121	TRIM68	RNF165	TRIM49B	RAPSN	SCAF11
	DCST1	RNFT1	TRIM39	BFAR	MID2	TRIM28	RNF122	RNF138	RNF166	TRIM49C	TRAIP	SHPRH
	DZIP3	RNFT2	RNF24	BIRC2	MKRN1	TRIM36	RNF123	RNF139	RNF167	TRIM49D1	RNF207	SH3RF3
	LNX1	RING1	RNF25	BIRC3	MKRN2	TRIM45	RNF125	DTX1	RNF168	TRIM49D2	RNF208	SIAH1
	LNX2	RNF2	RNF26	BIRC7	MKRN3	TRIM47	RNF126	RNF141	RNF169	TRIM50	TRIML1	SIAH2
	LRSAM1	PCGF3	TRIM8	BMI1	MKRN4P	TRIM48	LONRF3	SH3RF1	RNF170	TRIM51	RFPL4A	SYVN1
	MAP3K1	RNF4	TRIM63	BRAP	MKRN9P	TRIM52	RNF128	DTX3L	RNF185	TRIM58	RFPL4AL1	TOPORS
	MDM2	RNF5	TRIM55	BRCA1	MNAT1	RNF103	RNF130	RNF144A	RNF186	TRIM62	RFPL4B	TRIM31
	MDM4	RNF6	TRIM54	RFPL2	NEURL1	TRIM59	PJA2	RNF144B	RNF187	TRIM64	RNF212	TRIM32
	MIB1	RNF7	RNF31	HLTF	NEURL1B	TTC3	SH3RF2	RNF145	CBLL1	TRIM64B	RNF212B	TRIM33
	MIB2	RNF8	RNF32	**TRIM21**	PCGF1	UHRF1	PCGF5	RNF146	RFFL	TRIM64C	RNF213	TRIM35
	MKRN5P	TRIM10	TRIM60	TRIM24	PEX10	UHRF2	VPS41	TRIM25	LONRF1	TRIM65	RNF214	TRIM37
	MKRN6P	RNF10	RNF34	TRAF4	PJA1	VPS11	XIAP	RNF148	LONRF2	TRIM67	RNF215	TRIM41
	MKRN7P	RNF11	TRIM40	TRAF5	**TRIM19**	TRIM56	CBLL2	RNF149	MEX3D	TRIM71	RNF216	TRIM42
	MKRN8P	RLIM	TRIM61	TRAF6	PEX2	PCGF2	ZSWIM2	RNF150	MEX3C	TRIM72	RNF217	
	MYCBP2	RNF13	TRIM69	TRIM2	RAD18	RNF111	RNF180	RNF151	MEX3B	TRIM73	MUL1	
	MYLIP	RNF14	UBOX5	TRIM4	RAG1	RNF112	RNF181	RNF152	CHFR	TRIM74	RNF219	
	NFXL1	TRIM38	RNF38	**TRIM5**	RBX1	RNF113A	RNF182	DTX3	CGRRF1	TRIM75P	RNF220	
	NFX1	TRIM17	RNF39	TRIM6	TRIM27	RNF113B	RNF183	DTX4	RC3H1	TRIM77	PHRF1	
	NHLRC1	RNF17	RNF40	TRIM7	TRIM13	RNF114	RNF175	MGRN1	RCHY1	UNKL	RNF222	
	RBCK1	TRIM49	RNF41	NEURL3	RFPL1	RNF115	MSL2	RNF157	COP1	VPS8	RNF223	

Gene family	**Gene symbol**											
Tripartite motif containing	MID2	TRIM26BP	TRIM49B	TRIM62	TRIM10	TRIM36	TRIM51EP	TRIM66	MEFV	TRIM43CP	TRIM54	TRIM77
	TRIM2	TRIM27	TRIM49C	TRIM63	TRIM11	TRIM37	TRIM51FP	TRIM67	TRIM21	TRIM44	TRIM55	TRIM58
	TRIM3	TRIM28	TRIM49D1	TRIM64	TRIM13	TRIM38	TRIM51GP	TRIM68	**TRIM22**	TRIM45	TRIM56	TRIM59
	TRIM4	TRIM29	TRIM49D2	TRIM64B	**TRIM14**	TRIM39	TRIM51HP	TRIM69	TRIM23	TRIM46	CMYA5	TRIM74
	TRIM5	TRIM31	TRIM50	TRIM64C	TRIM15	TRIM40	TRIM51JP	TRIM71	TRIM24	TRIM47	**TRIM26**	TRIM75P
	TRIM6	**TRIM32**	TRIM51	TRIM64DP	TRIM16	TRIM41	TRIM52	TRIM72	TRIM25	TRIM48	TRIM60	TRIM53BP
	TRIM7	TRIM33	TRIM51BP	TRIM64EP	TRIM17	TRIM42	TRIM53AP	TRIM73	TRIM43B	TRIM49	TRIM61	TRIM53CP
	TRIM8	TRIM34	TRIM51CP	TRIM64FP	MID1	TRIM43	TRIM9	TRIM35	TRIM51DP	TRIM65	PML	
Gene family	**Gene symbol**											
PHD finger proteins	AIRE	BAZ2B	CHD4	DPF3	ING5	KDM5B	KMT2C	NFX1	PHF6	PHF11	JADE1	INTS12
	ASH1L	BPTF	CHD5	FBXL19	KAT6A	KDM5C	KMT2D	NSD1	PHF7	PHF12	PHF19	PHF23
	ASH2L	BRD1	CXXC1	ING1	KAT6B	KDM5D	KMT2E	PHF1	G2E3	PHF13	PHF20	
	BAZ1A	BRPF1	DIDO1	ING2	KDM2A	KDM7A	MLLT6	PHF2	PHF8	PHF14	PHF20L1	
	BAZ1B	BRPF3	DPF1	ING3	KDM2B	KMT2A	MLLT10	PHF3	FANCL	JADE2	PHF21A	
	BAZ2A	CHD3	DPF2	ING4	KDM5A	KMT2B	MTF2	PHF5A	PHF10	JADE3	PHF21B	
	RSF1	SP100	SP140	TAF3	TRIM24	TRIM33	UHRF1	NSD2	ZMYND8	NSD3	ZMYND11	
	SHPRH	SP110	SP140L	TCF19	TRIM28	TRIM66	UHRF2	PYGO2	PYGO1	PHRF1	PHF24	
Gene family	**Gene symbol**											
Tetratricopeptide repeat domain containing	ANAPC7	FKBPL	IFIT2	NASP	RANBP2	SGTA	ST13	TRANK1	TTC8	TRAPPC12	TTC23	TTC31
	BBS4	FKBP4	IFIT3	NCF2	RGPD1	SGTB	TANC1	TTC1	TTC9	TTC16	TTC24	TTC32
	CDC16	FKBP5	IFIT5	NPHP3	RGPD2	SH3TC1	TANC2	DNAJC7	TTC9B	TTC17	TTC25	TTC33
	CDC23	FKBP8	KDM6A	OGT	RGPD3	SH3TC2	TMTC1	TTC3	TTC9C	CFAP70	TTC26	TTC34
	CDC27	GPSM1	KLC1	PEX5	RGPD4	SNX21	TMTC2	TTC4	IFT88	TTC19	TTC27	EMC2
	CNOT10	GPSM2	KLC2	PEX5L	RGPD5	SPAG1	TMTC3	TTC5	FIS1	KIF1BP	TTC28	
	CTR9	GTF3C3	KLC3	PPID	RGPD6	SRP72	TMTC4	TTC6	TTC12	TTC21A	TTC29	
	DNAJC3	IFIT1	KLC4	PPP5C	RGPD8	STIP1	TOMM34	TTC7A	TTC13	TTC21B	TTC30A	
	DNAAF4	IFIT1B	NAA16	PPP5D1	RPAP3	STUB1	TOMM70	TTC7B	TTC14	TTC22	TTC30B	
	TTC39B	TTC39C	CFAP46	UTY	WDTC1	ZC3H7A	ZC3H7B	TTC39A	TTC38	TTC37	TTC36	
Gene family	**Gene symbol**											
Protein phosphatase 1 regulatory subunits	PPP1R1A	PPP1R10	PPP1R17	PPP1R32	AURKA	CEP192	AATK	IKZF1	MYO1D	PHACTR3	SFI1	TMEM225
	PPP1R1B	PPP1R11	PPP1R18	ARFGEF3	AURKB	CLCN7	AHCYL1	ITGA2B	NCOR1	PHACTR4	SFPQ	TNS1
	PPP1R1C	PPP1R12A	URI1	MARF1	AXIN1	CNST	ANKRD42	ITPR1	NEFL	PHRF1	SLC12A2	TRA2B
	PPP1R2	PPP1R12B	CCDC8	PPP1R35	BCL2	ANKRD28	CAMSAP3	ITPR3	NEK2	PKMYT1	SLC7A14	TRIM28
	PPP1R3A	PPP1R12C	PPP1R21	PPP1R36	BCL2L1	DZIP3	CDCA2	KCNA6	NOC2L	PLCL1	SLC9A1	TRPC4AP
	PPP1R3B	TP53BP2	CHCHD3	PPP1R37	BCL2L2	EIF2S2	DLG3	KCNK10	NOM1	POLD3	SMARCB1	
	PPP1R3C	PPP1R13B	CHCHD6	SH2D4A	BRCA1	ELL	**EIF2AK2**	KIF18A	NONO	PREX2	SPATA2	
	PPP1R3D	PPP1R14A	CSMD1	SH3RF2	CASC1	ZFYVE16	GPR12	LMTK2	OCLN	RB1CC1	SPOCD1	
	PPP1R3E	PPP1R14B	DDX31	TRIM42	KNL1	SH3GLB1	GRM1	LMTK3	OPN3	RBM26	SPRED1	
	PPP1R3F	PPP1R14C	PPP1R26	ZCCHC9	CASP9	PTK2	GRM5	MAP1B	ORC5	RIMBP2	SPZ1	
	PPP1R3G	PPP1R14D	PPP1R27	PPP1R42	CASP2	CSRNP2	GRM7	MAPT	PARD3	RPGRIP1L	SRSF10	
	PPP1R7	PPP1R15A	ELFN1	AKAP1	DLG2	CSRNP3	GRXCR1	MCM7	PCDH11X	RPL5	STAU1	
	PPP1R8	PPP1R15B	ELFN2	AKAP11	CD2BP2	FER	HCFC1	MKI67	PCDH7	RRP1B	SYTL2	
	PPP1R9A	PPP1R16A	GPATCH2	AKAP9	CDC25C	FARP1	HDAC6	MPHOSPH10	PCIF1	RYR1	TMEM132C	
	PPP1R9B	PPP1R16B	HYDIN	APC	CENPE	FKBP15	HSPB6	MYO16	PFKM	SACS	TMEM132D	
	YLPM1	WWC1	WNK1	WDR81	WBP11	VPS54	VDR	UBN1	TSKS	TSC2	TRPC5	
Gene family	**Gene symbol**											
Sterile alpha motif domain containing	ANKS1A	ARAP3	CNKSR2	EPHA3	EPHB1	KIF24	PHC3	PPP1R9A	SAMD8	SAMD14	SCMH1	
	ANKS1B	ASZ1	CNKSR3	EPHA4	EPHB2	LRSAM1	PPFIA1	SAMD1	SAMD9	SAMD15	SCML1	
	ANKS3	BFAR	DDHD2	EPHA5	EPHB3	L3MBTL1	PPFIA2	SAMD3	SAMD9L	**SAMHD1**	SCML2	
	ANKS4B	BICC1	DGKD	EPHA6	EPHB4	L3MBTL3	PPFIA3	SAMD4A	SAMD10	SAMSN1	SCML4	
	ANKS6	CASKIN1	DGKH	EPHA7	EPHB6	L3MBTL4	PPFIA4	SAMD4B	SAMD11	SARM1	SEC23IP	
	ARAP1	CASKIN2	EPHA1	EPHA8	INPPL1	PHC1	PPFIBP1	SAMD5	SAMD12	SASH1	SFMBT1	
	ARAP2	CNKSR1	EPHA2	EPHA10	KAZN	PHC2	PPFIBP2	SAMD7	SAMD13	SASH3	SFMBT2	
	TNKS2	USH1G	WDSUB1	ZCCHC14	TNKS	STIM2	STIM1	SHANK3	SHANK2	SHANK1	SGMS1	
Gene family	**Gene symbol**											
Apolipoprotein B mRNA editing enyzme catalytic subunits	AICDA	APOBEC1	APOBEC2	**APOBEC3A**	APOBEC3A_B	**APOBEC3B**	**APOBEC3C**	**APOBEC3D**	**APOBEC3F**	**APOBEC3G**	**APOBEC3H**	APOBEC4
Gene family	**Gene symbol**											
Minor histocompability antigens	AKAP13	BCL2A1	C19orf48	ERAP1	ARHGAP45	PUM3	MTHFD1	PI4K2B	P2RX5	SON	TMSB4Y	
	APOBEC3B	CD19	DDX3Y	ERBB2	HMHB1	RESF1	MYO1G	PKN3	RPS4Y1	SP110		
	ARHGDIB	CENPM	DPH1	GEMIN4	HMSD	LY75	NUP133	PRCP	SLC1A5	SSR1		
	BCAT2	CTSH	EBI3	HEATR1	KDM5D	MR1	PDCD11	PTK2B	SLC19A1	SWAP70		
	ZNF419	WNK1	UTY	USP9Y	UGT2B17	TRIP10	TYMP	TRIM42	TRIM22	TOR3A		
Gene family	**Gene symbol**											
Bardet-Biedl syndrome associated	BBS1	BBS2	ARL6	BBS4	MKS1	SDCCAG8	IFT27					
	BBS5	BBS7	BBS9	TRIM32	CEP290	LZTFL1	IFT172					
	MKKS	TTC8	BBS10	BBS12	WDPCP	BBIP1	C8orf37					
Gene family	**Gene symbol**											
Paf1/RNA polymerase II complex	CDC73	CTR9	LEO1	**PAF1**	**RTF1**	WDR61						
Gene family	**Gene symbol**											
Schlafen family	SLFN5	**SLFN11**	SLFN12	SLFN12L	SLFN13	SLFN14	SLFNL1					
Gene family	**Gene symbol**											
UPF1 like RNA helicases	AQR	DNA2	HELZ	HELZ2	IGHMBP2	**MOV10**	MOV10L1	SETX	UPF1	ZGRF1	ZNFX1	
Gene family	**Gene symbol**											
Bromodomain containing	ATAD2	BAZ1B	BPTF	BRD8	BRPF3	CECR2	KAT2A	ASH1L	SMARCA2	SP110		
	ATAD2B	BAZ2A	BRD1	BRD9	BRWD1	CREBBP	KAT2B	PBRM1	SMARCA4	SP140		
	BAZ1A	BAZ2B	BRD7	BRPF1	BRWD3	EP300	KMT2A	PHIP	SP100	SP140L		
	TRIM28	TRIM33	TRIM66	ZMYND8	ZMYND8	ZMYND11	TRIM24	TAF1L	TAF1			
Gene family	**Gene symbol**											
Interferon induced transmembrane proteins	**IFITM1**	**IFITM3**	IFITM8P	IFITM5								
	IFITM2	IFITM4P	IFITM9P	IFITM10								

Supplementary Table S8. List of genes from Group II that belong to the families of cellular restriction factors (RFs) restricting late stages of HIV life cycle. Connection between each genes and HIV infection was checked in HIV interaction database (https://www.ncbi.nlm.nih.gov/genome/viruses/retroviruses/hiv-1/interactions/) or in literature.

Gene symbol	Connection with HIV	Source of information
Aatk	Yes	https://www.ncbi.nlm.nih.gov/genome/viruses/retroviruses/hiv-1/interactions/browse/
Camsap3	Yes	https://www.ncbi.nlm.nih.gov/genome/viruses/retroviruses/hiv-1/interactions/browse/
Klrc2	Yes	https://www.ncbi.nlm.nih.gov/genome/viruses/retroviruses/hiv-1/interactions/browse/
Klrd1	Yes	https://www.ncbi.nlm.nih.gov/genome/viruses/retroviruses/hiv-1/interactions/browse/
Lrp1	Yes	https://www.ncbi.nlm.nih.gov/genome/viruses/retroviruses/hiv-1/interactions/browse/
Ncr1	Yes	https://www.ncbi.nlm.nih.gov/genome/viruses/retroviruses/hiv-1/interactions/browse/
Ncr3	Yes	https://www.ncbi.nlm.nih.gov/genome/viruses/retroviruses/hiv-1/interactions/browse/
Siglec7	Yes	https://www.ncbi.nlm.nih.gov/genome/viruses/retroviruses/hiv-1/interactions/browse/
Tlr2	Yes	https://www.ncbi.nlm.nih.gov/genome/viruses/retroviruses/hiv-1/interactions/browse/
Tlr4	Yes	https://www.ncbi.nlm.nih.gov/genome/viruses/retroviruses/hiv-1/interactions/browse/
Tnfrsf10d	Yes	https://www.ncbi.nlm.nih.gov/genome/viruses/retroviruses/hiv-1/interactions/browse/
Tnfsf11	Yes	https://www.ncbi.nlm.nih.gov/genome/viruses/retroviruses/hiv-1/interactions/browse/
Klrb1	Yes	https://academic.oup.com/intimm/article/19/8/943/707672
Klrc1	Yes	https://www.ncbi.nlm.nih.gov/pubmed/18976975
Lilra2	Yes	https://www.ncbi.nlm.nih.gov/pmc/articles/PMC3250304/
Lilrp2	Yes	https://www.ncbi.nlm.nih.gov/pmc/articles/PMC3250304/
Ncam1	Yes	https://www.ncbi.nlm.nih.gov/pmc/articles/PMC5892189/
Ncr2	Yes	https://www.ncbi.nlm.nih.gov/pubmed/19424050
Siglec5	Yes	https://www.ncbi.nlm.nih.gov/pubmed/22945238
Slfn13	Yes	https://www.nature.com/articles/s41467-018-03544-x
Tnfrsf18	Yes	https://www.ncbi.nlm.nih.gov/pmc/articles/PMC2872147/
Tnfsf4	Yes	https://www.ncbi.nlm.nih.gov/pubmed/24238037
Bcl2L2	No	
Plxnc1	No	
Slfn12	No	
Spred1	No	
Ppp1r26	No	
Ppp1r9A	No	

The results of this thesis will be soon submitted as a journal article; manuscript in preparation:

Schlafen12, a novel HIV restriction factor involved in latency

Katarína Smutná[1*], Mie Kobayashi-Ishihara[1*], Anna-Esteve Godina[2,3], Javier P. Martinez[1], Jennifer Jungfleisch[4], Rene Boettcher[4], Selina Rogenmoser[1], Makoto Yamagishi[5], Yasuko Tsunetsugu-Yokota[6], Juana Díez Antón[4, 7], Jordi Argilaguet[1] and Andreas Meyerhans[1,7]

[1] Infection Biology Group, Department of Experimental and Health Sciences, Universitat Pompeu Fabra, Barcelona, Spain
[2] CNAG-CRG, Center for Genomic Regulation (CRG), Barcelona Institute of Science and Technology, Barcelona, Spain
[3] Universitat Pompeu Fabra, Barcelona, Spain
[4] Molecular Virology Group, Department of Experimental and Health Sciences, Universitat Pompeu Fabra, Barcelona, Spain
[5] Graduate School of Frontier Sciences, University of Tokyo, Tokyo, Japan
[6] Department of Medical Technology, School of Human Sciences, Tokyo University of Technology, Tokyo, Japan
[7] Institució de Recerca i Estudis Avançats (ICREA), Barcelona, Spain

These authors contributed equally to this work
*Corresponding authors

Correspondence:
Andreas Meyerhans, Ph.D.
andreas.meyerhans@upf.edu

DISCUSSION

In this thesis, we aimed to identify cellular factors that may contribute to HIV latency via interference with post-transcriptional events of the HIV life cycle. Based on own observations of a differential behavior of latently infected naive and memory CD4 T cells towards HIV latency reversal (Tsunetsugu-Yokota et al. 2016b), the transcriptomes of primary CD4 T cells maintained under different culture conditions were determined and inspected for possible HIV regulators. Naive T cells that were maintained under HSP conditions show an upregulation of TLR and TLR-signalling genes, suggesting their readiness to receive danger signals from incoming pathogens. Furthermore, the TFs *Uaca* and *Tle1* that suppress NF-kB factor transcription were upregulated, as were the single-strand specific *RNase2* with an antiviral activity and *Irf8*, a TF that can maintain HIV proviruses in a latent state by repressing the HIV promoter. Interestingly, amongst the upregulated genes was also *Slfn12*, a member of a conserved family of proteins with antiviral activities. It includes SLFN11 that could inhibit HIV translation based on its non-optimal codon usage (M. Li et al. 2012). Since relatively little was known on the mechanism of their antiviral activity and their potential role in latency, SLFN11 and 12 were cloned and analyzed further. We could show that they both participate in the maintenance of HIV latency and inhibit HIV translation in a codon-usage dependent manner at the level of translation elongation. Together this increases our basic knowledge on virus latency and suggests target proteins for novel HIV cure strategies.

1. HIV latency and cure

The capacity of HIV to remain in a latent state that is non-visible for the immune system and antiretroviral drugs is a main obstacle for an HIV cure. Productive HIV infection proceeds most efficiently in activated CD4 T cells that (i) express high levels of CD4 and the co-receptors CCR5 or CXCR4 (Maier et al. 2000), (ii) have a high level of dNTPs necessary for efficient reverse transcription of the viral RNA genome (Meyerhans et al. 1994) and (iii) express the transcription factors NFAT and NFkB that activate the HIV promoter of the 5´LTR region (Kinoshita et al. 1997; Nabel and Baltimore 1987). However, such cells *in vivo* rapidly dye due to virus-mediated apoptosis or cytotoxic T cell-mediated killing and have a half-life of less than 1 day. As a consequence, these cells are rapidly lost once the HIV cycle is

interrupted by efficient cART (Bailey et al. 2006; Tobin et al. 2005). In contrast, latently infected CD4 T cells have an estimated half-life of about 44 months (J. D. Siliciano et al. 2003) and thus cART alone is not able to eliminate this so-called virus reservoir within the life-time of an infected patient. Once treatment is stopped, HIV usually rebounds rapidly within 2 weeks (Tae-Wook Chun et al. 1999; Davey et al. 1999) demonstrating that cure strategies against HIV require additional interventions.

The HIV reservoir is believed to consist mainly of latently infected memory CD4 T cells (Chomont et al. 2009; Guinevere Q. Lee 2016) . Latency can be established early in an HIV infection during the physiological transit from an effector to a memory T cell as this change in differentiation is associated with a number of events that favor latency including i.e. the downregulation of transcription factors necessary for HIV activation (Shan et al. 2017). The reservoir size consists of about 10^5 to 10^7 HIV-infected cells per infected individual (T-W Chun et al. 1998) or 0.03 to 3 infectious units per million resting CD4 T cells (J. D. Siliciano et al. 2003). Due to the dominance of defective proviruses in the latently infected cell population of over 90%, reservoir size determinations may vary significantly depending on the technique chosen. Interestingly, there is evidence that latently infected CD4 T cells can expand by both, homeostatic and antigen-specific proliferation, and still maintain HIV proviruses in a latent form (Chomont et al. 2009; Farber, Yudanin, and Restifo 2013; Simonetti et al. 2016). The mechanisms underlying this expansion are currently unknown. Our own work suggests at least 2 possibilities. First, antisense transcripts may exhibit a dominant suppressor activity and can lock an integrated HIV provirus into a non-reactivatable state thus allowing infected cell expansion without HIV reactivation (Kobayashi-Ishihara et al. 2018). While this work using latently infected T cell clones identified a novel mechanism of latency maintenance, frequency estimates would suggest that it is rather rare and does not apply to the majority of the latently infected cells in HIV patients. Furthermore, it is still unclear whether the antisense transcription-mediated lock of HIV proviruses is permanent *in vivo* or could be unlocked under specific T cell stimulatory conditions. Second, under HSP culture conditions, primary latently infected naive CD4 T cells can suppress HIV provirus expression by both, transcriptional and posttranscriptional mechanisms. RNAseq analyses suggested at least 3 transcription factors (*Uaca*, *Tle1*, and *Irf8*) that potentially could maintain latency by suppressing NF-kB (L. Liu et al. 2009;

Ghosh et al. 2007) and repressing the HIV promoter (Munier et al. 2005). Furthermore, latently infected resting naive CD4 T cells can suppress HIV provirus expression by a posttranscriptional block. Candidate cellular factors mediating this effect are SLFN11 and 12 that were further investigated here. Both genes contribute to dampen HIV protein expression in a codon usage-dependent manner acting at the level of translation elongation. Knock down of both genes in latently infected ACH2 cells lead to a 10 fold increase of HIV production after cell activation. This together with the expression of SLFN12 under HSP conditions suggests that the Schlafen proteins may contribute to keep HIV protein production well controlled even during cell proliferation. While their contribution *in vivo* has yet to be verified, it would not exclude other post-transcriptional contributors to latency such as lack of UPF1 (Rao et al. 2018) and MATR3 (Sarracino et al. 2018) that act at the levels of mRNA stability and nuclear export, respectively.

2. SLFNs against HIV and other viruses

SLFN11 and 12 are members of a conserved, IFN-inducible protein family that inhibit a broad spectrum of viruses. For example, SLFN11 was shown to inhibit HIV (M. Li et al. 2012), murine leukemia virus (MLV) and feline immunodeficiency virus (FIV) (Stabell et al. 2016), while SLFN13 and 14 inhibit influenza (Seong et al. 2017), Zika virus and HIV (Yang et al. 2018; Pisareva et al. 2015), and influenza and varicella-zoster virus (Seong et al. 2017), respectively. Mechanistic antiviral studies were only performed with SLFN11 demonstrating a codon usage-dependent translation inhibition of HIV-1, possibly mediated via limited tRNA availability through specific tRNA binding (M. Li et al. 2012). Subsequent structural and molecular biology studies of SLFN13 and 14 have shown that these proteins have RNAse activity and can cleave tRNAs (Yang et al. 2018; Pisareva et al. 2015), as well as rRNAs (Yang et al. 2018) and mRNAs (Pisareva et al. 2015), thus participating in the control of mRNA translation. Here we verify the codon-usage dependent inhibition of HIV-1 protein production by SLFN11 and demonstrate a similar activity for SLFN12. Both proteins do not affect HIV translation initiation but translation elongation (**Figure R6 D**). Preliminary data also suggest a binding of SLFN11 and 12 to HIV RNA, however,

it is yet unknown whether this interaction is direct or indirect, and whether it is codon-usage-specific or not. Respective experiments are underway.

Irrespective of the detailed mechanisms of how SLFN proteins inhibit HIV reactivation, why were SLFN11 and 12 not identified in a previous global screen for latency maintaining factors? Besnard and colleagues have used latently infected J-Lat T cells that contain a single copy of an integrated HIV construct with an eGFP marker gene (Jordan, Bisgrove, and Verdin 2003). These cells were then transfected with a library of shRNAs linked to mCherry covering the complete genome and the cells were partly stimulated with antibodies to the T cell receptor. Evidence for latency controlling elements then showed up in eGFP and mCherry double positive cells (Besnard et al. 2016). That the SLFN protein family members were not amongst the 335 latency-controlling factors identified by this experimental set-up is not surprising because the eGFP marker gene has an optimized codon usage. As such it is not under SLFN translational control as shown in our experiments with pHIV-NLE that carries an eGFP gene (**Figure R3 E**) and lack of control of codon-optimized HIV-1 Gag p24 (**Figure R5 D**).

Besides HIV, many other viruses including DENV, HCV, WNV, CHKV and ZKV have a non-optimal codon usage and thus a low CAI score (**Figure D1**). Thus, it seems feasible that organisms use “non-optimal codon usage sensing” as a mean of detecting pathogen invasion. Indeed the broad spectrum antiviral activity of the SLFN genes would argue in favor of such a possibility. However, since many cellular genes are also not optimized in their codon usage and have similar CAI score as viral genomes, how could the SLFNs distinguish between friend and foe? While this is not yet understood, this distinction may be controlled at the level of pathogenic RNA detection and IFN induction (Katsoulidis et al. 2009, 2010; Puck et al. 2015). Like the HIV restriction factors TRIM5 alpha, APOBEC3G, SAMHD1, MX2, Tetherin and IFITMs, the SLFN proteins are also IFN inducible and their antiviral effect may be potentiated after pathogen detection. By this way, SLFN proteins may have a physiological role beyond pathogen defence but may become restriction factors when needed. Along these lines, the cellular genes with low CAI scores may help in defining such functions. Respective genes are enriched in the GO terms cell cycle

control and mitosis suggesting that these processes are also under translation control. Future work in this direction clearly deserves attention.

3. Conclusions and Perspectives

In summary, homeostatically proliferating T cells express a multitude of factors that may control HIV latency at a transcriptional and post-transcriptional level. Among these are the SLFN family members 11 and 12 that restrict HIV translation at the level of elongation in a codon usage-dependent manner. This may help to explain latent HIV provirus expansion via cell division and restricted virus production after T cell reactivation. Given their possible role in cell cycle control under non-infectious conditions, their utility as targets in HIV cure strategies has yet to be determined.

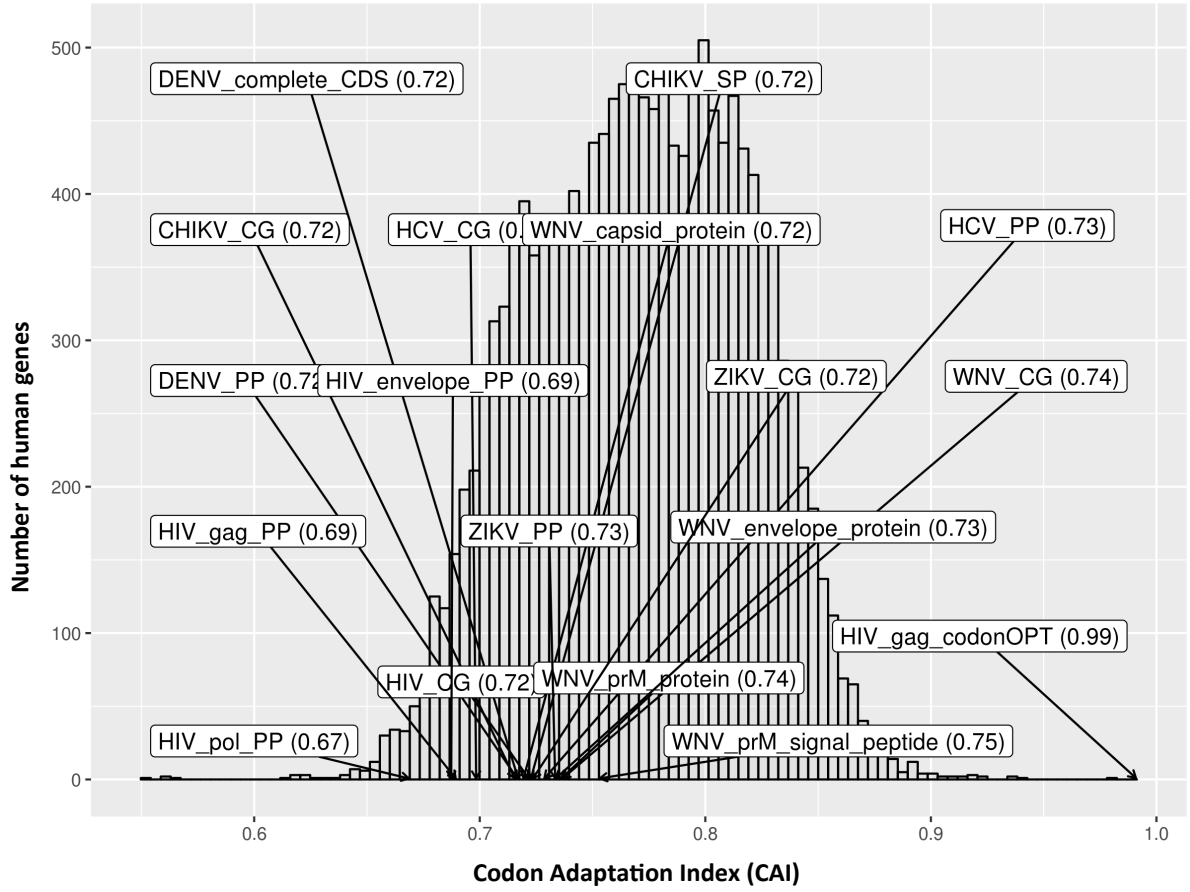

Figure D1. Histogram of codon adaptation indices (CAIs) of hg38 RefSeq transcripts. CAIs of several viral genomes and sequences are highlighted for comparison. DENV - Dengue virus; CHIKV - Chikungunya virus; HCV - Hepatitis C virus; HIV - Human immunodeficiency virus; WNV - West Nile virus; ZIKV - Zika virus. (PP - polyprotein; OPT – codon optimized sequence; CG - complete genome) Mean CAI for RefSeq transcripts: 0.77.

CONCLUSIONS

The main conclusions from the results presented in this thesis are as follows:

RNAseq analyses revealed different transcriptomic signatures of HSP-cultured naive and TCR-activated memory CD4 T cells

- Most of the genes upregulated in HSP-cultured CD4 T cells compared to TCR-activated CD4 T cells are enriched in GO terms such as immune defence and immune responses
- Several identified transcription factors from HSP-cultured CD4 T cells are known to play a role in control of HIV latency
- SLFN12 in HSP-cultured CD4 T cells was identified as a candidate HIV restriction factor involved in latency

SLFN11 and SLFN12 play a role in HIV latency maintenance

- HIV reactivation from latently infected ACH2 cells is enhanced by knock-down of SLFN11 and SLFN12
- HIV expression enhancement is due to an increase of the translation efficiency

SLFN12 inhibits HIV protein production in a codon-usage dependent manner at the level of translation elongation

- SLFN12 attenuates HIV protein synthesis from non-codon-optimized vital transcripts
- SLFN11 and SLFN12 bind to ribosomal subunits and ribosomes during HIV translation

ANNEXES

ANNEX 1

List of abbreviations

A	adenosine
Ag	antigen
AIDS	acquired immunodeficiency syndrome
Asp	asparagine
C	cytosine
CA	capsid
CAI	codon adaptation index
cART	combination antiretroviral therapy
CTLs	cytotoxic T lymphocytes
DE	differentially expressed genes
DNA	deoxyribonucleic acid
DNMDP	6-(4-(diethylamino)-3-nitrophenyl)-5-methyl-4,5-dihydropyridazin-3(2H)-one
dNTP	deoxynucleoside triphosphate
eGFP	enhanced green fluorescent protein
EIAV	equine infectious anemia virus
FIV	feline immunodeficiency virus
G	guanine
GAPDH	Glyceraldehyde 3-phosphate dehydrogenase
GFP	green fluorescent protein
HIV	human immunodeficiency virus
HSP	homeostatic proliferation
IFN	interferon
IL-15	interleukin 15
IL-2	interleukin 2
IL-7	interleukin 7
IN	integrase
IVDU	intravenous drug users
LAV	lymphadenopathy associated virus
Leu	leucine
LPA	latency promoting agent
LRA	latency reversal agent
LTR	long terminal repetition
MA	matrix
MLV	murine leukemia virus
mRNA	messenger RNA
MSM	men who have sex with men
NC	nucleocapsid

NF-κB	nuclear factor kappa-light-chain-enhancer of activated B cells
NFAT	nuclear factor of activated T cells
NLS	nuclear localization signal
opt	optimized
ORF	open reading frame
PBMC	peripheral blood mononuclear cell
PCR	polymerase chain reaction
PR	protease
RF	restriction factor
RNA	ribonucleic acid
RT	reverse transcriptase
SAHA	Suberoylanilide Hydroxamic Acid
Ser	serine
shRNA	short hairpin RNA
SIV	simian immunodeficiency virus
SLFN	Schlafen
ssRNA	single-stranded RNA
SU	surface
TCR	T-cell receptor
TF	transcription factor
TLR	Toll-like receptor
TM	transmembrane
tRNA	transfer RNA
Trp	tryptophan
VZV	varicella-zoster virus
wt	wild-type

ANNEX 2

Other contributions during PhD study

Fleta-Soriano E, Smutná K, Martínez JP, Lorca Oró C, Sadiq SK, Mirambeau G, et al. The Myxobacterial Metabolite Soraphen A Inhibits HIV-1 by Reducing Virus Production and Altering Virion Composition. Antimicrob Agents Chemother. 2017 Aug;61(8). DOI: 10.1128/AAC.00739-17

REFERENCES

A

Ajamian, Lara, Levon Abrahamyan, Miroslav Milev, Pavel V. Ivanov, Andreas E. Kulozik, Niels H. Gehring, and Andrew J. Mouland. 2008. “Unexpected Roles for UPF1 in HIV-1 RNA Metabolism and Translation.” *RNA* 14 (5): 914–27.

Akashi, H. 1994. “Synonymous Codon Usage in Drosophila Melanogaster: Natural Selection and Translational Accuracy.” *Genetics* 136 (3): 927–35.

Al-Jabri, Ali A. 2003. “How Does HIV-1 Infect a Susceptible Human Cell?: Current Thinking.” *Journal for Scientific Research. Medical Sciences* 5 (1-2): 31–44.

Archin, Nancie M., Amy Espeseth, Daniel Parker, Manzoor Cheema, Daria Hazuda, and David M. Margolis. 2009. “Expression of Latent HIV Induced by the Potent HDAC Inhibitor Suberoylanilide Hydroxamic Acid.” *AIDS Research and Human Retroviruses* 25 (2): 207–12.

Archin, N. M., A. L. Liberty, A. D. Kashuba, S. K. Choudhary, J. D. Kuruc, A. M. Crooks, D. C. Parker, et al. 2012. “Administration of Vorinostat Disrupts HIV-1 Latency in Patients on Antiretroviral Therapy.” *Nature* 487 (7408): 482–85.

B

Bailey, Justin R., Ahmad R. Sedaghat, Tara Kieffer, Timothy Brennan, Patricia K. Lee, Megan Wind-Rotolo, Christine M. Haggerty, et al. 2006. “Residual Human Immunodeficiency Virus Type 1 Viremia in Some Patients on Antiretroviral Therapy Is Dominated by a Small Number of Invariant Clones Rarely Found in Circulating CD4+ T Cells.” *Journal of Virology* 80 (13): 6441–57.

Barré-Sinoussi, F., J. C. Chermann, F. Rey, M. T. Nugeyre, S. Chamaret, J. Gruest, C. Dauguet, et al. 1983. “Isolation of a T-Lymphotropic Retrovirus from a Patient at Risk for Acquired Immune Deficiency Syndrome (AIDS).” *Science* 220 (4599): 868–71.

Bedoya, Victoria I., Adriano Boasso, Andrew W. Hardy, Susanna Rybak, Gene M. Shearer, and Maria T. Rugeles. 2006. “Ribonucleases in HIV Type 1 Inhibition: Effect of Recombinant RNases on Infection of Primary T Cells and Immune Activation-Induced RNase Gene and Protein Expression.” *AIDS Research and Human Retroviruses* 22 (9): 897–907.

Berger, Michael, Philippe Krebs, Karine Crozat, Xiaohong Li, Ben A. Croker, Owen M. Siggs, Daniel Popkin, et al. 2010. “An Slfn2 Mutation Causes Lymphoid and Myeloid Immunodeficiency due to Loss of Immune Cell Quiescence.” *Nature Immunology* 11 (4): 335–43.

Besnard, Emilie, Shweta Hakre, Martin Kampmann, Hyung W. Lim, Nina N. Hosmane, Alyssa Martin, Michael C. Bassik, et al. 2016. “The mTOR Complex Controls HIV Latency.” *Cell Host & Microbe* 20 (6): 785–97.

Bishop, Kate N., Mohit Verma, Eun-Young Kim, Steven M. Wolinsky, and Michael H. Malim. 2008. “APOBEC3G Inhibits Elongation of HIV-1 Reverse Transcripts.” *PLoS Pathogens* 4 (12): e1000231.

Bleul, C. C., L. Wu, J. A. Hoxie, T. A. Springer, and C. R. Mackay. 1997. “The HIV Coreceptors CXCR4 and CCR5 Are Differentially Expressed and Regulated on Human T Lymphocytes.” *Proceedings of the National Academy of Sciences* 94 (5): 1925–30.

Bocharov, G., V. Chereshnev, I. Gainova, S. Bazhan, B. Bachmetyev, J. Argilaguet, J. Martinez, and A. Meyerhans. 2012. “Human Immunodeficiency Virus Infection : From Biological Observations to Mechanistic Mathematical Modelling.” *Mathematical Modelling of Natural Phenomena* 7 (5): 78–104.
Boyman, O., J. Purton, C. Surh, and J. Sprent. 2007. “Cytokines and T-Cell Homeostasis.” *Current Opinion in Immunology* 19 (3): 320–26.
Brady, Gareth, Louise Boggan, Andrew Bowie, and Luke A. J. O’Neill. 2005. “Schlafen-1 Causes a Cell Cycle Arrest by Inhibiting Induction of Cyclin D1.” *The Journal of Biological Chemistry* 280 (35): 30723–34.
Bukrinsky, M. I., T. L. Stanwick, M. P. Dempsey, and M. Stevenson. 1991. “Quiescent T Lymphocytes as an Inducible Virus Reservoir in HIV-1 Infection.” *Science* 254 (5030): 423–27.
Bullen, C. Korin, C. Korin Bullen, Gregory M. Laird, Christine M. Durand, Janet D. Siliciano, and Robert F. Siliciano. 2014. “New Ex Vivo Approaches Distinguish Effective and Ineffective Single Agents for Reversing HIV-1 Latency in Vivo.” *Nature Medicine* 20 (4): 425–29.
Bustos, Olivia, Saijal Naik, Gayle Ayers, Claudio Casola, Maria A. Perez-Lamigueiro, Paul T. Chippindale, Ellen J. Pritham, and Elena de la Casa-Esperón. 2009. “Evolution of the Schlafen Genes, a Gene Family Associated with Embryonic Lethality, Meiotic Drive, Immune Processes and Orthopoxvirus Virulence.” *Gene* 447 (1): 1–11.

C

Calonge, Esther, Mercedes Bermejo, Francisco Diez-Fuertes, Isabelle Mangeot, Nuria González, Mayte Coiras, Laura Jiménez Tormo, et al. 2017. “Different Expression of Interferon-Stimulated Genes in Response to HIV-1 Infection in Dendritic Cells Based on Their Maturation State.” *Journal of Virology* 91 (8). https://doi.org/10.1128/JVI.01379-16.
Case, Kathleen. 1986. “Nomenclature: Human Immunodeficiency Virus.” *Annals of Internal Medicine* 105 (1): 133.
Castelli, Joann C., and Jay A. Levy. 2002. “HIV (Human Immunodeficiency Virus).” In *Encyclopedia of Cancer*, 407–16.
Castro-Gonzalez, Sergio, Marta Colomer-Lluch, and Ruth Serra-Moreno. 2018. “Barriers for HIV Cure: The Latent Reservoir.” *AIDS Research and Human Retroviruses* 34 (9): 739–59.
Chereshnev, V. A., G. Bocharov, S. Bazhan, B. Bachmetyev, I. Gainova, V. Likhoshvai, J. M. Argilaguet, et al. 2013. “Pathogenesis and Treatment of HIV Infection: The Cellular, the Immune System and the Neuroendocrine Systems Perspective.” *International Reviews of Immunology* 32 (3): 282–306.
Chojnacki, Jakub, Thorsten Staudt, Bärbel Glass, Pit Bingen, Johann Engelhardt, Maria Anders, Jale Schneider, Barbara Müller, Stefan W. Hell, and Hans-Georg Kräusslich. 2012. “Maturation-Dependent HIV-1 Surface Protein Redistribution Revealed by Fluorescence Nanoscopy.” *Science* 338 (6106): 524–28.
Chomont, Nicolas, Mohamed El-Far, Petronela Ancuta, Lydie Trautmann, Francesco A. Procopio, Bader Yassine-Diab, Geneviève Boucher, et al. 2009. “HIV Reservoir Size and Persistence Are Driven by T Cell Survival and Homeostatic Proliferation.” *Nature Medicine* 15 (8): 893–900.
Chun, Tae-Wook, Richard T. Davey, Delphine Engel, H. Clifford Lane, and Anthony S. Fauci. 1999. “Re-Emergence of HIV after Stopping Therapy.” *Nature* 401

(6756): 874–75.
Chun, T. W., D. Engel, M. M. Berrey, T. Shea, L. Corey, and A. S. Fauci. 1998. “Early Establishment of a Pool of Latently Infected, Resting CD4(+) T Cells during Primary HIV-1 Infection.” *Proceedings of the National Academy of Sciences of the United States of America* 95 (15): 8869–73.
Chun, T-W, T. -W. Chun, D. Engel, M. M. Berrey, T. Shea, L. Corey, and A. S. Fauci. 1998. “Early Establishment of a Pool of Latently Infected, Resting CD4 T Cells during Primary HIV-1 Infection.” *Proceedings of the National Academy of Sciences* 95 (15): 8869–73.
Clavel, F., D. Guétard, F. Brun-Vézinet, S. Chamaret, M. A. Rey, M. O. Santos-Ferreira, A. G. Laurent, C. Dauguet, C. Katlama, and C. Rouzioux. 1986. “Isolation of a New Human Retrovirus from West African Patients with AIDS.” *Science* 233 (4761): 343–46.

D

Dalgleish, A. G., P. C. Beverley, P. R. Clapham, D. H. Crawford, M. F. Greaves, and R. A. Weiss. 1984. “The CD4 (T4) Antigen Is an Essential Component of the Receptor for the AIDS Retrovirus.” *Nature* 312 (5996): 763–67.
Davey, R. T., N. Bhat, C. Yoder, T. -W. Chun, J. A. Metcalf, R. Dewar, V. Natarajan, et al. 1999. “HIV-1 and T Cell Dynamics after Interruption of Highly Active Antiretroviral Therapy (HAART) in Patients with a History of Sustained Viral Suppression.” *Proceedings of the National Academy of Sciences* 96 (26): 15109–14.
Dolgin, Elie. 2013. “Underestimate of HIV Reservoirs Threatens Purging Approach.” *Nature Medicine* 19 (4): 384–85.
Doyon, Geneviève, Jennifer Zerbato, John W. Mellors, and Nicolas Sluis-Cremer. 2013. “Disulfiram Reactivates Latent HIV-1 Expression through Depletion of the Phosphatase and Tensin Homolog.” *AIDS* 27 (2): F7–11.

F

Farber, Donna L., Naomi A. Yudanin, and Nicholas P. Restifo. 2013. “Human Memory T Cells: Generation, Compartmentalization and Homeostasis.” *Nature Reviews. Immunology* 14 (1): 24–35.
Finzi, D., M. Hermankova, T. Pierson, L. M. Carruth, C. Buck, R. E. Chaisson, T. C. Quinn, et al. 1997. “Identification of a Reservoir for HIV-1 in Patients on Highly Active Antiretroviral Therapy.” *Science* 278 (5341): 1295–1300.
Frankel, A. D., and J. A. Young. 1998. “HIV-1: Fifteen Proteins and an RNA.” *Annual Review of Biochemistry* 67: 1–25.

G

Gao, Feng, Elizabeth Bailes, David L. Robertson, Yalu Chen, Cynthia M. Rodenburg, Scott F. Michael, Larry B. Cummins, et al. 1999. “Origin of HIV-1 in the Chimpanzee Pan Troglodytes Troglodytes.” *Nature* 397 (6718): 436–41.
Gately, M. K., B. B. Desai, A. G. Wolitzky, P. M. Quinn, C. M. Dwyer, F. J. Podlaski, P. C. Familletti, F. Sinigaglia, R. Chizonnite, and U. Gubler. 1991. “Regulation of Human Lymphocyte Proliferation by a Heterodimeric Cytokine, IL-12 (cytotoxic Lymphocyte Maturation Factor).” *Journal of Immunology* 147 (3): 874–82.

Gendelman, H. E., L. M. Baca, H. Husayni, J. A. Turpin, D. Skillman, D. C. Kalter, J. M. Orenstein, D. L. Hoover, and M. S. Meltzer. 1990. “Macrophage-HIV Interaction: Viral Isolation and Target Cell Tropism.” *AIDS* 4 (3): 221–28.
Geserick, Peter, Frank Kaiser, Uwe Klemm, Stefan H. E. Kaufmann, and Jens Zerrahn. 2004a. “Modulation of T Cell Development and Activation by Novel Members of the Schlafen (slfn) Gene Family Harbouring an RNA Helicase-like Motif.” *International Immunology* 16 (10): 1535–48.
———. 2004b. “Modulation of T Cell Development and Activation by Novel Members of the Schlafen (slfn) Gene Family Harbouring an RNA Helicase-like Motif.” *International Immunology* 16 (10): 1535–48.
Ghosh, Hiyaa S., James V. Spencer, Bobby Ng, Michael W. McBurney, and Paul D. Robbins. 2007. “Sirt1 Interacts with Transducin-like Enhancer of Split-1 to Inhibit Nuclear Factor kappaB-Mediated Transcription.” *Biochemical Journal* 408 (1): 105–11.
Gingold, Hila, and Yitzhak Pilpel. 2011. “Determinants of Translation Efficiency and Accuracy.” *Molecular Systems Biology* 7 (April): 481.
“Global HIV & AIDS Statistics — 2018 Fact Sheet.” n.d. Accessed November 9, 2018. http://www.unaids.org/en/resources/fact-sheet.
“Global HIV and AIDS Statistics.” 2015a. AVERT. July 16, 2015. https://www.avert.org/global-hiv-and-aids-statistics.
Goldstone, David C., Valerie Ennis-Adeniran, Joseph J. Hedden, Harriet C. T. Groom, Gillian I. Rice, Evangelos Christodoulou, Philip A. Walker, et al. 2011. “HIV-1 Restriction Factor SAMHD1 Is a Deoxynucleoside Triphosphate Triphosphohydrolase.” *Nature* 480 (7377): 379–82.
Goonetilleke, Nilu, Michael K. P. Liu, Jesus F. Salazar-Gonzalez, Guido Ferrari, Elena Giorgi, Vitaly V. Ganusov, Brandon F. Keele, et al. 2009. “The First T Cell Response to Transmitted/founder Virus Contributes to the Control of Acute Viremia in HIV-1 Infection.” *The Journal of Experimental Medicine* 206 (6): 1253–72.
Goujon, Caroline, Olivier Moncorgé, Hélène Bauby, Tomas Doyle, Christopher C. Ward, Torsten Schaller, Stéphane Hué, Wendy S. Barclay, Reiner Schulz, and Michael H. Malim. 2013. “Human MX2 Is an Interferon-Induced Post-Entry Inhibitor of HIV-1 Infection.” *Nature* 502 (7472): 559–62.
Guinevere Q. Lee, Mathias Lichterfeld. 2016. “Diversity of HIV-1 Reservoirs in CD4 T Cell Subsets.” *Current Opinion in HIV and AIDS* 11 (4): 383.
Gulick, Roy M., John W. Mellors, Diane Havlir, Joseph J. Eron, Charles Gonzalez, Deborah McMahon, Douglas D. Richman, et al. 1997. “Treatment with Indinavir, Zidovudine, and Lamivudine in Adults with Human Immunodeficiency Virus Infection and Prior Antiretroviral Therapy.” *The New England Journal of Medicine* 337 (11): 734–39.
Guy, G. R., R. A. Jackson, P. Yusoff, and S. Y. Chow. 2009. “Sprouty Proteins: Modified Modulators, Matchmakers or Missing Links?” *The Journal of Endocrinology* 203 (2): 191–202.

H

Harbers, K., A. Schnieke, H. Stuhlmann, D. Jähner, and R. Jaenisch. 1981. “DNA Methylation and Gene Expression: Endogenous Retroviral Genome Becomes Infectious after Molecular Cloning.” *Proceedings of the National Academy of Sciences of the United States of America* 78 (12): 7609–13.

Harris, Reuben S., and Mark T. Liddament. 2004. “Retroviral Restriction by APOBEC Proteins.” *Nature Reviews. Immunology* 4 (11): 868–77.
Hayashi, Tsuyoshi, Maxime Jean, Huachao Huang, Sydney Simpson, Netty G. Santoso, and Jian Zhu. 2017. “Screening of an FDA-Approved Compound Library Identifies Levosimendan as a Novel Anti-HIV-1 Agent That Inhibits Viral Transcription.” *Antiviral Research* 146 (October): 76–85.
Henry, Curtis J., David A. Ornelles, Latoya M. Mitchell, Kristina L. Brzoza-Lewis, and Elizabeth M. Hiltbold. 2008. “IL-12 Produced by Dendritic Cells Augments CD8+ T Cell Activation through the Production of the Chemokines CCL1 and CCL17.” *Journal of Immunology* 181 (12): 8576–84.
Hirsch, M., R. Steigbigel, S. Staszewski, J. Mellors, E. Scerpella, B. Hirschel, J. Lange, et al. 1999. “A Randomized, Controlled Trial of Indinavir, Zidovudine, and Lamivudine in Adults with Advanced Human Immunodeficiency Virus Type 1 Infection and Prior Antiretroviral Therapy.” *The Journal of Infectious Diseases* 180 (3): 659–65.
Hope, Thomas J. 1997. “Viral RNA Export.” *Chemistry & Biology* 4 (5): 335–44.
Ho, Ya-Chi, Liang Shan, Nina N. Hosmane, Jeffrey Wang, Sarah B. Laskey, Daniel I. S. Rosenbloom, Jun Lai, Joel N. Blankson, Janet D. Siliciano, and Robert F. Siliciano. 2013. “Replication-Competent Noninduced Proviruses in the Latent Reservoir Increase Barrier to HIV-1 Cure.” *Cell* 155 (3): 540–51.
Huang, Da Wei, Brad T. Sherman, and Richard A. Lempicki. 2009. “Systematic and Integrative Analysis of Large Gene Lists Using DAVID Bioinformatics Resources.” *Nature Protocols* 4 (1): 44–57.
Huet, Thierry, Rémi Cheynier, Andreas Meyerhans, Georges Roelants, and Simon Wain-Hobson. 1990. “Genetic Organization of a Chimpanzee Lentivirus Related to HIV-1.” *Nature* 345 (6273): 356–59.
Hu, Wei-Shau, and Stephen H. Hughes. 2012a. “HIV-1 Reverse Transcription.” *Cold Spring Harbor Perspectives in Medicine* 2 (10). https://doi.org/10.1101/cshperspect.a006882.
———. 2012b. “HIV-1 Reverse Transcription.” *Cold Spring Harbor Perspectives in Medicine* 2 (10). https://doi.org/10.1101/cshperspect.a006882.

J

Jean, Maxime J., Tsuyoshi Hayashi, Huachao Huang, Justin Brennan, Sydney Simpson, Andrei Purmal, Katerina Gurova, et al. 2017. “Curaxin CBL0100 Blocks HIV-1 Replication and Reactivation through Inhibition of Viral Transcriptional Elongation.” *Frontiers in Microbiology* 8 (October): 2007.
Jenkins, M. K., A. Khoruts, E. Ingulli, D. L. Mueller, S. J. McSorley, R. L. Reinhardt, A. Itano, and K. A. Pape. 2001. “In Vivo Activation of Antigen-Specific CD4 T Cells.” *Annual Review of Immunology* 19: 23–45.
Jia, Xiaofei, Qi Zhao, and Yong Xiong. 2015. “HIV Suppression by Host Restriction Factors and Viral Immune Evasion.” *Current Opinion in Structural Biology* 31 (April): 106–14.
Jordan, Albert, Dwayne Bisgrove, and Eric Verdin. 2003. “HIV Reproducibly Establishes a Latent Infection after Acute Infection of T Cells in Vitro.” *The EMBO Journal* 22 (8): 1868–77.

K

Kane, Melissa, Trinity M. Zang, Suzannah J. Rihn, Fengwen Zhang, Tonya Kueck, Mudathir Alim, John Schoggins, Charles M. Rice, Sam J. Wilson, and Paul D. Bieniasz. 2016. “Identification of Interferon-Stimulated Genes with Antiretroviral Activity.” *Cell Host & Microbe* 20 (3): 392–405.

Katsikis, Peter D., Yvonne M. Mueller, and François Villinger. 2011. “The Cytokine Network of Acute HIV Infection: A Promising Target for Vaccines and Therapy to Reduce Viral Set-Point?” *PLoS Pathogens* 7 (8): e1002055.

Katsoulidis, Efstratios, Nathalie Carayol, Jennifer Woodard, Iwona Konieczna, Beata Majchrzak-Kita, Alison Jordan, Antonella Sassano, Elizabeth A. Eklund, Eleanor N. Fish, and Leonidas C. Platanias. 2009. “Role of Schlafen 2 (SLFN2) in the Generation of Interferon α-Induced Growth Inhibitory Responses.” *The Journal of Biological Chemistry* 284 (37): 25051–64.

Katsoulidis, Efstratios, Evangelos Mavrommatis, Jennifer Woodard, Mario A. Shields, Antonella Sassano, Nathalie Carayol, Konrad T. Sawicki, Hidayatullah G. Munshi, and Leonidas C. Platanias. 2010. “Role of Interferon α (IFNα)-Inducible Schlafen-5 in Regulation of Anchorage-Independent Growth and Invasion of Malignant Melanoma Cells.” *The Journal of Biological Chemistry* 285 (51): 40333–41.

Keating, Cameron P., Melissa K. Hill, David J. Hawkes, Redmond P. Smyth, Catherine Isel, Shu-Yun Le, Ann C. Palmenberg, et al. 2009. “The A-Rich RNA Sequences of HIV-1 Pol Are Important for the Synthesis of Viral cDNA.” *Nucleic Acids Research* 37 (3): 945–56.

Ke, Ruian, Sharon R. Lewin, Julian H. Elliott, and Alan S. Perelson. 2015. “Modeling the Effects of Vorinostat In Vivo Reveals Both Transient and Delayed HIV Transcriptional Activation and Minimal Killing of Latently Infected Cells.” *PLoS Pathogens* 11 (10): e1005237.

Kim, Hong, Myung-Soo Choi, Kyung-Soo Inn, and Bum-Joon Kim. 2016. “Inhibition of HIV-1 Reactivation by a Telomerase-Derived Peptide in a HSP90-Dependent Manner.” *Scientific Reports* 6 (1). https://doi.org/10.1038/srep28896.

Kinoshita, Shigemi, Lishan Su, Masahiko Amano, Luika A. Timmerman, Hideto Kaneshima, and Garry P. Nolan. 1997. “The T Cell Activation Factor NF-ATc Positively Regulates HIV-1 Replication and Gene Expression in T Cells.” *Immunity* 6 (3): 235–44.

Kitchen, S. G., and J. A. Zack. 1999. “Distribution of the Human Immunodeficiency Virus Coreceptors CXCR4 and CCR5 in Fetal Lymphoid Organs: Implications for Pathogenesis in Utero.” *AIDS Research and Human Retroviruses* 15 (2): 143–48.

Kobayashi-Ishihara, Mie, Kazutaka Terahara, Javier P. Martinez, Makoto Yamagishi, Ryutaro Iwabuchi, Christian Brander, Manabu Ato, Toshiki Watanabe, Andreas Meyerhans, and Yasuko Tsunetsugu-Yokota. 2018. “HIV LTR-Driven Antisense RNA by Itself Has Regulatory Function and May Curtail Virus Reactivation From Latency.” *Frontiers in Microbiology* 9 (May): 1066.

Korber, B., M. Muldoon, J. Theiler, F. Gao, R. Gupta, A. Lapedes, B. H. Hahn, S. Wolinsky, and T. Bhattacharya. 2000. “Timing the Ancestor of the HIV-1 Pandemic Strains.” *Science* 288 (5472): 1789–96.

Korin, Y. D., and J. A. Zack. 1999. “Nonproductive Human Immunodeficiency Virus Type 1 Infection in Nucleoside-Treated G0 Lymphocytes.” *Journal of Virology* 73 (8): 6526–32.

Kovalenko, Pavlo L., and Marc D. Basson. 2014. “Schlafen 12 Expression Modulates Prostate Cancer Cell Differentiation.” *The Journal of Surgical Research* 190 (1): 177–84.

Kramer, Holger B., Kerry J. Lavender, Li Qin, Andrea R. Stacey, Michael K. P. Liu, Katalin di Gleria, Alison Simmons, et al. 2010. “Elevation of Intact and Proteolytic Fragments of Acute Phase Proteins Constitutes the Earliest Systemic Antiviral Response in HIV-1 Infection.” *PLoS Pathogens* 6 (5): e1000893.

Kumar, Nitasha A., Julia B. McBrien, Diane G. Carnathan, Maud Mavigner, Cameron Mattingly, Erick R. White, Federico Viviano, et al. 2018. “Antibody-Mediated CD4 Depletion Induces Homeostatic CD4 T Cell Proliferation without Detectable Virus Reactivation in Antiretroviral Therapy-Treated Simian Immunodeficiency Virus-Infected Macaques.” *Journal of Virology* 92 (22). https://doi.org/10.1128/JVI.01235-18.

L

Laird, Gregory M., C. Korin Bullen, Daniel I. S. Rosenbloom, Alyssa R. Martin, Alison L. Hill, Christine M. Durand, Janet D. Siliciano, and Robert F. Siliciano. 2015. “Ex Vivo Analysis Identifies Effective HIV-1 Latency-Reversing Drug Combinations.” *The Journal of Clinical Investigation* 125 (5): 1901–12.

Lavie, Laurence, Milena Kitova, Esther Maldener, Eckart Meese, and Jens Mayer. 2005. “CpG Methylation Directly Regulates Transcriptional Activity of the Human Endogenous Retrovirus Family HERV-K(HML-2).” *Journal of Virology* 79 (2): 876–83.

Levesque, Marc C., M. Anthony Moody, Kwan-Ki Hwang, Dawn J. Marshall, John F. Whitesides, Joshua D. Amos, Thaddeus C. Gurley, et al. 2009. “Polyclonal B Cell Differentiation and Loss of Gastrointestinal Tract Germinal Centers in the Earliest Stages of HIV-1 Infection.” *PLoS Medicine* 6 (7): e1000107.

Levy, Jay A. 1989. “Pathogenesis of Human Immunodeficiency Virus Infection.” *Annals of the New York Academy of Sciences* 567 (1 Viral Oncogen): 58–68.

Li, Gene-Wei, Eugene Oh, and Jonathan S. Weissman. 2012. “The Anti-Shine-Dalgarno Sequence Drives Translational Pausing and Codon Choice in Bacteria.” *Nature* 484 (7395): 538–41.

Li, Manqing, Elaine Kao, Xia Gao, Hilary Sandig, Kirsten Limmer, Mariana Pavon-Eternod, Thomas E. Jones, et al. 2012. “Codon-Usage-Based Inhibition of HIV Protein Synthesis by Human Schlafen 11.” *Nature* 491 (7422): 125–28.

Lin, Yue-Zhi, Liu-Ke Sun, Dan-Tong Zhu, Zhe Hu, Xue-Feng Wang, Cheng Du, Yu-Hong Wang, Xiao-Jun Wang, and Jian-Hua Zhou. 2016. “Equine Schlafen 11 Restricts the Production of Equine Infectious Anemia Virus via a Codon Usage-Dependent Mechanism.” *Virology* 495: 112–21.

Liu, Furao, Pingting Zhou, Qian Wang, Meichao Zhang, and Dong Li. 2018. “The Schlafen Family: Complex Roles in Different Cell Types and Virus Replication.” *Cell Biology International* 42 (1): 2–8.

Liu, Li, Takashi Sakai, Nam Hoang Tran, Rika Mukai-Sakai, Ryuji Kaji, and Kiyoshi Fukui. 2009. “Nucling Interacts with Nuclear Factor-kappaB, Regulating Its Cellular Distribution.” *The FEBS Journal* 276 (5): 1459–70.

Liu, Zhenlong, Qinghua Pan, Shilei Ding, Jin Qian, Fengwen Xu, Jinming Zhou, Shan Cen, Fei Guo, and Chen Liang. 2013. “The Interferon-Inducible MxB Protein Inhibits HIV-1 Infection.” *Cell Host & Microbe* 14 (4): 398–410.

Lloyd, A. 1996. “HIV Infection and AIDS.” *Papua and New Guinea Medical Journal* 39 (3): 174–80.

M

Madrid-Elena, Nadia, María Laura García-Bermejo, Sergio Serrano-Villar, Alberto Díaz-de Santiago, Beatriz Sastre, Carolina Gutiérrez, Fernando Dronda, et al. 2018. “Maraviroc Is Associated with Latent HIV-1 Reactivation through NF-κB Activation in Resting CD4 T Cells from HIV-Infected Individuals on Suppressive Antiretroviral Therapy.” *Journal of Virology*, February. https://doi.org/10.1128/JVI.01931-17.

Maier, R., M. M. Bartolomé-Rodríguez, C. Moulon, H. U. Weltzien, and A. Meyerhans. 2000. “Kinetics of CXCR4 and CCR5 up-Regulation and Human Immunodeficiency Virus Expansion after Antigenic Stimulation of Primary CD4(+) T Lymphocytes.” *Blood* 96 (5): 1853–56.

Marsden, Matthew D., and Jerome A. Zack. 2010. “Establishment and Maintenance of HIV Latency: Model Systems and Opportunities for Intervention.” *Future Virology* 5 (1): 97–109.

Martinez, M. A., J. P. Vartanian, and S. Wain-Hobson. 1994. “Hypermutagenesis of RNA Using Human Immunodeficiency Virus Type 1 Reverse Transcriptase and Biased dNTP Concentrations.” *Proceedings of the National Academy of Sciences of the United States of America* 91 (25): 11787–91.

Mattei, Simone, Florian Km Schur, and John Ag Briggs. 2016. “Retrovirus Maturation-an Extraordinary Structural Transformation.” *Current Opinion in Virology* 18 (June): 27–35.

Mavrommatis, Evangelos, Eleanor N. Fish, and Leonidas C. Platanias. 2013a. “The Schlafen Family of Proteins and Their Regulation by Interferons.” *Journal of Interferon & Cytokine Research: The Official Journal of the International Society for Interferon and Cytokine Research* 33 (4): 206–10.

———. 2013b. “The Schlafen Family of Proteins and Their Regulation by Interferons.” *Journal of Interferon & Cytokine Research: The Official Journal of the International Society for Interferon and Cytokine Research* 33 (4): 206–10.

———. 2013c. “The Schlafen Family of Proteins and Their Regulation by Interferons.” *Journal of Interferon & Cytokine Research: The Official Journal of the International Society for Interferon and Cytokine Research* 33 (4): 206–10.

Meyerhans, A., J. P. Vartanian, C. Hultgren, U. Plikat, A. Karlsson, L. Wang, S. Eriksson, and S. Wain-Hobson. 1994. “Restriction and Enhancement of Human Immunodeficiency Virus Type 1 Replication by Modulation of Intracellular Deoxynucleoside Triphosphate Pools.” *Journal of Virology* 68 (1): 535–40.

Mohammadi, Pejman, Julia di Iulio, Miguel Muñoz, Raquel Martinez, István Bartha, Matthias Cavassini, Christian Thorball, et al. 2014. “Dynamics of HIV Latency and Reactivation in a Primary CD4 T Cell Model.” *PLoS Pathogens* 10 (5): e1004156.

Montagnier, Luc. 1999. “HUMAN IMMUNODEFICIENCY VIRUSES (RETROVIRIDAE) | General Features.” In *Encyclopedia of Virology*, 763–74.

Moore, John P., Alexandra Trkola, and Tatjana Dragic. 1997. “Co-Receptors for HIV-1 Entry.” *Current Opinion in Immunology* 9 (4): 551–62.

Mousseau, Guillaume, Cari F. Kessing, Rémi Fromentin, Lydie Trautmann, Nicolas Chomont, and Susana T. Valente. 2015. “The Tat Inhibitor Didehydro-Cortistatin A Prevents HIV-1 Reactivation from Latency.” *mBio* 6 (4): e00465.

Munier, Sandie, Delphine Delcroix-Genête, Laëtitia Carthagéna, Audrey Gumez, and Uriel Hazan. 2005. “Characterization of Two Candidate Genes, NCoA3 and IRF8, Potentially Involved in the Control of HIV-1 Latency.” *Retrovirology* 2 (November): 73.

Murray, Alexandra J., Kyungyoon J. Kwon, Donna L. Farber, and Robert F. Siliciano. 2016. “The Latent Reservoir for HIV-1: How Immunologic Memory and Clonal Expansion Contribute to HIV-1 Persistence.” *Journal of Immunology* 197 (2): 407–17.

N

Nabel, Gary, and David Baltimore. 1987. “An Inducible Transcription Factor Activates Expression of Human Immunodeficiency Virus in T Cells.” *Nature* 326 (6114): 711–13.

Neil, Stuart J. D., Virginie Sandrin, Wesley I. Sundquist, and Paul D. Bieniasz. 2007. “An Interferon-Alpha-Induced Tethering Mechanism Inhibits HIV-1 and Ebola Virus Particle Release but Is Counteracted by the HIV-1 Vpu Protein.” *Cell Host & Microbe* 2 (3): 193–203.

Neil, Stuart J. D., Trinity Zang, and Paul D. Bieniasz. 2008. “Tetherin Inhibits Retrovirus Release and Is Antagonized by HIV-1 Vpu.” *Nature* 451 (7177): 425–30.

Neumann, Brent, Liang Zhao, Kathleen Murphy, and Thomas J. Gonda. 2008. “Subcellular Localization of the Schlafen Protein Family.” *Biochemical and Biophysical Research Communications* 370 (1): 62–66.

Nogales, Vanesa, William C. Reinhold, Sudhir Varma, Anna Martinez-Cardus, Catia Moutinho, Sebastian Moran, Holger Heyn, et al. 2016. “Epigenetic Inactivation of the Putative DNA/RNA Helicase SLFN11 in Human Cancer Confers Resistance to Platinum Drugs.” *Oncotarget* 7 (3): 3084–97.

Norose, Kazumi, Akitoshi Kikumura, Andrew D. Luster, Christopher A. Hunter, and Tajie H. Harris. 2011. “CXCL10 Is Required to Maintain T-Cell Populations and to Control Parasite Replication during Chronic Ocular Toxoplasmosis.” *Investigative Ophthalmology & Visual Science* 52 (1): 389–98.

Nyamweya, Samuel, Andrea Hegedus, Assan Jaye, Sarah Rowland-Jones, Katie L. Flanagan, and Derek C. Macallan. 2013. “Comparing HIV-1 and HIV-2 Infection: Lessons for Viral Immunopathogenesis.” *Reviews in Medical Virology* 23 (4): 221–40.

P

Patel, Vaishali B., Yingjie Yu, Jayanta K. Das, Bhaumik B. Patel, and Adhip P. N. Majumdar. 2009. “Schlafen-3: A Novel Regulator of Intestinal Differentiation.” *Biochemical and Biophysical Research Communications* 388 (4): 752–56.

Perelson, A. S., P. Essunger, Y. Cao, M. Vesanen, A. Hurley, K. Saksela, M. Markowitz, and D. D. Ho. 1997. “Decay Characteristics of HIV-1-Infected Compartments during Combination Therapy.” *Nature* 387 (6629): 188–91.

Pierson, Theodore C., Yan Zhou, Tara L. Kieffer, Christian T. Ruff, Christopher Buck, and Robert F. Siliciano. 2002. “Molecular Characterization of Preintegration Latency in Human Immunodeficiency Virus Type 1 Infection.” *Journal of Virology* 76 (17): 8518–31.

Pierson, T., T. L. Hoffman, J. Blankson, D. Finzi, K. Chadwick, J. B. Margolick, C. Buck, J. D. Siliciano, R. W. Doms, and R. F. Siliciano. 2000. “Characterization of Chemokine Receptor Utilization of Viruses in the Latent Reservoir for Human Immunodeficiency Virus Type 1.” *Journal of Virology* 74 (17): 7824–33.

Pisareva, Vera P., Ilham A. Muslimov, Andrew Tcherepanov, and Andrey V. Pisarev. 2015. “Characterization of Novel Ribosome-Associated Endoribonuclease SLFN14 from Rabbit Reticulocytes.” *Biochemistry* 54 (21): 3286–3301.

Puck, Alexander, Regina Aigner, Madhura Modak, Petra Cejka, Dieter Blaas, and Johannes Stöckl. 2015. “Expression and Regulation of Schlafen (SLFN) Family Members in Primary Human Monocytes, Monocyte-Derived Dendritic Cells and T Cells.” *Results in Immunology* 5: 23–32.

Q

Qian, Wenfeng, Jian-Rong Yang, Nathaniel M. Pearson, Calum Maclean, and Jianzhi Zhang. 2012. “Balanced Codon Usage Optimizes Eukaryotic Translational Efficiency.” *PLoS Genetics* 8 (3): e1002603.

R

Ramratnam, B., J. E. Mittler, L. Zhang, D. Boden, A. Hurley, F. Fang, C. A. Macken, A. S. Perelson, M. Markowitz, and D. D. Ho. 2000. “The Decay of the Latent Reservoir of Replication-Competent HIV-1 Is Inversely Correlated with the Extent of Residual Viral Replication during Prolonged Anti-Retroviral Therapy.” *Nature Medicine* 6 (1): 82–85.

Rao, Shringar, Raquel Amorim, Meijuan Niu, Abdelkrim Temzi, and Andrew J. Mouland. 2018. “The RNA Surveillance Proteins UPF1, UPF2 and SMG6 Affect HIV-1 Reactivation at a Post-Transcriptional Level.” *Retrovirology* 15 (1). https://doi.org/10.1186/s12977-018-0425-2.

Recher, Mike, Marja-Liisa Karjalainen-Lindsberg, Mikael Lindlöf, Maria Söderlund-Venermo, Gaetana Lanzi, Elina Väisänen, Arun Kumar, et al. 2014. “Genetic Variation in Schlafen Genes in a Patient with a Recapitulation of the Murine Elektra Phenotype.” *The Journal of Allergy and Clinical Immunology* 133 (5): 1462–65.e5.

Robinson, Mark D., and Alicia Oshlack. 2010. “A Scaling Normalization Method for Differential Expression Analysis of RNA-Seq Data.” *Genome Biology* 11 (3): R25.

Roney, Kelly, Eda Holl, and Jenny Ting. 2013. “Immune Plexins and Semaphorins: Old Proteins, New Immune Functions.” *Protein & Cell* 4 (1): 17–26.

Rugeles, Maria T., Charles M. Trubey, Victoria I. Bedoya, Ligia A. Pinto, Joost J. Oppenheim, Susanna M. Rybak, and Gene M. Shearer. 2003. “Ribonuclease Is Partly Responsible for the HIV-1 Inhibitory Effect Activated by HLA Alloantigen Recognition.” *AIDS* 17 (4): 481–86.

Rullas, Joaquín, Mercedes Bermejo, Javier García-Pérez, Manuela Beltán, Nuria González, Marjan Hezareh, Stephen J. Brown, and José Alcamí. 2004. “Prostratin Induces HIV Activation and Downregulates HIV Receptors in Peripheral Blood Lymphocytes.” *Antiviral Therapy* 9 (4): 545–54.

S

Sarracino, Ambra, Lavina Gharu, Anna Kula, Alexander O. Pasternak, Veronique Avettand-Fenoel, Christine Rouzioux, Maryana Bardina, et al. 2018. “Posttranscriptional Regulation of HIV-1 Gene Expression during Replication and Reactivation from Latency by Nuclear Matrix Protein MATR3.” *mBio* 9 (6). https://doi.org/10.1128/mBio.02158-18.

Sassano, Antonella, Evangelos Mavrommatis, Ahmet Dirim Arslan, Barbara Kroczynska, Elspeth M. Beauchamp, Satya Khuon, Ten-Leong Chew, et al. 2015. “Human Schlafen 5 (SLFN5) Is a Regulator of Motility and Invasiveness of Renal Cell Carcinoma Cells.” *Molecular and Cellular Biology* 35 (15): 2684–98.

Schaller, Torsten, Caroline Goujon, and Michael H. Malim. 2012. “AIDS/HIV. HIV Interplay with SAMHD1.” *Science* 335 (6074): 1313–14.

Schoggins, John W. 2014. “Interferon-Stimulated Genes: Roles in Viral Pathogenesis.” *Current Opinion in Virology* 6: 40–46.

Schoggins, John W., and Charles M. Rice. 2011. “Interferon-Stimulated Genes and Their Antiviral Effector Functions.” *Current Opinion in Virology* 1 (6): 519–25.

Schwarz, D. A., C. D. Katayama, and S. M. Hedrick. 1998. “Schlafen, a New Family of Growth Regulatory Genes That Affect Thymocyte Development.” *Immunity* 9 (5): 657–68.

Seddon, Benedict, Peter Tomlinson, and Rose Zamoyska. 2003. “Interleukin 7 and T Cell Receptor Signals Regulate Homeostasis of CD4 Memory Cells.” *Nature Immunology* 4 (7): 680–86.

Sengupta, Srona, and Robert F. Siliciano. 2018. “Targeting the Latent Reservoir for HIV-1.” *Immunity* 48 (5): 872–95.

Seong, Rak-Kyun, Seong-Wook Seo, Ji-Ae Kim, Sarah J. Fletcher, Neil V. Morgan, Mukesh Kumar, Young-Ki Choi, and Ok Sarah Shin. 2017. “Schlafen 14 (SLFN14) Is a Novel Antiviral Factor Involved in the Control of Viral Replication.” *Immunobiology* 222 (11): 979–88.

Shan, Liang, Kai Deng, Hongbo Gao, Sifei Xing, Adam A. Capoferri, Christine M. Durand, S. Alireza Rabi, et al. 2017. “Transcriptional Reprogramming during Effector-to-Memory Transition Renders CD4 T Cells Permissive for Latent HIV-1 Infection.” *Immunity* 47 (4): 766–75.e3.

Shan, Liang, Kai Deng, Neeta S. Shroff, Christine M. Durand, S. Alireza. Rabi, Hung-Chih Yang, Hao Zhang, Joseph B. Margolick, Joel N. Blankson, and Robert F. Siliciano. 2012. “Stimulation of HIV-1-Specific Cytolytic T Lymphocytes Facilitates Elimination of Latent Viral Reservoir after Virus Reactivation.” *Immunity* 36 (3): 491–501.

Shan, Liang, and Robert F. Siliciano. 2013. “From Reactivation of Latent HIV-1 to Elimination of the Latent Reservoir: The Presence of Multiple Barriers to Viral Eradication.” *BioEssays: News and Reviews in Molecular, Cellular and Developmental Biology* 35 (6): 544–52.

Sharp, Paul M., and Beatrice H. Hahn. 2011. “Origins of HIV and the AIDS Pandemic.” *Cold Spring Harbor Perspectives in Medicine* 1 (1): a006841.

Sharp, P. M., and W. H. Li. 1987. “The Codon Adaptation Index--a Measure of Directional Synonymous Codon Usage Bias, and Its Potential Applications.” *Nucleic Acids Research* 15 (3): 1281–95.

Sheehy, Ann M., Nathan C. Gaddis, and Michael H. Malim. 2003. “The Antiretroviral Enzyme APOBEC3G Is Degraded by the Proteasome in Response to HIV-1 Vif.” *Nature Medicine* 9 (11): 1404–7.

Sherer, Nathan M., Jing Jin, and Walther Mothes. 2010. “Directional Spread of Surface-Associated Retroviruses Regulated by Differential Virus-Cell Interactions.” *Journal of Virology* 84 (7): 3248–58.
Shioda, Tatsuo, Jay A. Levy, and Cecilia Cheng-Mayer. 1991. “Macrophage and T Cell-Line Tropisms of HIV-1 Are Determined by Specific Regions of the Envelope gp!20 Gene.” *Nature* 349 (6305): 167–69.
Short, J. A. L. 2009. “Viral Evasion of Interferon Stimulated Genes.” *Bioscience Horizons* 2 (2): 212–24.
Siliciano, Janet D., Joleen Kajdas, Diana Finzi, Thomas C. Quinn, Karen Chadwick, Joseph B. Margolick, Colin Kovacs, Stephen J. Gange, and Robert F. Siliciano. 2003. “Long-Term Follow-up Studies Confirm the Stability of the Latent Reservoir for HIV-1 in Resting CD4+ T Cells.” *Nature Medicine* 9 (6): 727–28.
Siliciano, Robert F., and Warner C. Greene. 2011. “HIV Latency.” *Cold Spring Harbor Perspectives in Medicine* 1 (1): a007096.
Simonetti, Francesco R., Michele D. Sobolewski, Elizabeth Fyne, Wei Shao, Jonathan Spindler, Junko Hattori, Elizabeth M. Anderson, et al. 2016. “Clonally Expanded CD4+ T Cells Can Produce Infectious HIV-1 in Vivo.” *Proceedings of the National Academy of Sciences of the United States of America* 113 (7): 1883–88.
Spencer, Paige S., Efraín Siller, John F. Anderson, and José M. Barral. 2012. “Silent Substitutions Predictably Alter Translation Elongation Rates and Protein Folding Efficiencies.” *Journal of Molecular Biology* 422 (3): 328–35.
Spivak, Adam M., and Vicente Planelles. 2018. “Novel Latency Reversal Agents for HIV-1 Cure.” *Annual Review of Medicine* 69 (1): 421–36.
Stabell, Alex C., John Hawkins, Manqing Li, Xia Gao, Michael David, William H. Press, and Sara L. Sawyer. 2016. “Non-Human Primate Schlafen11 Inhibits Production of Both Host and Viral Proteins.” *PLoS Pathogens* 12 (12): e1006066.
Stacey, A. R., P. J. Norris, L. Qin, E. A. Haygreen, E. Taylor, J. Heitman, M. Lebedeva, et al. 2009. “Induction of a Striking Systemic Cytokine Cascade prior to Peak Viremia in Acute Human Immunodeficiency Virus Type 1 Infection, in Contrast to More Modest and Delayed Responses in Acute Hepatitis B and C Virus Infections.” *Journal of Virology* 83 (8): 3719–33.
Stopak, Kim S., Ya-Lin Chiu, Jerry Kropp, Robert M. Grant, and Warner C. Greene. 2007. “Distinct Patterns of Cytokine Regulation of APOBEC3G Expression and Activity in Primary Lymphocytes, Macrophages, and Dendritic Cells.” *The Journal of Biological Chemistry* 282 (6): 3539–46.
Stremlau, Matthew, Michel Perron, Mark Lee, Yuan Li, Byeongwoon Song, Hassan Javanbakht, Felipe Diaz-Griffero, Donovan J. Anderson, Wesley I. Sundquist, and Joseph Sodroski. 2006. “Specific Recognition and Accelerated Uncoating of Retroviral Capsids by the TRIM5alpha Restriction Factor.” *Proceedings of the National Academy of Sciences of the United States of America* 103 (14): 5514–19.
Surh, Charles D., and Jonathan Sprent. 2008. “Homeostasis of Naive and Memory T Cells.” *Immunity* 29 (6): 848–62.

T

Tian, Li, Santai Song, Xiaojing Liu, Yan Wang, Xiaoguang Xu, Yi Hu, and Jianming Xu. 2014. “Schlafen-11 Sensitizes Colorectal Carcinoma Cells to Irinotecan.” *Anti-Cancer Drugs* 25 (10): 1175–81.

Tobin, Nicole H., Gerald H. Learn, Sarah E. Holte, Yang Wang, Ann J. Melvin, Jennifer L. McKernan, Diane M. Pawluk, et al. 2005. “Evidence That Low-Level Viremias during Effective Highly Active Antiretroviral Therapy Result from Two Processes: Expression of Archival Virus and Replication of Virus.” *Journal of Virology* 79 (15): 9625–34.

Tree, Timothy I. M., Gaby Duinkerken, Sabine Willemen, René R. P. de Vries, and Bart O. Roep. 2004. “HLA-DQ-Regulated T-Cell Responses to Islet Cell Autoantigens Insulin and GAD65.” *Diabetes* 53 (7): 1692–99.

Tsujimoto, Yoshihide. 1998. “Role of Bcl-2 Family Proteins in Apoptosis: Apoptosomes or Mitochondria?” *Genes to Cells: Devoted to Molecular & Cellular Mechanisms* 3 (11): 697–707.

Tsunetsugu-Yokota, Yasuko, Mie Kobayahi-Ishihara, Yamato Wada, Kazutaka Terahara, Haruko Takeyama, Ai Kawana-Tachikawa, Kenzo Tokunaga, Makoto Yamagishi, Javier P. Martinez, and Andreas Meyerhans. 2016a. “Homeostatically Maintained Resting Naive CD4 T Cells Resist Latent HIV Reactivation.” *Frontiers in Microbiology* 7 (December): 1944.

———. 2016b. “Homeostatically Maintained Resting Naive CD4 T Cells Resist Latent HIV Reactivation.” *Frontiers in Microbiology* 7 (December): 1944.

V

Van Damme, Nanette, Daniel Goff, Chris Katsura, Rebecca L. Jorgenson, Richard Mitchell, Marc C. Johnson, Edward B. Stephens, and John Guatelli. 2008. “The Interferon-Induced Protein BST-2 Restricts HIV-1 Release and Is Downregulated from the Cell Surface by the Viral Vpu Protein.” *Cell Host & Microbe* 3 (4): 245–52.

Van Heuverswyn, Fran, Yingying Li, Cecile Neel, Elizabeth Bailes, Brandon F. Keele, Weimin Liu, Severin Loul, et al. 2006. “Human Immunodeficiency Viruses: SIV Infection in Wild Gorillas.” *Nature* 444 (7116): 164.

Van Lint, C., S. Emiliani, M. Ott, and E. Verdin. 1996. “Transcriptional Activation and Chromatin Remodeling of the HIV-1 Promoter in Response to Histone Acetylation.” *The EMBO Journal* 15 (5): 1112–20.

Vartanian, Jean-Pierre, Michel Henry, and Simon Wain-Hobson. 2002. “Sustained G→A Hypermutation during Reverse Transcription of an Entire Human Immunodeficiency Virus Type 1 Strain Vau Group O Genome.” *The Journal of General Virology* 83 (4): 801–5.

Vartanian, J. P., A. Meyerhans, B. Asjö, and S. Wain-Hobson. 1991. “Selection, Recombination, and G----A Hypermutation of Human Immunodeficiency Virus Type 1 Genomes.” *Journal of Virology* 65 (4): 1779–88.

Vartanian, J. P., U. Plikat, M. Henry, R. Mahieux, L. Guillemot, A. Meyerhans, and S. Wain-Hobson. 1997. “HIV Genetic Variation Is Directed and Restricted by DNA Precursor Availability.” *Journal of Molecular Biology* 270 (2): 139–51.

Verdin, E., P. Paras Jr, and C. Van Lint. 1993. “Chromatin Disruption in the Promoter of Human Immunodeficiency Virus Type 1 during Transcriptional Activation.” *The EMBO Journal* 12 (8): 3249–59.

W

Waal, Luc de, Timothy A. Lewis, Matthew G. Rees, Aviad Tsherniak, Xiaoyun Wu, Peter S. Choi, Lara Gechijian, et al. 2016. “Identification of Cancer-Cytotoxic Modulators of PDE3A by Predictive Chemogenomics.” *Nature Chemical Biology* 12 (2): 102–8.

Weissenhorn, W., A. Dessen, S. C. Harrison, J. J. Skehel, and D. C. Wiley. 1997. “Atomic Structure of the Ectodomain from HIV-1 gp41.” *Nature* 387 (6631): 426–30.

Whitney, James B., Alison L. Hill, Srisowmya Sanisetty, Pablo Penaloza-MacMaster, Jinyan Liu, Mayuri Shetty, Lily Parenteau, et al. 2014. “Rapid Seeding of the Viral Reservoir prior to SIV Viraemia in Rhesus Monkeys.” *Nature* 512 (7512): 74–77.

Wilen, C. B., J. C. Tilton, and R. W. Doms. 2012. “HIV: Cell Binding and Entry.” *Cold Spring Harbor Perspectives in Medicine* 2 (8): a006866–a006866.

Y

Yang, Jin-Yu, Xiang-Yu Deng, Yi-Sheng Li, Xian-Cai Ma, Jian-Xiong Feng, Bing Yu, Yang Chen, et al. 2018. “Structure of Schlafen13 Reveals a New Class of tRNA/rRNA- Targeting RNase Engaged in Translational Control.” *Nature Communications* 9 (1): 1165.

Yoshizawa, I., Y. Soda, T. Mizuochi, S. Yasuda, T. A. Rizvi, T. Mizuochi, T. Takemori, and Y. Tsunetsugu-Yokota. 2001. “Enhancement of Mucosal Immune Response against HIV-1 Gag by DNA Immunization.” *Vaccine* 19 (20-22): 2995–3003.

Yu, Chien-Hung, Yunkun Dang, Zhipeng Zhou, Cheng Wu, Fangzhou Zhao, Matthew S. Sachs, and Yi Liu. 2015. “Codon Usage Influences the Local Rate of Translation Elongation to Regulate Co-Translational Protein Folding.” *Molecular Cell* 59 (5): 744–54.

Z

Zack, J. A., S. J. Arrigo, S. R. Weitsman, A. S. Go, A. Haislip, and I. S. Chen. 1990. “HIV-1 Entry into Quiescent Primary Lymphocytes: Molecular Analysis Reveals a Labile, Latent Viral Structure.” *Cell* 61 (2): 213–22.

Zack, J. A., A. M. Haislip, P. Krogstad, and I. S. Chen. 1992. “Incompletely Reverse-Transcribed Human Immunodeficiency Virus Type 1 Genomes in Quiescent Cells Can Function as Intermediates in the Retroviral Life Cycle.” *Journal of Virology* 66 (3): 1717–25.

Zhang, L., T. He, A. Talal, G. Wang, S. S. Frankel, and D. D. Ho. 1998. “In Vivo Distribution of the Human Immunodeficiency Virus/simian Immunodeficiency Virus Coreceptors: CXCR4, CCR3, and CCR5.” *Journal of Virology* 72 (6): 5035–45.

Zhang, L., B. Ramratnam, K. Tenner-Racz, Y. He, M. Vesanen, S. Lewin, A. Talal, et al. 1999. “Quantifying Residual HIV-1 Replication in Patients Receiving Combination Antiretroviral Therapy.” *The New England Journal of Medicine* 340 (21): 1605–13.

Zhou, Xiaobei, Helen Lindsay, and Mark D. Robinson. 2014. “Robustly Detecting Differential Expression in RNA Sequencing Data Using Observation Weights.” *Nucleic Acids Research* 42 (11): e91.

Zhou, Yan, Haili Zhang, Janet D. Siliciano, and Robert F. Siliciano. 2005. “Kinetics of Human Immunodeficiency Virus Type 1 Decay Following Entry into Resting CD4+ T Cells.” *Journal of Virology* 79 (4): 2199–2210.
Zuylen, Wendy J. van, Valerie Garceau, Adi Idris, Kate Schroder, Katharine M. Irvine, Jane E. Lattin, Dmitry A. Ovchinnikov, et al. 2011. “Macrophage Activation and Differentiation Signals Regulate Schlafen-4 Gene Expression: Evidence for Schlafen-4 as a Modulator of Myelopoiesis.” *PloS One* 6 (1): e15723.